LOS ALAMOS SCIENTIFIC LABORATORY
OF THE UNIVERSITY OF CALIFORNIA o LOS ALAMOS NEW MEXICO

DETONATION PROPERTIES OF CONDENSED EXPLOSIVES CALCULATED WITH AN EQUATION OF STATE BASED ON INTERMOLECULAR POTENTIALS

Printed in USA. Price $ 2.75. Available from the

Office of Technical Services
U. S. Department of Commerce
Washington 25, D. C.

LA-2712
PHYSICS
TID-4500 (18th Ed.)

LOS ALAMOS SCIENTIFIC LABORATORY
OF THE UNIVERSITY OF CALIFORNIA LOS ALAMOS NEW MEXICO

REPORT WRITTEN: May 1962

REPORT DISTRIBUTED: December 14, 1962

DETONATION PROPERTIES OF CONDENSED EXPLOSIVES CALCULATED WITH AN EQUATION OF STATE BASED ON INTERMOLECULAR POTENTIALS

by

Wildon Fickett

Contract W-7405-ENG. 36 with the U. S. Atomic Energy Commission

ABSTRACT

The best available statistical-mechanical theories consistent with a reasonable expenditure of computer time are used to calculate a detonation product equation of state for condensed explosives and are tested by comparison of calculated detonation properties with experiment.

Chemical equilibrium among up to nine product species, including a separate solid phase, is assumed. The LJD cell model is the basic equation of state. For application to mixtures, a variant of the Longuet-Higgins conformal solution theory is chosen, although some other forms are also considered.

The sensitivity of the results to variation of the uncertain intermolecular potentials and other doubtful elements of the theory is sufficient to rule out an a priori calculation, but rough adjustment of one parameter gives fair agreement with experiment for a variety of CHON explosives. Although some insight into the problem is gained, the performance of this relatively complex theory is comparable to that of simpler forms previously tried. It appears that still more complicated theories and better knowledge of the intermolecular potentials are required for further progress.

ACKNOWLEDGMENT

The author wishes to acknowledge helpful discussions with W. W. Wood, Z. W. Salsburg and C. Mader. Thanks are also due W. C. Davis and B. G. Craig for discussions concerning the experimental data and its interpretation.

CONTENTS

CONTENTS

(continued)

INTRODUCTION

If a cylinder of explosive is suddenly heated or struck at one end, a detonation wave propagates down the length of the charge with approximately constant velocity. This phenomenon is often treated by the model of von Neumann and Zeldovich (Ref. 1, Chap. 3). Transport properties are neglected, and the wave consists of a plane shock followed by a short reaction zone of constant length in which the explosive material is rapidly transformed into its decomposition or detonation products. The material at the end of the reaction zone is in a state of chemical equilibrium and enters a time-dependent expansion wave extending to the rear boundary of the charge. This model, with the aid of the so-called Chapman-Jouguet (CJ) hypothesis, (Ref. 1, Chap. 3) reduces the problem of calculating the state at the rear boundary of the reaction zone (termed the CJ plane) to the solution of a set of algebraic equations, provided that the equation of state of the detonation products is known. The CJ state and the corresponding propagation velocity are unaffected by the details of the flow in the reaction zone ahead or in the expansion wave behind.

This simple theory has inspired a number of efforts to calculate the detonation properties of both gaseous and solid explosives. These

calculations have been fairly successful for gaseous explosives, where the equation of state is known, but less so for condensed explosives, where it is not. The calculations for condensed explosives, many of which are based on semi-empirical equations of state, have been reviewed recently by Jacobs.[2]

Calculations made to date have not completely exploited the available equation of state theories, partly because fairly extensive numerical work is required. However, a reasonably complete test of existing theory is practical with present computing equipment, and this is what we attempt here: to calculate a detonation product equation of state from the best available analytic statistical-mechanical theories consistent with a reasonable expenditure of computer time, and to test the theory through comparison of calculated and experimental results for plane, steady detonation waves.

In order to limit the scope of the investigation and because most of the experimental work has been done on materials of this class, we consider only explosives containing the elements C, H, O, and N. An initial investigation limited to a single explosive with fixed-product composition has been published.[3] In the present work, a number of explosives are considered and equilibrium product composition is used.

Chapter 1

THE MODEL AND RELATED ASSUMPTIONS

1.1 The Molecular Model

We assume that the molecular model is appropriate up to the highest pressures we will consider. Since this assumption, which underlies most of the others, has been questioned, (Ref. 4, p. 286) we examine it first.

To get a general idea of the conditions of interest, take the explosive RDX and assume the decomposition reaction

$$C_3H_6N_6O_6 \rightarrow 3N_2 + 3O_2 + 3CO \quad .$$

For RDX of initial density ρ_o = 1.8 g/cc, the experimental value of relative volume v_{CJ}/v_o is about 0.75,[5] which gives a CJ volume of about 0.42 g/cc. With the mean molecular weight of this product mixture, about 24, we have for the molar volume

$$V = 10.5 \text{ cc/mole} \quad .$$

For a face-centered cubic lattice this gives a mean nearest-neighbor distance of

2.91 A.

Two nitrogen molecules placed end-to end on a pair of neighboring sites would look like:

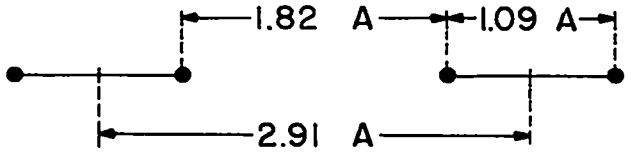

so that for this molecule the distance between nonbonded atoms is about 1.7 times the bond distance. To estimate the intermolecular repulsion energy, we use the pair potentials of reference 3 which were determined to give the experimental RDX detonation velocity in a calculation with fixed product composition. All of these potentials give about the same result at this distance: an interaction energy, divided by Boltzmann's constant, of about 3500 °K.* To compare this with the dissociation

---

One of the best-known pair potentials is that of argon. It can also be used to estimate the repulsion energy in the following way. The radius r of the potential minimum for N_2 obtained from second-virial coefficient measurements is about 4.05 A (Ref. 6, p. 1111) so that at the value of r = 2.91 A given above, the reduced distance r/r* is about 0.7. Using the best available potential for argon in this distance range (obtained from molecular scattering),[7] we obtain at the same reduced distance an interaction energy of 3000 °K. The Lennard-Jones potentials determined from second-virial coefficient measurements give an energy two or three times as large at this distance,[3] but they represent a considerable extrapolation from the data for which they were determined.

energy, we recall that in a face-centered cubic lattice, there are six pair interactions per molecule, corresponding to a total interaction energy of

$$16{,}500\ ^{\circ}\mathrm{K/mole} \cong 1.4\ \mathrm{ev/mole} \cong 32\ \mathrm{kcal/mole} \cong 1.3\ \mathrm{kcal/g}\ ,$$

whereas the dissociation energy of N_2 is about 9 ev. These simple considerations indicate that molecules exist under such conditions. Since the CJ temperatures are probably of the order of 2000 to 4000 °K, however, the intermolecular interaction energy will be several times the molecular kinetic energy, and the so-called "imperfection" terms in the equation of state will dominate.

1.2 Separation of the Partition Function

For calculational convenience, we assume that the partition function is separable, that is, that the overall partition function, after integration over momentum, can be expressed as a product of the configurational and internal partition functions, and that the internal partition function (for vibration, rotation, etc.) is the same as that at infinite dilution. While this assumption is probably not badly wrong, it does introduce some uncertainty.

An estimate of the effect of compression on the vibrational partition function has been made by Cottrell,[8] who has done a quantum-mechanical calculation for the H_2^+ molecule ion confined in an ellipsoidal box. At a pressure of 0.6 mb, a volume of 14 A^3/molecule or 8.4 cc/mole, and a temperature of 3000 °K, he finds that the vibrational energy has increased

by about 1 kcal/mole, or about 1/6 RT, over its value in free space.

A rough estimate of the effects of restricted rotation can be obtained by consideration of molecules having hindered internal rotation. In ethane at 1000 °K, for example, the contribution to the heat capacity from internal rotation is about 1/4 R greater than it would be for free rotation. (Ref. 9, p. 118) Thus the use of this assumption introduces non-negligible errors of perhaps 10-15% of the contribution of the internal partition function.

1.3 Non-Additivity of Pair Forces

Most statistical mechanical theories use the assumption that the total energy of a system of molecules in a given configuration can be expressed as a sum of pair interactions, that is,

$$U(\vec{r}_1, \vec{r}_2, \cdots, \vec{r}_N) = \sum_{\substack{i,j=1 \\ i<j}}^{N} u_{ij}(\vec{r}_i, \vec{r}_j) \quad , \tag{1.1}$$

where the $\vec{r}$'s are the vector positions of the N molecules, U is the total configurational energy, and u_{ij} is the interaction energy of the i-j pair. For a dilute system this description is appropriate. As the system is compressed, however, it must eventually fail, until finally the appropriate type of theory, such as metallic band theory or the Fermi-Thomas model, makes no reference to pair potentials. The failure of this assumption may be one of the more important sources of error, since its magnitude in repulsive regions is so difficult to estimate. However, a first order

quantum-mechanical calculation by Rosen [10] (See also Refs. 11 and 12.) gives encouragingly small results. He finds for helium

$$\frac{E_{abc}}{E_{ab} + E_{bc} + E_{ac}} = 1.15\ e^{-r} \text{ for the configuration } \bullet \leftarrow r \rightarrow \bullet,$$

$$= 9.8\ e^{-(8/3)r} \text{ for the configuration } \bullet \leftarrow r \rightarrow \bullet \qquad \bullet,$$

where E_{abc} is the energy of the three-body configuration shown, the denominator is the sum of the three-pair interactions, and r is in units of Bohr radii (0.529 A). The diameter of the potential well for helium is $r^* = 2.95$ A (Ref. 6, p. 1111). To obtain results for conditions comparable to those in detonations, we take the reduced distance $r/r^* = 0.7$, and thus use $r = 0.7r^*$ or 2.1 A. At this distance we find

$$\frac{E_{abc}}{E_{ab} + E_{bc} + E_{ac}} \cong -0.02 \text{ for the triangular configuration,}$$

$$\cong +0.0002 \text{ for the linear configuration.}$$

Another way of reassuring oneself about this problem is to compare results from a pair-potential model with those from a theory appropriate to higher densities, such as the Fermi-Thomas model. To facilitate this comparison we have calculated the pair potential which would give to a system of like molecules on a face-centered cubic lattice the same energies at all compressions as those calculated from the Fermi-Thomas model for a temperature of 0 °K.[13] This fictitious potential for argon is compared with some potentials estimated from experimental data in Fig. 1.1. Molecules with the pair potential labeled FTD placed on the sites of a face-centered cubic lattice reproduce the Fermi-Thomas-Dirac results for argon

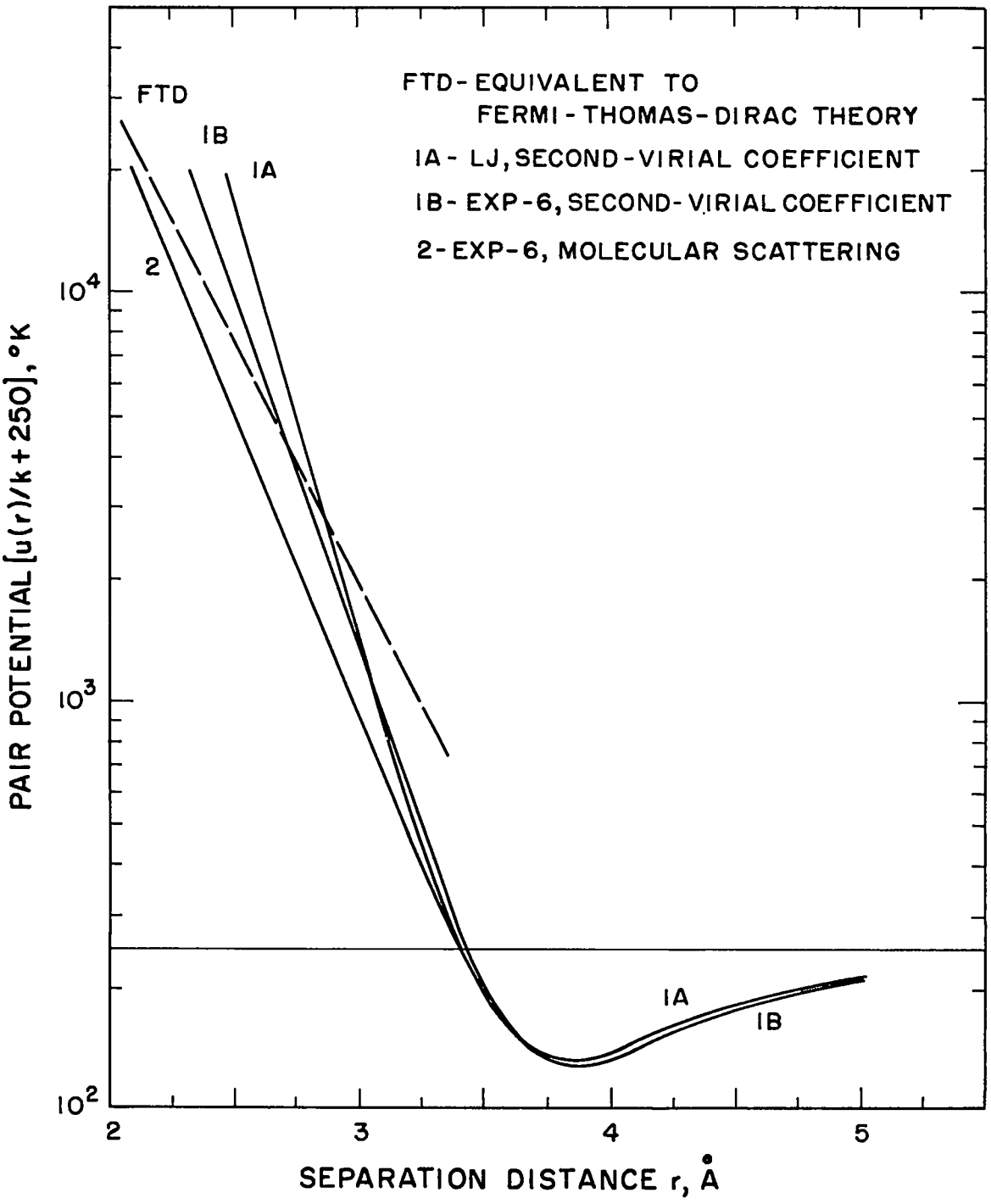

Fig. 1.1 Comparison of experimental pair potentials for argon with that equivalent to the Fermi-Thomas-Dirac theory.

at 0 °K. The other potentials are obtained from experimental results quoted in reference 14. The fictitious potential is seen to come fairly close to the experimental potential obtained from molecular scattering data at its lower limit of validity. This result is encouraging, but perhaps fortuitous.

1.4 The Metallic Transition

We have stated above our assumption that the molecular model is the appropriate one, but that at some high pressure it becomes inappropriate. This comes about in the following way (Ref. 15, Chap. 10). At low densities, the energy levels of a regular array of atoms or molecules correspond to those of the isolated molecules but are highly degenerate because of the large number of particles. As the material is compressed, these degenerate levels split up due to the perturbations of near neighbors, but are so large in number that "bands" of energy levels are formed. As the compression is continued, these bands eventually overlap. If the substance is initially nonconducting (lowest band filled with electrons) then it takes on metallic character when the ground state band overlaps (or is separated by an energy of about kT from) the first excited band.

Some attempts have been made to calculate the point at which this metallic transition occurs in simple substances. For H_2,[16] it was concluded that the metallic transition may never occur, but if it does the transition pressure is greater than 250 kb. For helium, which has a very high ionization energy, the transition pressure has been estimated to be 100 to 200 mb.[17] Both of these calculations are for a temperature of

0 °K. The point at which this type of transition might occur in systems of interest to us is uncertain. The high temperature probably tends to lower the transition pressure by increasing the kinetic energy of the electrons, but the perturbation of the regular lattice structure through molecular motion probably has the opposite effect. In a similar fashion, the variety of molecular species probably increases the transition pressure. Hirschfelder (Ref. 6, p. 264) states that the metallic state is probably reached at pressures of about 1 mb.

Chapter 2

THEORY

Since we limit our consideration to CHON explosives, it should be sufficient to consider a system of detonation products consisting of two phases: one, solid carbon in some form, and the other, a fluid mixture of the remaining product species. Thus we require an equation of state for a pure solid, an equation of state for a fluid mixture (which we hereafter call the gas equation of state), and a method of calculating the equilibrium composition of such a two-phase system. These define the overall equation of state of the mixture; the hydrodynamic conservation equations must then be solved with this equation of state.

This chapter is devoted to a qualitative discussion of the required theory. The corresponding equations are collected in Appendix A, and a description of the machine code is given in Appendix B.

2.1 Ideal Thermodynamic Functions

For fluids it is convenient to separate the equation of state calculation into ideal and imperfection parts corresponding to the factoring of the partition function into internal and configurational terms. The solid

equation of state is formally separated in the same way into an ideal part at the temperature of interest and one atmosphere pressure and an imperfection part depending on both temperature and pressure. The ideal parts, usually referred to as ideal thermodynamic functions, have been tabulated by the National Bureau of Standards and others for all of the species of interest to us. For use in the calculation, the results are represented by analytic fits constructed to give a thermodynamically consistent set of functions.

2.2 Solid Equation of State

From the phase diagram of carbon,[18] Fig. 2.1, we see that our region of interest probably contains the diamond-graphite transition curve. For simplicity, and because this transition is rather slow, we assume that the carbon is always present as graphite.

The particle size of the precipitated carbon may be limited by several effects such as nucleation, rate of reaction, and diffusion. To obtain an estimate of the maximum particle size, we calculate an approximate upper size limit for a diffusion-controlled precipitation. The simple theory for diffusion-limited crystal growth[19] gives

$$r = \alpha(dt)^{1/2} \quad ,$$

where r is the particle radius at time t, d is the diffusion coefficient, and α is a dimensionless function of concentration ranging from 0.1 to 10. The principal uncertainty in applying this equation is the value of the diffusion coefficient under detonation conditions. In the absence of

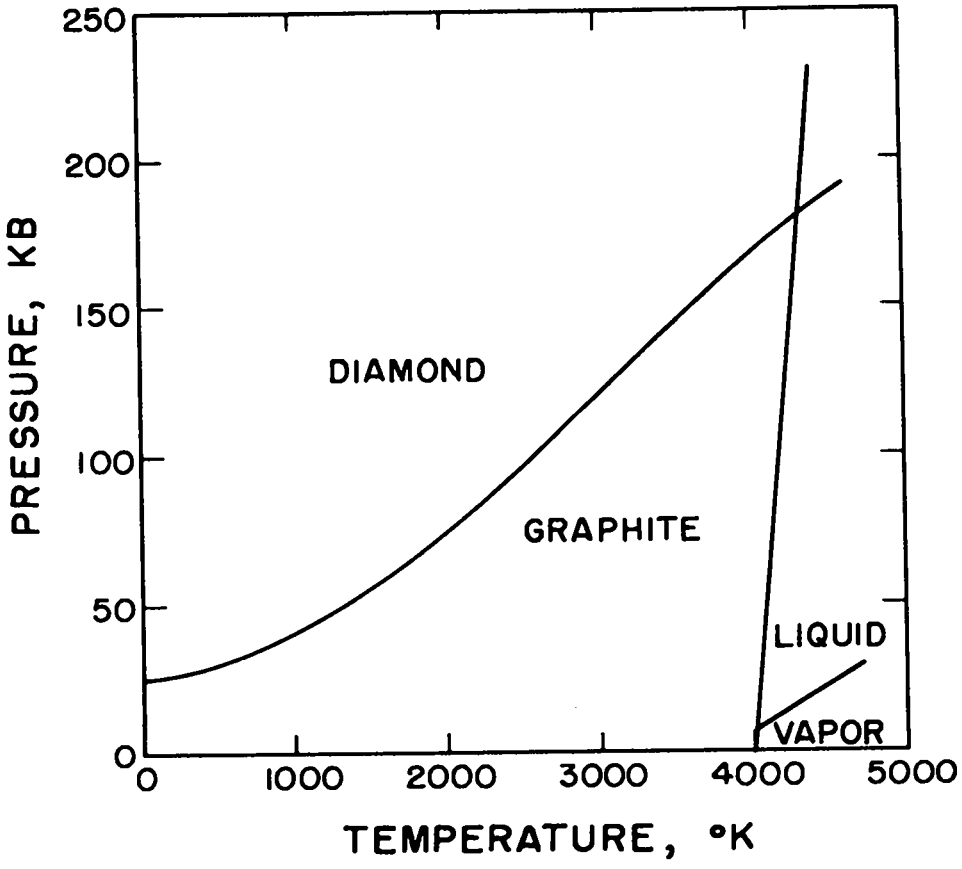

Fig. 2.1. Phase diagram of carbon.

experimental information and reliable theory, we assume that it lies in the range of values measured for liquids under normal conditions: about 10^{-5} cm^2/sec. This choice appears to be at least consistent with the trends of experimental measurements of self-diffusion in CO_2.[20] For a time of 1 μsec, it gives a particle radius of about 300 A.

Thus the carbon particles are not large, and it is possible that the other effects mentioned above could completely prevent their precipitation in the reaction zone even when they are present at equilibrium. In any case, we allow the carbon to be present as a separate phase, and represent the effects of small particle size by allowing small increases in its heat of formation as an additional parameter.

The graphite equation of state is constructed from the experimental Hugoniot curve by a method similar to that described by Rice et al. (Ref. 21, p. 1) It is assumed that:

(1) The energy is known along some reference curve in the p-v plane.

(2) At a given volume, the energy is a linear function of pressure.

(3) The Gruneisen number,

$$G = \left[\frac{1}{v} \left(\frac{\partial E}{\partial p} \right)_v \right]^{-1} \qquad (2.1)$$

is constant.

Thus the equation of state takes the form

$$E = E_r(v) + (G/v)[p - p_r(v)] \quad . \qquad (2.2)$$

The reference curve (subscript r) is taken to be

the experimental Hugoniot[22] for $v/v_o < 1$,

the curve $p = 0$ for $v/v_o > 1$.

The energies on the Hugoniot are known from the experimental pressures and volumes and the Hugoniot equation; the energies and volumes on $p = 0$ are obtained by assuming constant values of the heat capacity C_v and thermal expansion coefficient α:

$$E - E_o = C_v T \quad ,$$

$$\frac{v - v_o}{v_o} = \alpha T \quad . \tag{2.3}$$

The value of G is obtained from the thermodynamic relation

$$G = \frac{v}{Cv}\frac{\alpha}{\kappa} \qquad \kappa = \frac{1}{v}\left(\frac{\partial v}{\partial p}\right)_T$$

applied at normal volume.

For our calculations, the thermodynamic variables p, v, and T are more convenient than p, v, and E. The details of this transformation are given in Appendix A. It results in a more complicated set of equations, and an iteration is required to determine v, given p and T. The constants used are

$C_v/R = 2.5$ (Ref. 23)

$\alpha = 8.03 \times 10^{-6}(°K)^{-1}$ (mean value for all directions)[24]

$v_o = 0.444$ cc/g (Ref. 25, pp. 2-18)

$T_o = 298\ °K$

$G = 0.1656$.

This value of C_v is an approximate mean for the range 300-2000 °K. Similarly, the value of G corresponds to an approximate mean value of κ(Ref. 26) over the range of the experimental data. The equation of state is rather insensitive to the choice of α and κ.

This equation of state gives results which are similar to those obtained with a different form used in earlier work.[27] This is not surprising, since both are fitted to the experimental Hugoniot, and all of the displacements from it are quite small.

2.3 Gas Equation of State

In classical statistical mechanics the imperfection part of the equation of state is derived from the partition function or phase integral

$$Q = \int^{V} \cdots \int^{V} \exp\left[- U(\vec{r}_1, \cdots, \vec{r}_N)/kT \right] d\vec{r}_1 \cdots d\vec{r}_N \qquad (2.4)$$

in which the vectors $\vec{r}$ denote the molecular positions, U is the total energy of any configuration, and the integration is over the volume v of the system. As pointed out in Chapter 1, it is usually assumed that U is expressible as a sum of pair interactions

$$U(\vec{r}_1, \vec{r}_2, \cdots, \vec{r}_N) = \sum_{\substack{i,j=1 \\ i<j}}^{N} u_{ij}(\vec{r}_i, \vec{r}_j) \quad , \qquad (2.5)$$

where u_{ij}, hereafter called the pair potential, is the interaction energy of the i-j pair of molecules. The problem thus separates into two parts: determination of the pair potentials u_{ij}, and calculation of the phase integral given these functions.

The pair potentials must be determined indirectly from various kinds of experimental data, for quantum-mechanical calculation of them is practical for only the simplest molecules. (Several recent theoretical calculations for helium agree with each other to within 20-30%, and with experiment (molecular scattering data) to within 30-50%.[28]) For pure fluids, at least, the problem of evaluating the phase integral is in much better shape. The cell or free volume theory of Lennard-Jones and Devonshire and its various modifications and improvements provide a fairly good approximation above the critical density.

The problem becomes much more complicated for a mixture. With c different kinds of molecules there are $c(c + 1)/2$ different pair potentials, and there is very little experimental information on the interactions between unlike molecules. The problem of evaluating the phase integral becomes more complicated, and it is doubtful whether any simple theory such as the cell model can give satisfactory results. Most of the tractable theories of mixtures are obtained by perturbing the pure fluid equation of state; if these methods are used, it is still of considerable interest.

Pair Potentials

At the high pressures and densities produced by detonations in condensed explosives, the attractive parts of the pair potentials are relatively unimportant; the equation of state depends largely on their shapes in the repulsive region which is, unfortunately, poorly determined

by the usual methods. These consist of measuring, in dilute systems, bulk properties which can be calculated exactly from the pair potential. The determination is made by calculating the measured property with a variety of assumed potentials until one is found which reproduces the experimental data. The experiments are usually done at low temperatures, where the small fraction of energetic collisions makes the results insensitive to the shape of the repulsive part of the potential. In the last few years, however, a number of potential curves have been determined from the scattering of molecular beams. This method gives results in the repulsive range of interest to us but can be used only when one member of the interacting pair is in monatomic form. With the help of quantum-mechanical ideas, however, appropriate collections of such results can be used to estimate potentials for diatomic or polyatomic species. Another source of information is data on shock Hugoniots orginating in condensed materials. Subject to the uncertainty in the equation of state used, the Hugoniot can be calculated from an assumed pair potential and the results compared with experiment. We have done this where the necessary data were available.

The three most commonly used analytic representations of the pair potential are:

Lennard-Jones (L-J)

$$u(r) = k\Gamma^*\left[\frac{6}{n-6}\left(\frac{r}{r^*}\right)^{-n} - \frac{n}{n-6}\left(\frac{r}{r^*}\right)^{-6}\right] \tag{2.6a}$$

Mason-Rice (MR)

$$u(r) = k\Gamma^*\left[\frac{6}{\alpha-6}\, e^{\alpha\left(1-\frac{r}{r^*}\right)} - \frac{\alpha}{\alpha-6}\left(\frac{r}{r^*}\right)^{-6}\right] \tag{2.6b}$$

Modified Morse (MM)

$$u(r) = kT^*\left[\frac{6}{\alpha - 6} e^{\alpha\left(1 - \frac{r}{r^*}\right)} - \frac{\alpha}{\alpha - 6} e^{6\left(1 - \frac{r}{r^*}\right)}\right] \quad , \tag{2.6c}$$

where r is the separation distance, kT^* is the well depth (value of minimum energy) at separation r^*, k is Boltzmann's constant, and α and n are adjustable parameters which may range from 9 to 15. Since the exponential form of repulsion is probably more realistic, the latter two forms are preferred. The second is most commonly used but causes trouble at high densities because of its spurious descent to minus infinity at zero separation. The third removes this defect at the cost of a slight distortion of the correct form at large separations.

The mixture equations of state that we use require that the potentials be expressible as

$$u(r) = kT^* f(r/r^*) \quad , \tag{2.7}$$

with the same functional form $f(r/r^*)$ for all interactions. To satisfy this requirement, we assume that one of the above analytic forms (with the same value of n or α throughout) applies to all pairs of like molecules and that, for each such pair, values of r^* and T^* are given. Then we use for the unlike pairs a common analytic form (with the same n or α), and determine the values of r^* and T^* from the empirical combining rules

$$r^*_{ij} = \tfrac{1}{2}(r^*_i \pm r^*_j) \qquad T^*_{ij} = (T^*_i T^*_j)^{\frac{1}{2}} \quad . \tag{2.8}$$

These appear to hold within 2 or 3% for spherical and slightly nonspherical molecules like argon and nitrogen, but for mixtures like CO_2 that contain

more nonspherical molecules, deviations of 10 to 15% have been found (Ref. 6, pp. 169, 222; Ref. 29, p. 52; Ref. 30).

In a separate report[31] we have described the pertinent experimental information on the product species we plan to use, the calculation of the shock Hugoniots where experimental data are available, and the resulting choice of a potential for each species. The results are summarized in Table 2.1 and Fig. 2.2. A brief description of the extent of knowledge about each species follows.

Table 2.1. Potential Constants Chosen (exp-six form)[a]

Species	α	r*(A)	T*(°K)
A	12	3.83	119
N_2	15	4.05	120
CO	15	4.05	120
H_2O	14	3.35	138
NO	15[b]	3.97	105
H_2	14	3.34	37
CO_2	15[b]	4.20	200
O_2	15	3.73	132
CH_4	14	4.29	154

[a]The MM form was used for H_2O and O_2.

[b]These values of α were guessed.

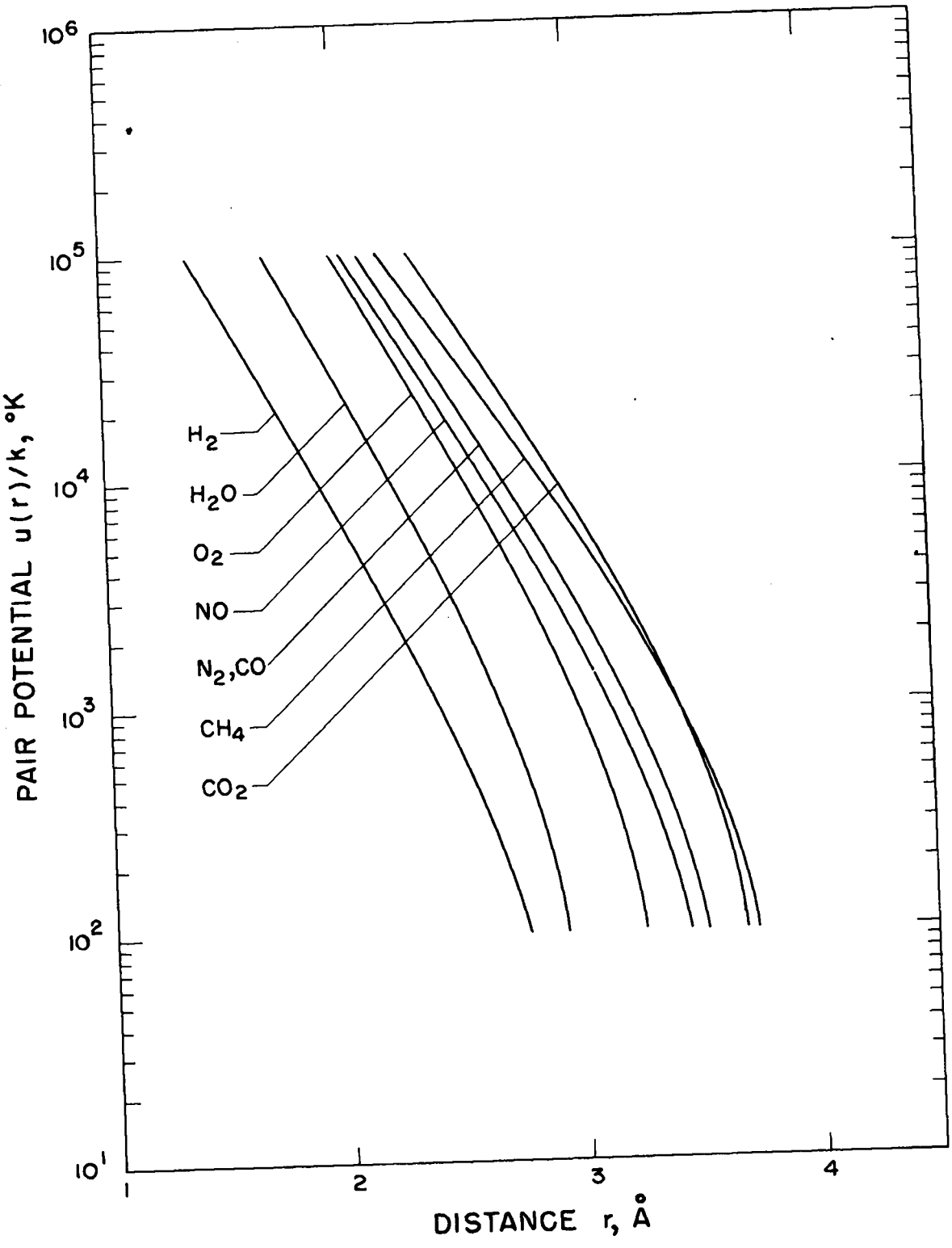

Fig. 2.2. The pair potentials chosen for each species.

Nitrogen, Carbon Monoxide, Hydrogen, and Methane. For all of these except carbon monoxide, both bulk measurements and molecular scattering data are available, and pair potentials consistent with both sets of data have been proposed. Only bulk measurements are available for carbon monoxide, but they give results very close to those for nitrogen, with which it is isoelectronic, and the carbon monoxide potential is, therefore, taken to be identical to that of nitrogen.

Nitric Oxide. For this substance, only bulk measurements and the potential determined from them are available. Since there is an unpaired electron, it is possible that the form of the potential is different from those of the other species.

Water. Water has a strong dipole moment and is nonspherical in shape. A spherically symmetric potential function of the sort commonly used may be a poor approximation, and several angle-dependent forms have been proposed. To avoid excessive complication in the equation of state calculation, we tried a spherically symmetric form and made a number of calculations of the Hugoniot curve to compare with the extensive experimental data available. None of the potentials tried agreed well with experiment; the choice was made to minimize the disagreement.

Carbon Dioxide. This molecule, like water, is nonspherical, and the bulk measurements using different properties give different potentials, depending on the property chosen and on the temperature range over which it is measured. There are no molecular scattering results. Our choice represents a compromise among the available data.

2.4 Pure-Fluid Equation of State

In the fixed-product-composition detonation calculations mentioned in the introduction, several different gas equations of state were used. All of them gave results which were fairly close together, particularly at high initial densities. This suggests that the pure-component equation of state (given the pair potential) is not one of the major uncertainties of the problem. We feel that the best equation of state consistent with the available computing time is the free-volume theory of Lennard-Jones and Devonshire, and its modifications (Ref. 6, Chap. 4).

In its simplest form, this model (hereafter called the LJD theory) imagines the available space to be divided into cells whose centers form a regular lattice spanning the available volume. Each cell contains a single molecule; all but one are assumed fixed at their cell centers, and this one is allowed to move in the force field of its neighbors which are "smeared out" onto a sphere of radius equal to the nearest-neighbor distance.

A number of improvements and modifications of this theory have been made. Kirkwood[32] provided a consistent statistical-mechanical derivation of the cell model which does not fix the neighbors while one molecule moves, but provides for the calculation of the probability of all positions within the cell, under the assumption that this probability is the same in all cells. His result takes the form of an integral equation for the cell probability and contains the earlier theory as a zeroth order approximation to the solution. Both Kirkwood's theory and the original one assume that

each cell contains exactly one molecule. A number of later investigations have elaborated the theory to include the presence of "holes" (empty cells) and multiply-occupied cells. In the region of interest to us, these complications have very little effect because of the high pressures and densities.*

To date, no one has presented an exact solution of Kirkwood's integral equation for a nonsingular pair potential. Wood[33] has solved it exactly for the case of hard spheres, with a result which is exactly that given by the simple LJD theory. An earlier numerical calculation by Hirschfelder[34] for hard spheres which removed the approximation of spherical smoothing but otherwise retained the inconsistent LJD approach (i.e., did not solve Kirkwood's integral equation, but did hold the neighbors at their lattice positions) gave a different answer. Thus for hard spheres, the effects of these two approximations--spherical smoothing, and the approximation of the integral equation solution by the LJD model of fixed neighbors exactly cancel each other to give the correct result.

The so-called "improved free-volume" theory for which, with the Lennard-Jones pair potential, extensive numerical results have recently been published by Dahler and Hirschfelder,[35] may not be an improvement at all, since, although the integral equation is solved, the approximation of spherical smoothing is still made. Thus it is not surprising to find that their theory agrees less well with Monte Carlo calculations made with the same pair potential than does the original LJD theory.

---

* This is not true, of course, at sufficiently low pressures on the isentrope through the CJ state.

Therefore, we use the original LJD cell theory. Some more recent developments in this field are not without interest, but we have retained the LJD theory, partly on the grounds of vested interest in machine codes already prepared. Moreover, it gives reasonably good agreement with the Monte Carlo results at high densities, and in the calculation of Hugoniot curves the errors in E and P appear to cancel each other to some extent.[14]

Mixtures

The Problem. Getting a tractable statistical-mechanical theory for the equation of state of a mixture is a formidable problem, particularly with molecules of appreciably different sizes. An extended discussion of this problem, with applications of most of the current theories to mixtures of hard spheres, is given in a separate report.[36] The results described there are qualitatively similar to those given in the next chapter for systems of more realistic molecules at high pressure, for under these conditions the size differences are the controlling factors.

Some of the difficulties are brought out by comparison with the simpler but still difficult problem of determining the equation of state of a pure fluid at high density. In a highly compressed pure fluid, the average positions of the molecules are close to the sites of a regular lattice, and the LJD cell theory, which allows only small displacements from the lattice sites, gives a fairly good approximation to the true equation of state.

In a mixture the problem is far from solved even if the molecules are assumed to lie on regular lattice sites, for the most probable

arrangement of the molecules on the sites must still be determined. Although this order-disorder problem has inspired a number of very complex theories,[37] it has not been solved in closed form for any three-dimensional lattice. The approximate methods which have been developed are of doubtful validity when the interaction energies are large compared to kT.

In a mixture, the lattice approximation itself is, of course, very poor, for the differences in molecular size produce an average configuration with a very irregular structure. The extremely complicated problem of determining this structure is well illustrated by Bernal's studies of the geometrical structure of pure liquids of normal density.[38] This problem bears some resemblance to that of the mixture, since a normal-density liquid has a rather open structure which can be roughly described as a mixture of molecules and holes.

The theory of mixtures is in a rather unsatisfactory state. Although much work has been done, much more remains. The present theories do not agree even on the sign of the corrections to ideal mixing. In view of their character, this is hardly a surprise. They simply do not go deeply enough into the details of the very complex problem.

Several different ways of attacking the problem are discussed in reference 36. Here we consider only two: the perturbation method and the pseudopotential method.

Perturbation Theories. The theories which use this approach can be divided into two classes: conformal solution theory, and what we choose to call n-fluid theory. It has only recently become clear that these

both stem from a common approach, viz., perturbation from a pure fluid whose properties are assumed known.[39] They differ mainly in the choice of expansion variable. The conformal solution method (Ref. 29, Chap. 9, 10; Ref. 40; 41) begins with the assumption that all of the intermolecular interaction potentials have the same functional form,

$$u_{ij}(r) = kT^*_{ij} f(r/r^*_{ij}) \tag{2.9}$$

where T^*_{ij} and r^*_{ij} may have different values for each component pair. Thus each pure component obeys the same reduced equation of state

$$F'_r = F'_r\left(\frac{T}{T^*_r}, \frac{pV^*_r}{RT}\right) , \qquad V^* = (N/\sqrt{2})r^{*3} \quad . \tag{2.10}$$

To obtain the equation of state of the mixture, some reference fluid obeying this common reduced equation of state is chosen, and the mixture partition function is expanded about that of the reference fluid in powers of $(r^*_{ij} - r^*_r)$ and $(T^*_{ij} - T^*_r)$, where the subscript r denotes the reference fluid. This expansion can be carried out exactly; for F', the imperfection Gibbs free energy of the mixture, it takes the form

$$F'(T,p,\vec{x}) = F'_r\left(\frac{T}{T^*_r}, \frac{pV^*_r}{RT}\right) + 3(pV_r - RT)\sum_{i,j=1}^{c} x_i x_j\left(\frac{r^*_{ij}}{r^*_r} - 1\right)$$

$$+ E'_r \sum_{i,j=1}^{c} x_i x_j\left(\frac{T^*_{ij}}{T^*_r} - 1\right) + \cdots, \tag{2.11}$$

where x_i is the mole fraction of component i, and c is the number of components. The coefficients of the first-order terms have the convenient property of being expressed entirely in terms of the macroscopic properties

of the reference fluid (and the composition). Unfortunately, the coefficients of the higher-order terms cannot be so simply expressed; they contain statistical-mechanical integrals of the molecular distribution functions of the reference fluid, and thus depend on its microscopic properties.

In the original formulation by Longuet-Higgins,[40] one of the pure components was chosen as the reference fluid. We refer to this form of the conformal solution theory as the LH theory. Nosanow's recent work[39] suggests that the reference fluid be chosen so that the first-order terms of Eq. 2.11 vanish. Thus, if we choose as the reference fluid a composition-dependent fictitious substance obeying the common reduced equations of state with potential constants

$$r_r^* = \sum_{i,j=1}^{c} x_i x_j r_{ij}^* \quad , \qquad T_r^* = \sum_{i,j=1}^{c} x_i x_j T_{ij}^* \quad , \tag{2.12}$$

the extensive properties of the mixture become, in first order, just those of the reference fluid. We call this form of the conformal solution theory the corresponding states, or "CS" theory. Unfortunately, this approximation criterion does not yield a unique reference fluid, since any functions of r_{ij}^* may be used as the expansion variables. For example, if the expansion is made in powers $(r_{ij}^*)^n$ and $(T_{ij}^*)^n$, with n an adjustable parameter, we have:

$$(r_r^*)^n = \sum_{i,j=1}^{c} x_i x_j (r_{ij}^*)^n \quad , \qquad (T_r^*)^n = \sum_{i,j=1}^{c} x_i x_j (T_{ij}^*)^n \quad . \tag{2.13}$$

Theories of the second class, which we call n-fluid theories, have received wide attention. Recently Nosanow[39] has provided a unified statistical-mechanical derivation of them. The method is quite similar to that of the conformal solution theory. As before, it is assumed that the properties of any pure fluid with given pair potential are known, i.e., that the function $F_r'[T,p,u(r)]$ is given. The principal differences are in the choice of the expansion variable and of the reference fluid.

The expansion is made in the differences between the individual pair-potential functions and the potential function of the reference fluid

$$u_{ij}(r) - u_r(r) \quad , \tag{2.14}$$

and these functional differences are treated as the variables of the Taylor series. It is thus no longer necessary that the potential functions have the same functional form, but only that their differences be, in some sense, sufficiently small. Of course, for molecules of different sizes these differences become large at sufficiently small separations, and there the expansion may become invalid. The hope is that such configurations are sufficiently improbable that the final result is correct, but this has not been proved. As in the conformal solution theory, the expansion is exact, but only the first-order coefficients can be expressed entirely in terms of the macroscopic properties of the reference fluid.

The form of the expansion is then generalized to a linear combination of expansions about a set of reference fluids whose maximum number is equal to the number of different pairs of components. The coefficients of this linear combination and the potentials of the reference fluids

are then chosen so that the first-order terms of the overall expansion vanish.

There are three ways of doing this; each yields a system which serves as a model of the mixture, correct to first order in the expansion variable.

(1) A single substance with potential function

$$u(r) = \sum_{i,j=1}^{c} x_i x_j u_{ij}(r) \quad . \tag{2.15}$$

The imperfection free energy of the mixture is just that of this substance.

(2) A set of c substances with potential functions

$$u_\alpha(r) = \sum_{j=1}^{c} x_j u_{\alpha j}(r) \ , \qquad (\alpha = 1, \cdots, c) \quad . \tag{2.16a}$$

The imperfection free energy of the mixture is given by

$$F'(T,p,\vec{x}) = \sum_{\alpha=1}^{c} x_\alpha F_r'[T,p,u_\alpha(r)] \quad . \tag{2.16b}$$

(3) A set of $c(c+1)/2$ substances with potential functions

$$u_{\alpha\beta}(r) = u_{ij}(r) \ , \qquad (\alpha, \beta = 1, \cdots c) \quad . \tag{2.17a}$$

The imperfection free energy of the mixture is given by

$$F'(T,p\vec{x}) = \sum_{\alpha,\beta=1}^{c} x_\alpha x_\beta F_r'\left[T,p,u_{\alpha\beta}(r)\right] \quad . \tag{2.17b}$$

Pseudopotential Theories. These theories are obtained by an approach completely different from the perturbation methods. The partition function for a mixture is rearranged to the form

$$\int^{V}\cdots\int^{V}\left\langle e^{-\beta U(\vec{R})}\right\rangle_{Av} d\vec{R} = \int\cdots\int^{V} e^{-\beta\Phi(\vec{R},\vec{x},T)} d\vec{R} \quad ,$$

$$\Phi(\vec{R},\vec{x},T) = -\beta^{-1}\,\ell n\left\langle e^{-\beta\vec{U}(\vec{R})}\right\rangle_{Av} ,$$

$$\beta = 1/kT , \qquad \vec{R} \equiv (\vec{r}_1, \cdots, \vec{r}_N) \quad . \tag{2.18}$$

where $\vec{x}$ represents the chemical composition of the system. The brackets denote an a priori average, for each set of position vectors occurring in the integration, over all possible interchanges of the molecules among these positions, so that evaluation of this integrand at each set of position vectors occurring in the integration requires the solution of a complicated order-disorder problem. Thus the problem has been formally rearranged to represent a single fictitious substance with an extremely complicated composition- and temperature-dependent potential function Φ, called the pseudopotential. The fictitious substance corresponding to this potential is clearly not conformal with the components of the mixture, in the sense of Eq. 2.9.

The order-disorder problem required for the calculation of the pseudopotential has been solved approximately by three different methods.[42-44] In the moment method, the pseudopotential is expanded in powers of the $u_{ij}(r)/kT$. Its first term is equivalent to the one-fluid theory. The higher-order terms are quite complicated. The series is known to converge, but the convergence is slow in systems of interest to us, where u_{ij}/kT is large, and there is no guarantee that two or three terms will give a better result than one. The pair-correlation method gives a more interesting first-order result: a rather complicated expression for the effective

potential function, which contains both the composition and the temperature and gives the one-fluid result only in the high-temperature limit. Higher approximations can be obtained in principle by this method also, but the result does not take the form of a power series, and no expansion variable can be identified. In the pseudo-pair-potential method, the moment method series is rearranged into a sum of pair interaction terms plus a sum of triplet interaction terms, etc. The pair interaction terms are summed in closed form to give

$$\Phi = \sum_{i<j} \varphi(r_{ij}) , \qquad \varphi(r) = - kT \ln \sum_{\alpha=1}^{c} \sum_{\gamma=1}^{c} x_\alpha x_\gamma e^{-\beta u_{\alpha\gamma}(r)} . \qquad (2.19)$$

It can be shown that the first-order result of the moment method (one-fluid theory) is a rigorous upper bound to the Gibbs free energy, and that the pseudo-pair-potential result is a rigorous lower bound to the same quantity. However, these bounds are so widely separated as to be of mostly theoretical interest.

Discussion. The LH theory suffers from the arbitrary choice of reference fluid. Once this is chosen as one of the pure components, the theory gives wrong results for the special case of a mixture consisting of any other pure component.

The CS theory does not have this disadvantage, for in the above special case the fictitious pure fluid representing the mixture reduces to the pure component in question. However, both of these theories suffer from the arbitrariness in the choice of the expansion variables.

The one-fluid theory is poor in several ways. The predicted mixture free energy is known to be too high. In the framework of the cell theory, it implies that all cells must be of the same size. Thus, the large components are squeezed too hard, and their chemical potentials are almost certainly too high. The one-fluid theory has been derived in a number of ways, but since it so often turns up as a first approximation to some other theory, one suspects that it could be improved.

The two-fluid theory almost certainly represents an improvement. It has also been derived in several different ways, but these are generally more sophisticated and reasonable than those leading to the one-fluid theory. In the cell theory framework, it corresponds to taking a different size cell for each component, which seems more reasonable than the one-fluid limitation to cells of equal size. Both theories suffer from a practical disadvantage: they yield effective potential constants only for a power-law potential function such as the L-J form. That is, the sums in Eqs. 2.15 and 2.16a which become, with a common functional form for the potential,

$$\sum_{j=1}^{c} x_j T^*_{\alpha j} f\left(\frac{r}{r^*_{\alpha j}}\right) \quad , \qquad \sum_{i,j=1}^{c} x_i x_j T^*_{ij} f\left(\frac{r}{r^*_{ij}}\right) \quad , \tag{2.20}$$

can be expressed in the form

$$\overline{T}^* f(r/\overline{r}^*) \quad , \tag{2.21}$$

with

$$\overline{T}^* = \overline{T}^*(\vec{x}, \underline{\underline{T}}^*, \underline{\underline{r}}^*), \qquad \overline{r}^* = \overline{r}^*(\vec{x}, \underline{\underline{T}}^*, \underline{\underline{r}}^*) \quad ,$$

(where $\underset{\sim}{T}^*$ and $\underset{\sim}{r}^*$ denote the sets of all T^*_{ij} and r^*_{ij}) only for a power-law potential function.[45] Thus, for the exp-six and MM potentials, Eq. 2.6, for example, the effective pair potential of the mixture in the one-fluid model or the pair potentials of the reference fluids in the two-fluid model should be used in the form of Eq. 2.20, rather than in the simpler form of Eq. 2.21.

Of the pseudopotential theories, the only practical result of the moment method is the one-fluid theory, which is probably much too hard. The results given in reference 36 indicate that the pseudo-pair-potential results are much too soft, at least at high pressures. This leaves the pair correlation method, whose worth is difficult to assess. None of the pseudopotential results are simple enough for use in the complete detonation calculation, although some limited results for the pair-correlation theory are given in the next chapter.

2.5 Chemical Equilibrium

The method proposed by Brinkley[46,47] is used, with some refinements, to solve for the chemical composition.

2.6 Hydrodynamic Conservation Equations

These are standard, (Ref. 1, Chap. 3) with the exception of the Chapman-Jouguet condition. The correct form of this hypothesis is open to question, but the best guess on the basis of the present theory[48] is that the equilibrium CJ condition — tangency of the Rayleigh line

$$D^2 = v_o^2 \frac{p - p_o}{v_o - v} \tag{2.22}$$

(with D the detonation velocity) to the equilibrium detonation Hugoniot — should at least be approached asymptotically with time. Therefore, we have used this form of the CJ condition, which is equivalent to finding the point on the equilibrium detonation Hugoniot at which the calculated detonation velocity is a minimum.

Chapter 3

ILLUSTRATIVE NUMERICAL RESULTS

In this chapter we give numerical results illustrating some properties of various portions of the theory and show the relative importance of the different contributions to the equation of state.

3.1 Solid Equation of State

An isotherm calculated from the graphite equation of state is shown in Fig. 3.1, together with the experimental Hugoniot. The isentrope with the same temperature at $p = 0$ lies very close to the isotherm; the isentropic temperature rise is small due to the small value of the Gruneisen constant G.

This equation of state gives results similar to those obtained from a different form used in earlier work.[27]

3.2 Gas Equation of State for Pure Fluids

Calculated isotherms for argon at 300, 1000, and 3000 °K and an isentrope through the 3000° isotherm at 0.3 mb pressure are shown in

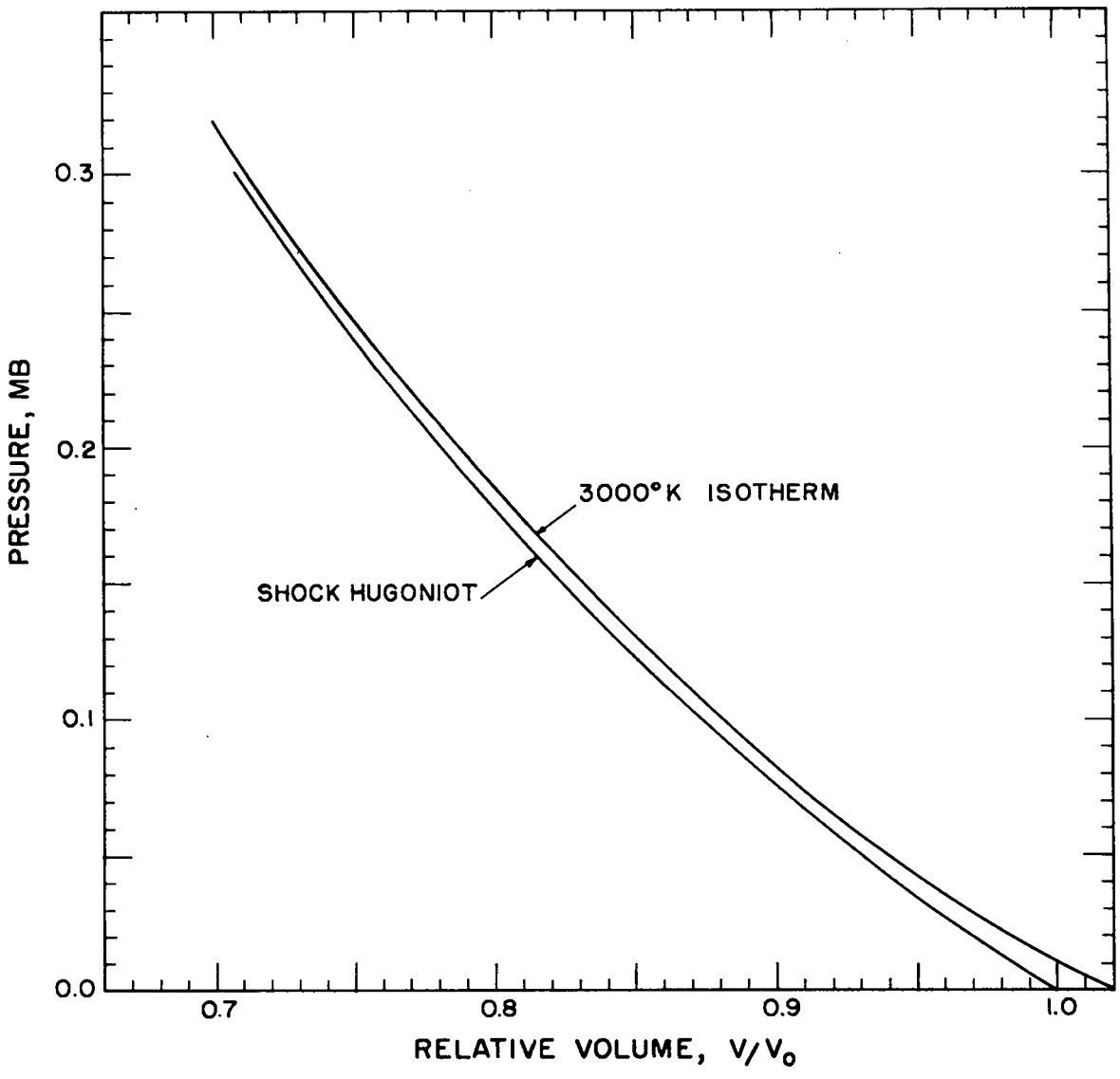

Fig. 3.1 Shock Hugoniot (experimental) and 3000 °K isotherm (calculated) for graphite.

Figure 3.2. The pair potential used in the exp-six form adjusted to fit molecular scattering data as described in Ref. 31. An experimental isentrope through the point T = 300 °K , p = 0.001 mb is also shown,[49] and is seen to be in fairly good agreement with the calculated one. In spite of the dips in the isotherms, the isentrope is quite smooth. This is probably somewhat fortuitous: the isentrope chosen enters the phase transition region shortly below its lower end in the figure. Isentropes of higher entropy probably look somewhat like the 3000° isotherm.

As discussed in Chapter 2, the equation of state is often thought of as divided into ideal and imperfection parts, the latter arising from the intermolecular forces. Under detonation conditions, the average intermolecular distances correspond to strong repulsion, and the intermolecular forces make the main contributions to the internal energy and pressure of the system. As an illustration, take the argon state point:

$p = 0.3$ mb.

$T = 3000$ °K.

$V = 10.2$ cc/mole

$E/RT = 4.57$ (relative to 0 °K.)

$pV/RT = 12.3$.

The energy and pressure are divided into ideal and imperfection parts as follows:

	ideal	imperfection
E/RT	33%	67%
pV/RT	8%	92%

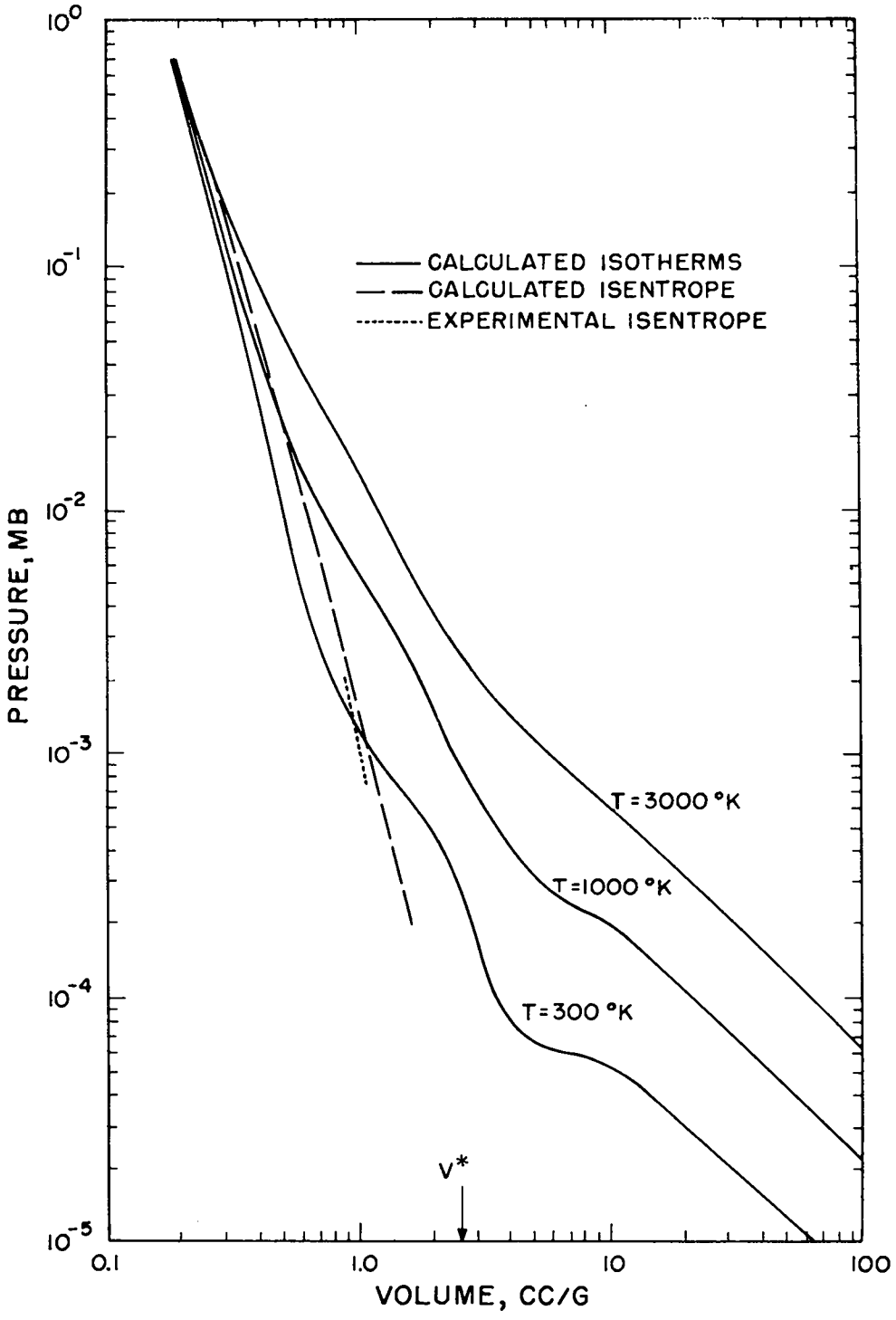

Fig. 3.2. Isotherms and isentropes for argon. Illustrating the characteristics of the gas equation of state for pure fluids.

The imperfection part is often thought of as further subdivided into "lattice" and "excess-over-lattice" parts. The lattice part corresponds to a (classical) face-centered cubic crystal at 0 °K, is thus independent of the statistical-mechanical equation of state, and depends only on the pair potential. When the imperfection parts of the energy and pressure are divided in this way, the results are

	lattice	excess over lattice
E'/RT	45%	55%
$pV/RT - 1$	74%	26% .

Also of interest is the question of what part of the potential curve makes the major contribution to the equation of state. To see this, we make use of the inverted form of the cell integrals given in the Appendix of reference 14. These express the imperfection energy and pressure in the form

$$E' \propto \int_0^\infty u(r)G(r)dr, \qquad pV - RT \propto \int_0^\infty ru'(r)G(r)dr,$$

where $u(r)$ is the pair potential and $G(r)$ is the weighting function or effective radial distribution function for the cell theory. Figure 3.3 shows the normalized weighting function and integrands of these integrals. The range of significant distances is sufficiently small, with half-width on the order of 0.5 A, that the attractive portion of the potential has almost no effect on the equation of state.

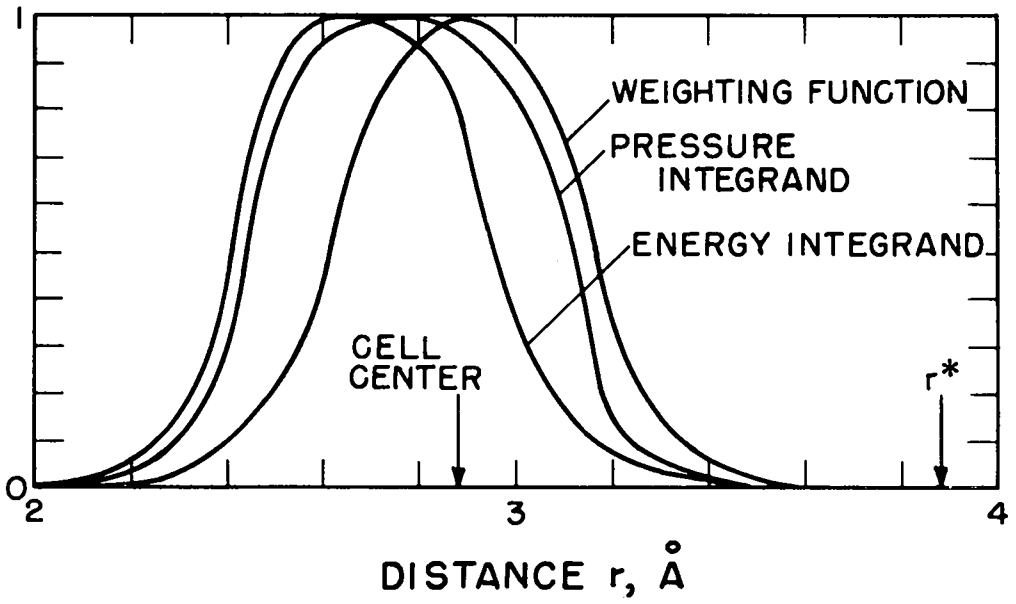

Fig. 3.3. Normalized weighting function and integrands for the LJD cell integrals transformed to integrals over the intermolecular separation r, evaluated for argon at p = 0.3 mb, T = 3000 °K. Not shown is the negative delta-function portion of the weighting function, which is located at its maximum and has an area equal to half that under the weighting function curve shown.

3.3 Gas Equation of State for Mixtures

Since presently available comparisons of the mixture theories are limited to low pressures, we give here a high-pressure comparison, and present some properties of the theories under detonation conditions. The LH, CS, one-fluid, and two-fluid theories are used. Limited consideration is also given to the Salsburg pair-correlation theory, which is too complicated for complete calculations, even in the simple binary system.

Thermodynamic Functions

The model used is a binary system at a pressure of 0.3 mb and a temperature of 2000 °K, whose components have pair potential constants in the ratios

$$\frac{r_2^*}{r_1^*} = \frac{5}{6} \quad , \qquad \frac{T_2^*}{T_1^*} = \frac{2}{3} \quad .$$

The L-J form of the pair potential is chosen because it is the only one for which simple average pair potentials are consistently defined in the statistical-mechanical sense by the mixture theories used. For the pair potential of component one, we take one of those chosen for least disagreement with experiment in reference 3:

$$n = 12, \qquad T^* = 100, \qquad r^* = 3.59 \quad .$$

Figure 3.4 shows the pair potentials for the pure components and the effective pair potentials for the equimolar binary system as given by the CS, one-fluid, pair-correlation, and pseudo-pair-potential theories.

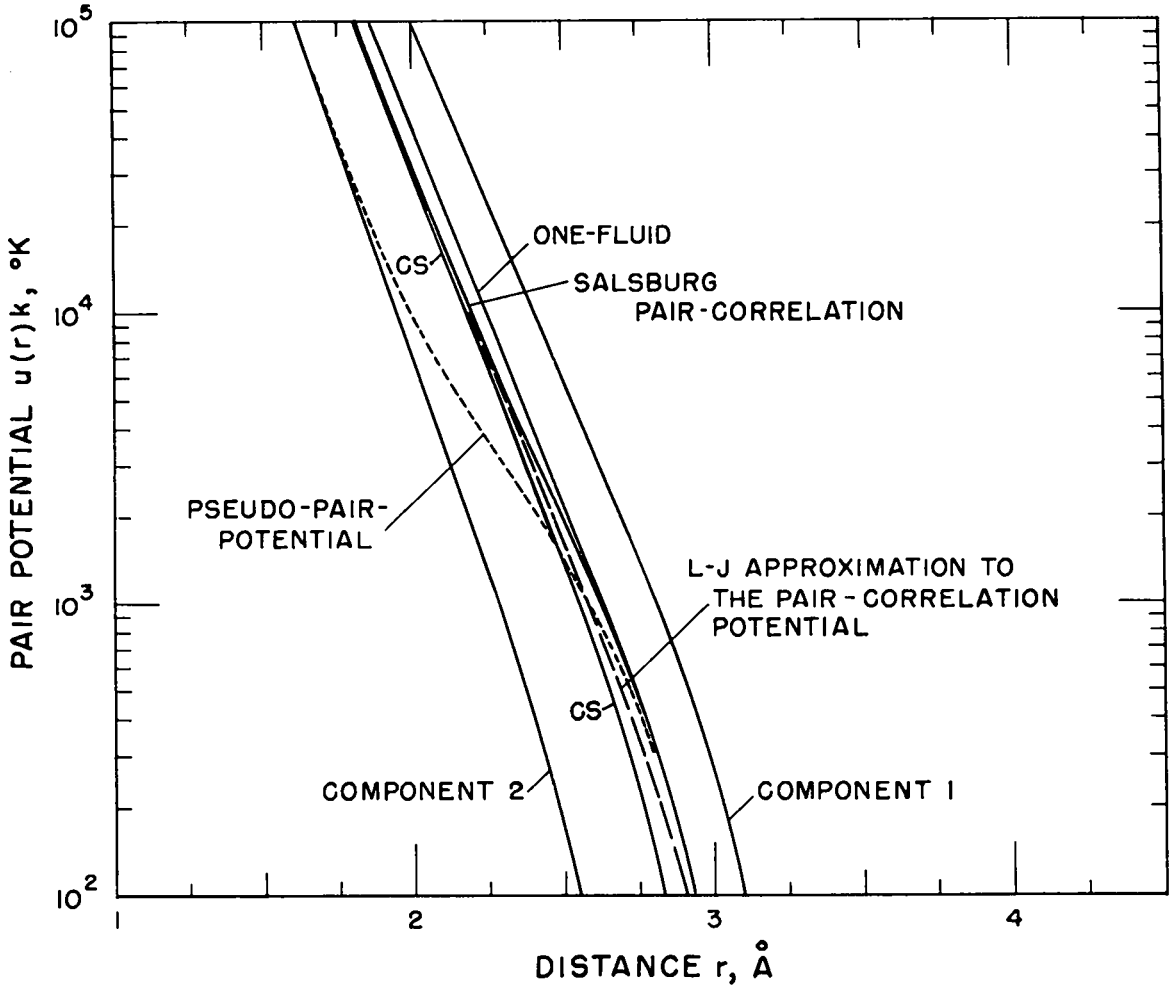

Fig. 3.4. The pair potentials of the pure components and the effective pair potentials given by the different mixture theories.

The thermodynamic functions* calculated for this system with the different mixture theories are shown in Figs. 3.5 and 3.6. Figure 3.7 shows the effective values of $\overline{T}^*$ and $\overline{r}^*$ given by the CS and one-fluid theories together with those for each of the reference fluids of the two-fluid theory. In order to do an approximate mixture calculation for the complicated pair-correlation potential, we have approximated it by the L-J potential shown with long dashes in Fig. 3.4. The thermodynamic functions for a substance with this potential are shown as points at $x_1 = \frac{1}{2}$ in Fig. 3.5.

From these results and more extensive calculations not reported here, we conclude:

(1) The different mixture theories give different signs for the excess thermodynamic functions.

---

* Some of the results of the calculations are expressed as excess thermodynamic functions, denoted by the superscript e. These are defined as the difference between the calculated value of the imperfection thermodynamic function for the mixture and the corresponding value for ideal mixing.

$$F^e(T,p,\vec{x}) = F'(T,p,\vec{x}) - \sum_{i=j}^{c} x_i F'_r\left(\frac{T}{T^*_i}, \frac{pV^*_i}{RT^*_i}\right) + x_i \ln x_i \text{ , etc.}$$

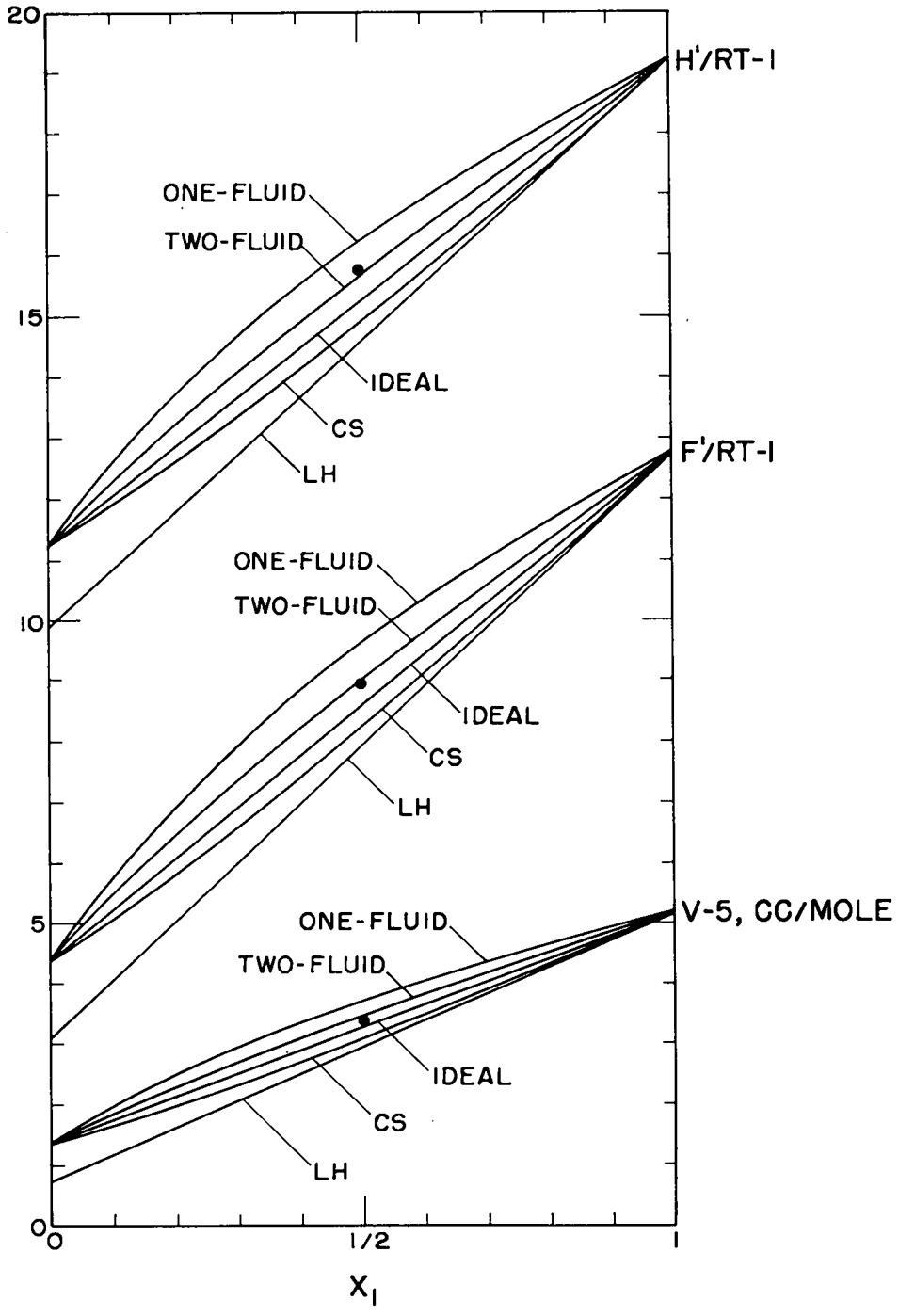

Fig. 3.5. Imperfection thermodynamic functions for the binary mixture. The dots at $x = \frac{1}{2}$ are for the pair-correlation potential approximated as described in the text.

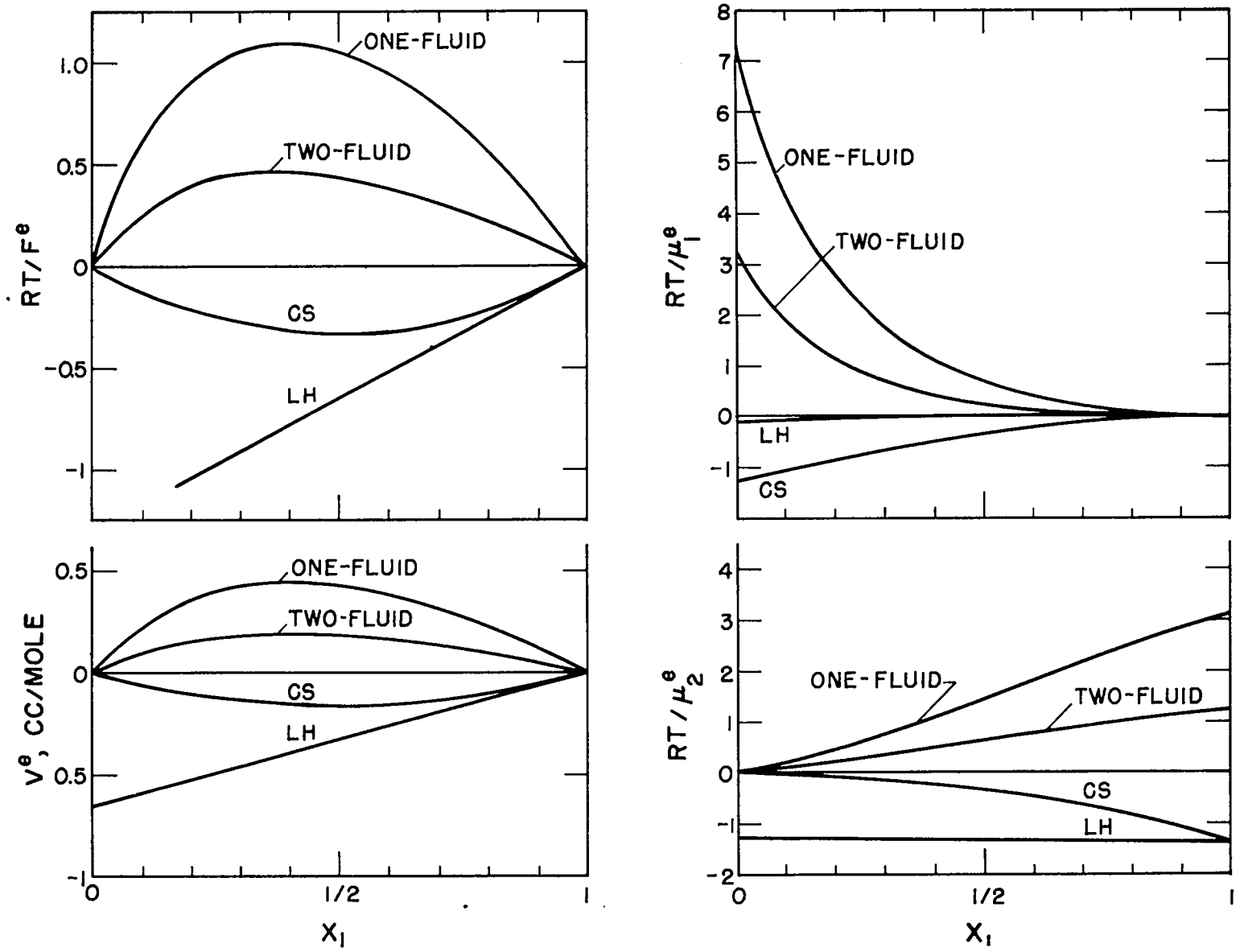

Fig. 3.6. Excess thermodynamic functions, including the chemical potentials, for the binary mixture.

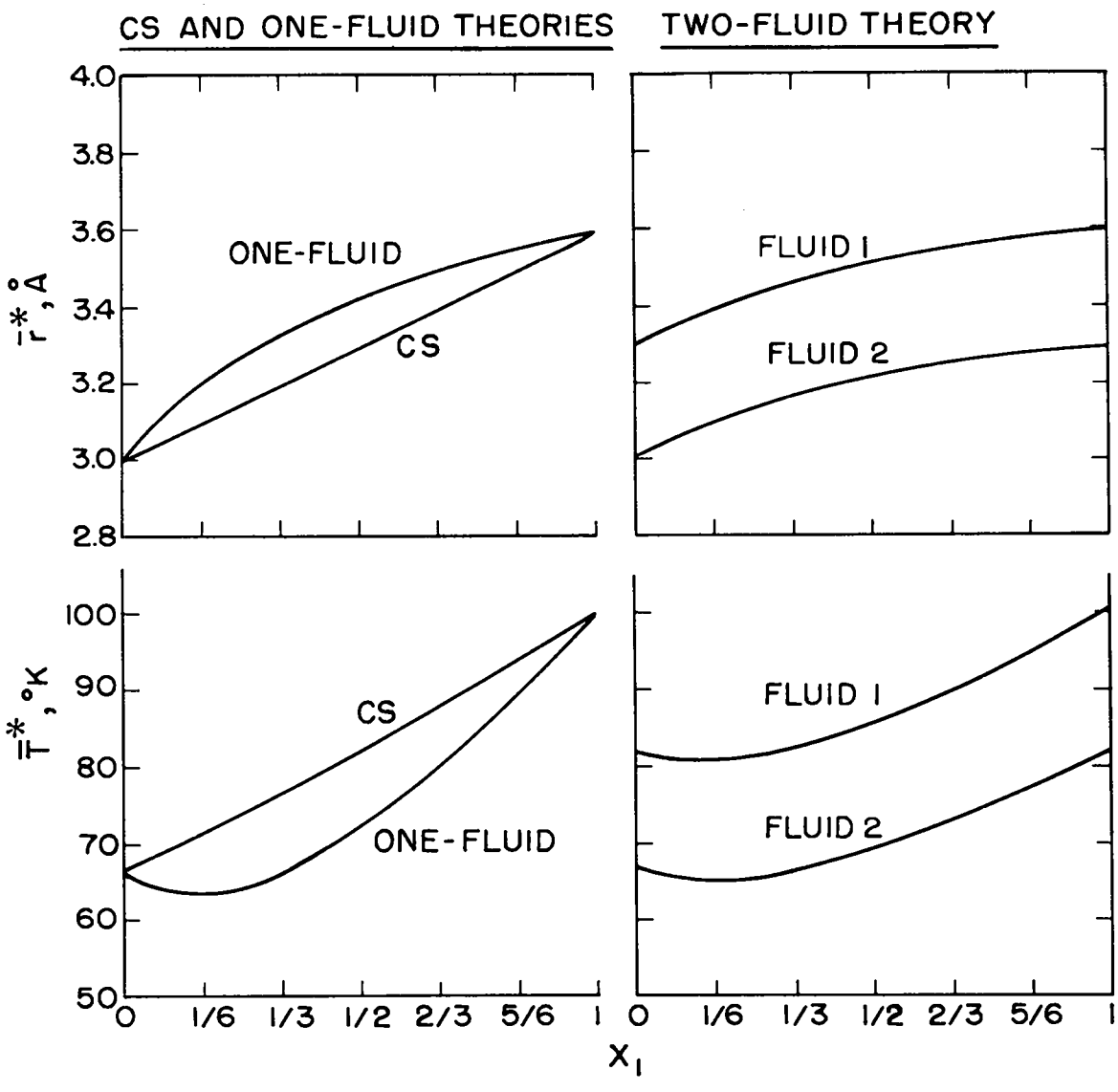

Fig. 3.7. Effective pair potential constants for the binary mixture.

(2) At $x_i = \frac{1}{2}$, the range of the results for the free energy and volume of the mixture is about 6-10% of their values for ideal mixing. The range of the calculated chemical potentials corresponds to changes of the equilibrium constants by factors of ten or more. The greatest range is found for compositions having small amounts of large molecules.

(3) The differences in potential constants chosen for this study are of the order of those in our system of product species. Under these conditions, the effect of differences in r^* is much larger than the effect of differences in T^*.

(4) One deficiency of the L-H theory — its failure for compositions far removed from the reference fluid — is shown.

(5) Although the CS and one-fluid theories are the two extremes when the r_i^* are appreciably different, they give the same results for the case of equal r_i^*.

(6) Calculations at points on an isentrope through p = 0.3 mb, T = 3000 °K show that over a wide range of temperature and pressure the excess thermodynamic functions, expressed as a percentage of the imperfection functions for ideal mixing, are of the same order of magnitude. The qualitative relationships are also unchanged: throughout, the one- and two-fluid theories give positive excess quantities, while the CS theory gives negative ones.

(7) Equilibrium calculations for mixtures of the species listed in Section 3.4 using the L-J, n = 12 potential and one-fluid theory give isotherms with mechanically unstable sections characterized by the rapid

shifting of the reaction

$$N_2 + CO_2 \rightarrow 2NO + C(S) \quad .$$

Under these conditions the system is presumably unstable with respect to separation into additional phases. What the composition of these might be was not determined. Since in this case both the mixture theory and the pair potential are unrealistically hard, the instability should probably be regarded as just an interesting curiosity (and, perhaps, as a warning). It was never encountered in any of the detonation calculations described in later chapters, for which more realistic pair potentials were used.

Continuous Variations of the Potential Constants

The LH, CS, and one-fluid theories are all obtained by expansion about a system in which the pair potentials of all components are the same, namely, a pure fluid. In each case, the expansion variables correspond to differences in the potential functions, and the first-order terms are given correctly. While none of these theories attempts to compute the second-order terms properly, nonlinearity is introduced into the latter two by their special choices of the reference fluids, which change both with the composition and with the pair potentials. The same type of expansion can be made for a pure fluid, and gives the properties of a second pure fluid with a different pair potential in terms of the properties of the first and the differences between the potential constants. Since the second-order terms in this expansion are probably comparable to those for

a mixture, this system is also of interest.

Figure 3.8 shows the imperfection thermodynamic functions of a pure fluid as a function of r^* and T^*, at constant T and p. The deviations of these curves from the straight lines tangent to them at the center of the range give a rough measure of the importance of the second-and higher-order terms in an expansion of the type used in the mixture theories. For the range of r^* and T^* found in our set of components, these results suggest that errors of the order of 5 to 10% in the volume might be attributed to the uncertainty in the second-order terms of the expansion.

Similar presentations for the binary mixture are given in Fig. 3.9, where the imperfection thermodynamic functions of the mixture are shown as functions of r_2^* and T_2^* with r_1^* and T_1^* fixed. All of these theories give the correct slopes at the central point ($r_1^* = r_2^*$, $T_1^* = T_2^*$), but differ in the curvature. The LH theory is linear in r_{11}^*, r_{12}^*, and r_{22}^*; since the arithmetic-mean combining rule is used for r_{12}^*, the curve for r_2^* becomes a straight line. This is not the case for T_2^*, for which the geometric-mean combining rule ($T_{12}^* = \sqrt{T_{11}^* T_{22}^*}$) is used. The other theories are linear in their initial formulation, but in each case the special choice of reference fluids effectively introduces nonlinear terms as pointed out above. Ideal mixing can be shown to give the wrong slope at the central point in the T_2^* plot; in the r_2^* plot it accidentally gives the right slope because terms cancel through the use of the arithmetic-mean combining rule for r_{12}^*. Since for small deviations the geometric and arithmetic means are nearly the same, however, the amount by which the ideal mixing curve deviates from the

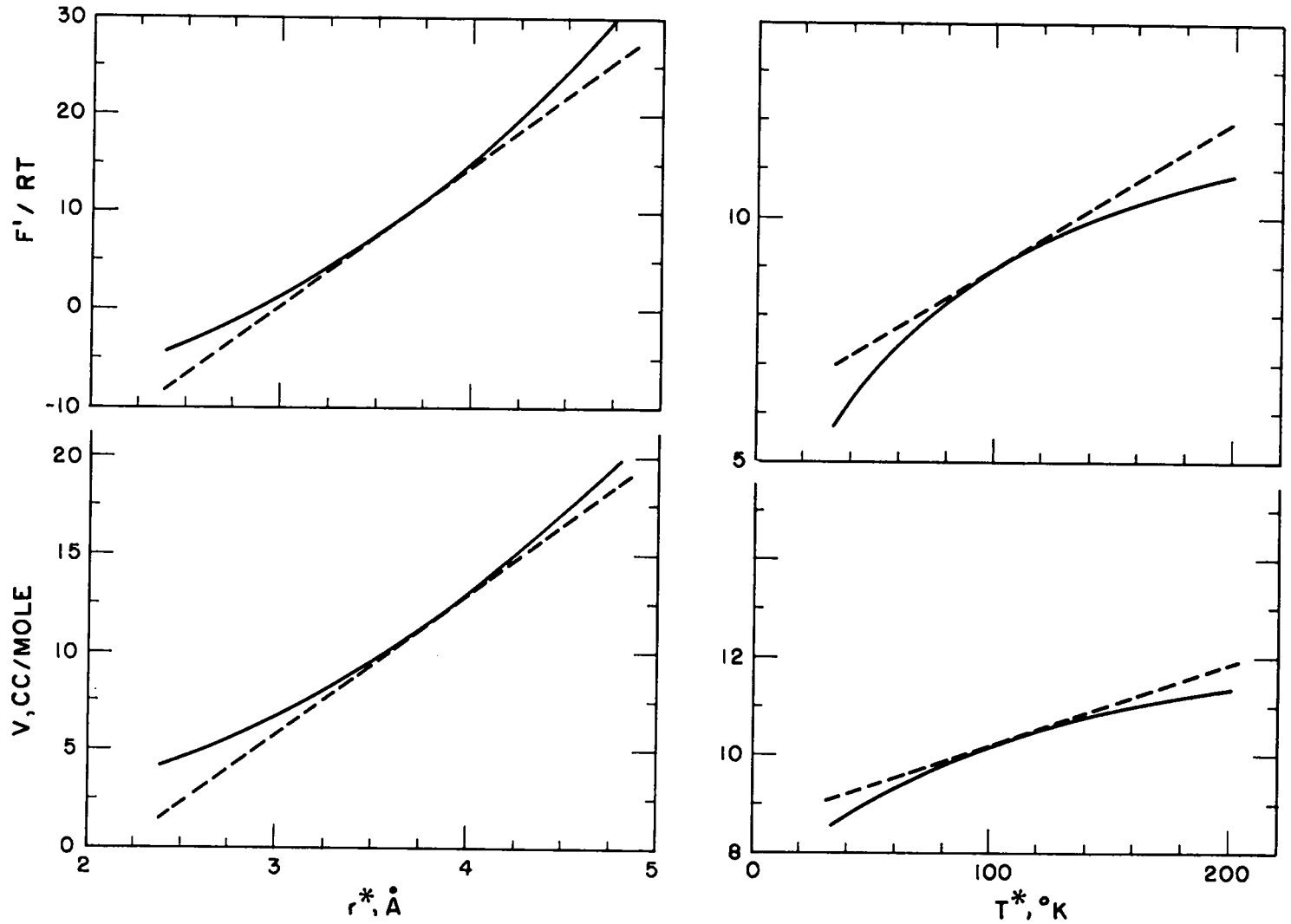

Fig. 3.8. Variation of the imperfection thermodynamic functions of a pure substance with the potential constants r* and T* at constant T and p. For the r* variation, T* is held constant at the central value, and vice versa. The dashed tangents at the central points are included to show the deviations from linearity.

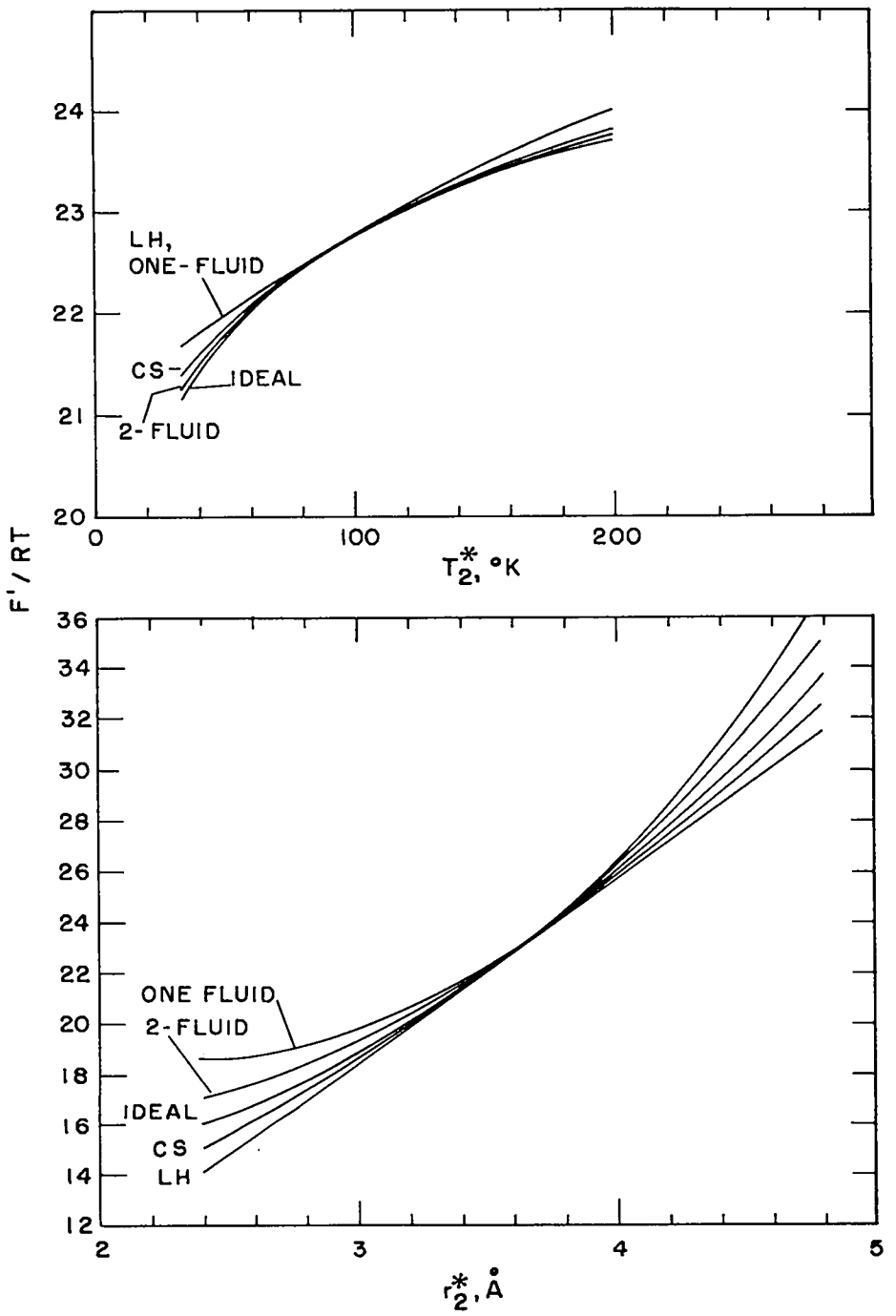

Fig. 3.9. Variation of the imperfection free energy of a binary mixture with the potential constants r_2^* and T_2^* at constant T and p (T = 2000 °K, p = 0.3 mb). For the r_2^* variation, T_2^* is held constant at the central value, and vice versa.

correct slope at the central point is too small to be seen in the figure.

From this point of view, the failure of the different mixture theories to agree even on the sign of the excess functions is not surprising. The deviation from ideal mixing depends, in all practical cases, on the amount of curvature in these curves, a property which is not given with any degree of confidence by any of these essentially linear theories.

3.4 Chemical Composition and Fugacities

Under the conditions of interest, fugacity corrections to the ideal gas equilibrium constants are important. We give here some numerical examples. For an equation of state point, we take the calculated CJ state for the explosive RDX ($C_3H_6O_6N_6$) at density 1.8 g/cc, using the pair-potential constants given in Chapter 2, the CS mixture theory, and the MM form of the pair potential. For the potential exponent, the value $\alpha = 13$ is chosen to give approximate agreement with the experimental detonation velocity.

A chemical reaction may be represented by

$$\sum_{i=1}^{c} \nu_i X_i = 0 \quad ,$$

where c is the total number of chemical species present, X_i represents one mole of species 1, and ν_i is the stoichiometric coefficient for species i, i.e., the number of moles of species i transformed by the reaction. At equilibrium, the mole fractions x_i of the species involved in each reaction must satisfy a relation of the form

$$\prod_{\substack{\text{(gas}\\\text{species)}}} x_i^{\nu_i} = k(T,p,\vec{x}) \quad ,$$

where k can be expressed as

$$\ell n\ k = \ell n\ K(T) - (\Delta\nu)(\ell n\ p + F_g'/RT) - \sum_{\substack{\text{(gas}\\\text{species)}}} \nu_i(\mu_i' - F_g')/RT - \nu_s F_s'/RT \quad ,$$

$$\ell n\ K(T) = - \sum_{\substack{\text{(all}\\\text{species)}}} \frac{\nu_i\left[F^o(T) - H_o^o + \Delta H_f^o\right]_i}{RT} \quad .$$

Here K(T) is the ideal gas equilibrium constant (which is expressed in terms of the standard free energies, as shown), $\Delta\nu$ is the change in the number of moles of gas as the reaction goes from left to right, F_g' is the total imperfection free energy of the gas,* F_s' is the corresponding quantity for the solid, and μ_i' is the imperfection chemical potential of species i. The terms $\mu_i' - F_g'$ in the expression for ℓn k can be given a simple physical interpretation. Since from thermodynamics

$$F_g' = \sum_{\substack{\text{(gas}\\\text{species)}}} x_i\mu_i' \quad ,$$

they represent, roughly speaking, differences in size and interaction energy; molecules which are larger and "harder" than average have $\mu_i' > F_g'$, and vice versa for those which are smaller and "softer."

---

* The fugacity is defined as $pe^{(F_g'/RT)}$.

In Table 3.1 we give numerical values of some of these quantities including the equilibrium constants for several reactions (not an independent set) for the calculated detonation state described above.

3.5 Kinetic, Internal, and Chemical Bond Energy

It may be of interest to give results for a simple hydrodynamic model which produces the detonation products in a constant state.[50] This is done by supposing that the detonation wave is followed by a piston moving with the mass velocity of the products, so that the state variables everywhere behind the wave are constant. For this model it can be shown that

$$Q + W = K.E. + E(T,p) - E(T_o,p_o) \quad ,$$

where W is the work done by the piston, Q is the "chemical bond energy" (the change in internal energy when the H.E. reacts at constant T and p to form products), K. E. is the kinetic energy of the products, and E is the internal energy of the products. Writing this equation as percentages of the total on each side for the calculation described in the previous section gives

$$\underset{60\%}{Q} + \underset{40\%}{W} = \underset{20\%}{K.E.} + \underbrace{E(T,p) - E(T_o,p_o)}_{80\%} \quad .$$

Thus, in this system which produces the detonation products in a constant state, only 60% of the energy which maintains the detonation comes from the breaking of chemical bonds, and the remainder is supplied by the piston. In the reaction products, 20% of this total energy appears as (macroscopic)

Table 3.1. Equilibrium Constants and Related Quantities for Several Reactions.

($p = 0.33$ mb, $T = 4040\ ^\circ K$, $\ln p = 12.7$, $\frac{F'_g}{RT} = 14.8$.)

Species	Ideal Chemical Potential $\frac{(F^\circ(T) - H^\circ_o - \Delta H^\circ_f)_i}{RT}$	Imperfection Chemical Potential $\frac{\mu'_i}{RT}$
C(s)	-4.4	4.4
N_2	-29.2	16.4
CO	-33.4	16.4
H_2O	-37.8	11.0
NO	-29.0	15.5
H_2	-21.6	8.4
CO_2	-47.4	19.1
O_2	-31.2	14.0
CH_4	-37.1	19.1

Reaction	Gas Mole Change ($\Delta\nu$)	Equilibrium Constants: For Ideal Gas at p=1 atm $\ln K(T)$	Equilibrium Constants: For Ideal Gas at p=0.33 mb $\ln K(T) - (\Delta\nu) \ln p$	Equilibrium Constants: With Fugacity Corrections $\ln k(T)$
(1) $CO \rightarrow \frac{1}{2}CO_2 + \frac{1}{2}C(s)$	$-\frac{1}{2}$	-7.5	-1.2	+3.5
(2) $H_2O \rightarrow H_2 + \frac{1}{2}O_2$	$+\frac{1}{2}$	-0.5	-6.9	-11.3
(3) $H_2O + \frac{1}{2}N_2 \rightarrow H_2 + NO$	$+\frac{1}{2}$	-1.7	-8.1	-12.8
(4) $CO + H_2O \rightarrow CO_2 + H_2$	0	-2.1	-2.1	-2.2
(5) $C(s) + \frac{2}{3}H_2O \rightarrow \frac{2}{3}CO + \frac{1}{3}CH_4$	$+\frac{1}{3}$	+5.1	+0.8	-4.8

kinetic energy, and the remaining 80% as increased internal energy of the products.

3.6 Some Gross Parameter Variations

In this section we show the effects of certain gross changes in the calculation. Included are the effects of the heat of explosion and of the number of moles of gas in the detonation products, two quantities often used in rough engineering evaluations of new explosives.

The explosive is RDX at density 1.8 g/cc. The calculation is made as described in Section 3.4, but with fixed, instead of equilibrium, product composition. The variations are listed in Table 3.2. In run 2 the number of moles of gas is increased by converting all of the CO_2 according to the equation

$$CO_2 + C(s) \rightarrow 2CO \quad .$$

In run 3 the solid is made incompressible. Run 4 shows the effect of increasing the heat of explosion Q, and in run 5 the LJD cell theory is replaced by the ideal gas equation of state. The heat of formation of the explosive is artifically adjusted as required to give the desired heat of explosion.

The results are given in Table 3.2 and Fig. 3.10.

Table 3.2. Description of the Parameter Variations.

Run	Description	Product Composition	Heat of Explosion (kcal/g)	Moles of Gas	P_{CJ} (mb)	$(v/v_o)_{CJ}$	T_{CJ} (°K)	$\gamma_{CJ} \equiv \left(\frac{\partial \ln p}{\partial \ln v}\right)_S$	D (m/s)
1	Reference	1[a]	1.51	7.5	0.315	0.771	4063	3.36	8741
2[b]	Increased number of moles of gas	2[c]	1.51	9	0.421	0.777	3833	3.48	10227
3	Incompressible solid	1	1.51	7.5	0.320	0.785	4053	3.66	9100
4[d]	Heat of explosion increased 50%	1	2.26	7.5	0.384	0.757	5858	3.12	9374
5	Ideal gas	1	1.51	7.5	0.050	0.566	5011	1.30	2539

[a] $1.5C(s) + 3H_2O + 1.5CO_2$.

[b] In run 2 the heat of formation of the explosive has been artificially reduced to keep the heat of explosion constant.

[c] $3N_2 + 3CO + 3H_2O$.

[d] In run 4 the heat of formation of the explosive has been artificially increased to give the desired heat of explosion.

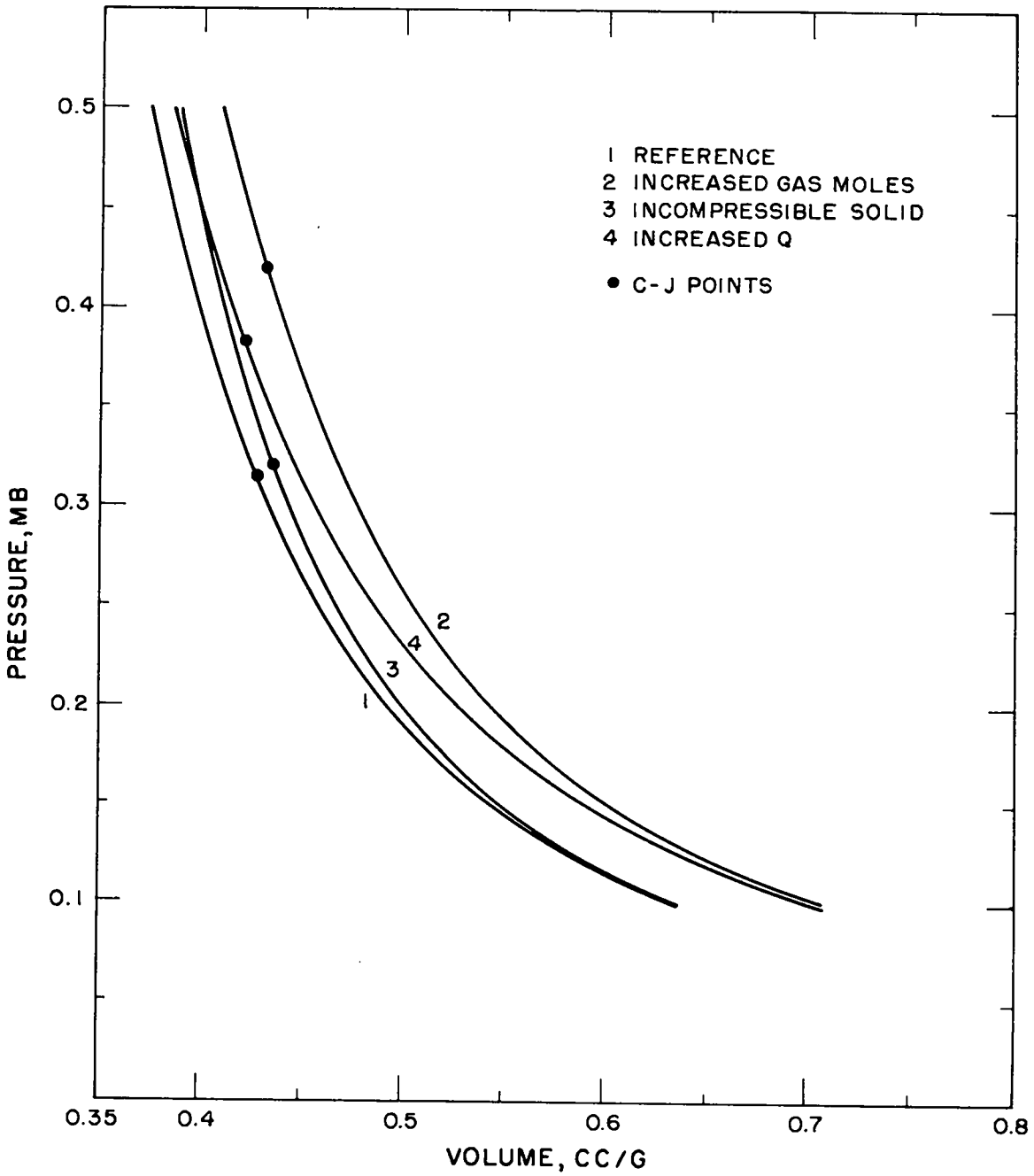

Fig. 3.10. Detonation Hugoniots for RDX under some gross parameter variations.

Chapter 4

VARIATION OF PARAMETERS

Because of the imperfect state of the theory, the calculation contains a number of adjustable parameters, such as the pair-potential constants. To assess the effect of this uncertainty, we first compare with experiment the results of a calculation which is a priori in the sense that the values of the parameters are chosen from the information presented in Chapters 2 and 3, making no use of the measured detonation properties of the explosives for which the calculations are done. We then examine the effects of a systematic variation of the parameters. Before describing any of the calculations, we discuss the parameters themselves.

4.1 The Parameters

We describe here the parameters which may be varied, listing them according to the main subdivisions of the theory.

Gas Equation of State

As pointed out in Chapter 2, this problem may be divided into the microscopic one of determining the forces (pair potentials) acting between

the molecules, and the macroscopic one of finding the behavior of the system once these force laws are given. For mixtures, most theoretical treatments divide the latter problem into the determination of a pure-fluid equation of state and of a mixture theory which gives the properties of the mixture as a perturbation on the pure fluid.

Pair Potentials. These are determined experimentally. In the simple case of interaction between monatomic molecules, the important repulsive part of the potential can be obtained directly from observations of molecular scattering. For more complicated molecules, pair potentials can be derived from this type of data, but only at the cost of introducing some assumptions. Even these less-certain results are not available for all of the interactions that we need to know.

As the potentials are usually represented, there are four parameters for each interaction: the analytic form, the repulsion exponent α or n, the characteristic distance r*, and the well depth T*. The conformal assumption requires that the analytic form and repulsion exponent be the same for all interactions so that a single analytic form and value of the repulsive exponent apply to all interactions of the system. The values of r* and T* for each interaction must still be chosen. For interactions of like molecules, they are taken from the experimental information on the pair potential; for unlike interactions, the combining rules

$$r^*_{ij} = \tfrac{1}{2}\,(r^*_i + r^*_j) \quad , \qquad T^*_{ij} = (T^*_i T^*_j)^{\frac{1}{2}}$$

are used. These rules are of course only approximate, and one could introduce many more parameters to modify them, but we will use them in this form and consider only the r^*_i and T^*_i of the like interactions as parameters.

Thus, for a system of c components, there are 2c + 2 parameters: the analytic form and repulsive index of the potential, and the individual parameters r_i^* and T_i^*. It will often be convenient to keep the ratios of the individual parameters constant and vary the average parameters for the mixture by scaling all of them by the same factor.

Pure Fluid Equation of State

Consideration is limited to a single form, the LJD cell theory, so that there are no adjustable parameters in this part of the theory.

Mixture Theory. The practical theories give quite different results, but there are no high-pressure experiments with which to compare. The crudeness of the theories compared to the problem to which they apply makes an a priori assessment of their worth difficult. We therefore try several, including the extreme ones, and regard this choice as another parameter.

Solid Equation of State. The principal uncertainty here is the particle size of the solid; if it is small enough, surface forces become important. To represent this effect, we vary the heat of formation of the solid by amounts up to about ten per cent of the sublimation energy.

4.2 An A Priori Calculation

For this calculation and for the parameter variations, we have chosen a minimum number of explosives covering a fairly wide range of atomic composition, oxygen balance, and density. These are listed in Table 4.1.

Table 4.1. Explosives Used in the Parameter Studies.

Explosive	Empirical Formula for 1 Mole	Reduced Atomic Composition C	H	O	N	Oxygen Balance[a] (to CO)	Enthalpy of Formation at 25°C (kcal/mole)
RDX	$C_3H_6O_6N_6$	0.5	1	1	1	0	14.71
Comp. B (65/35)	$C_{4.4}H_{5.7}O_6N_{4.9}$	0.73	0.95	1	0.82	-0.20	3.49
TNT	$C_7H_5O_6N_3$	1.15	0.83	1	0.5	-0.58	-17.81
Nitromethane (NM)	$C_3H_9O_6N_3$	0.5	1.5	1	0.5	-0.25	-21.28
Nitromethane/ nitric acid/ water[b] (NM/HNO_3)	$C_{1.1}H_{5.2}O_6N_{2.2}$	0.19	0.87	1	0.37	+0.38	-37.5

	ρ_o	Q (kcal/g)	Moles of Gas per Gram	Moles of Solid per Gram	Total Moles per Gram
RDX	1.800	1.49	0.034	0.007	0.041
Comp. B	1.714	1.41	0.031	0.012	0.043
TNT	1.640	1.28	0.026	0.022	0.048
NM	1.131	1.37	0.040	0.006	0.046
NM/HNO_3	1.293	1.04	0.037	0.0	0.037

All of these quantities are calculated at the densities given with the set of parameters described in the text. They are included to aid in characterizing the explosives.

[a] For an explosive $C_aH_bO_cN_d$ of molecular weight M, oxygen balance is defined as $\frac{1600}{M}(c - a - \frac{1}{2}b)$.

[b] This mixture is prepared by mixing 1 mole of nitromethane with an amount of 91% HNO_3, containing 1 mole of HNO_3. The molar composition is $CH_3NO_2/HNO_3/H_2O$: 1/1/0.346.

The parameters chosen are

(1) The MM potential

$$u(r) = kT^*\left[\frac{6}{\alpha - 6} e^{\alpha(1-\frac{r}{r^*})} - \frac{\alpha}{\alpha - 6} e^{6(1-\frac{r}{r^*})}\right]$$

with $\alpha = 14$.

(2) The species

C(graphite), N_2, CO, H_2O, NO, H_2, O_2, CH_4

with values of r_i^* and T_i^* from Table 2.1.

(3) The CS mixture theory.

(4) The value zero for the heat of formation of graphite.

Many of these choices are rather arbitrary. The repulsive exponent could have been chosen to be 15, but all of the $\alpha = 15$, exp-six potentials lie above the repulsive potentials derived from molecular scattering data over most of the distance range (see reference 31), so we have chosen $\alpha = 14$ instead. What mixture theory to choose is really an open question. The results reported in reference 36 suggest that, where anything is known about the problem, ideal mixing gives good results. The CS theory is close to ideal mixing and has the advantage that average potential constants are defined. The value of the graphite heat of formation is unknown; we have taken the bulk value. Thus, while we term this calculation a priori, there is considerable arbitrariness in its specification. How much the results are affected can be judged from the parameter variations presented later.

The results of this calculation are compared with experiment in Figs. 4.1 and 4.2 and in Table 4.2.* Most of the calculated detonation velocities are too high, the calculated Hugoniots do not come very close to the experimental CJ points, and the calculated values of γ** are all too high. Thus it appears that the parameter variations described in the next section may effect some improvement.

4.3 Single Parameter Variations

One of the first variations tried was to change the value of the repulsive exponent α from 14 to 13. With the exception of NM/HNO_3, this moved the calculated Hugoniots closer to the experimental CJ points in the p-v plane (Fig. 4.3), and brought the deviations from the experimental velocities closer together. We therefore decided to take this calculation as the starting point. In what follows we term this parameter set, that

---

*The figures and tables containing the results are at the end of this Chapter.

**The CJ pressure is given by $P = \frac{\rho_o D^2}{\gamma + 1}$; $\gamma \equiv \left(\frac{\partial \ln p}{\partial \ln v}\right)_S$. The quantity γ is chosen for comparison instead of the pressure, since it is a much less sensitive function of the thermodynamic state. For simplicity, we use in this chapter only the experimental data from this laboratory, which probably form a fairly consistent set. This should be sufficient here, where the main object is to show the effects of the parameters on the calculated results. More complete comparisons with most of the available experimental data are made in Chapter 5.

used for the a priori calculation with α changed from 14 to 13, the "central point."

The list of variations chosen is given in Table 4.2. Since there are so many parameters which can be varied, we have tried to select a limited set. Without actually assigning numbers, we have taken as a rough figure of merit for inclusion the product of the range of uncertainty of the parameter in question and its effect on the results. The range of variation of most of the parameters was chosen to correspond roughly to the uncertainty in their values. Some comments on the choices follow. The results will be discussed in Section 4.5.

Potential Parameters Common to All Species

In addition to α, the repulsive exponent in the analytic form of the pair potential, we define another common potential parameter: a scale factor S_{r^*} on all of the molecular sizes. The change in this scale factor (run 4) was chosen to give about the same effect on the results as changing α by 1 (runs 1-3). One calculation was also done with the L-J, n = 9 potential (run 5).

Potential Parameters For the Individual Species

The most uncertain of the pair-potential constants are the values of r* for carbon dioxide and water. These also have a marked effect on the calculated results and were therefore chosen for variation. The observed effects were large enough to make it desirable to take both

positive and negative changes (runs 6-9). The individual values of T^* apparently have little effect. This was suggested by some of the mixture studies mentioned in Chapter 3, and is confirmed by run 10 in which all T_i^* were made approximately equal to the middle of the range of the calculated average $\overline{T}^*$ for the central point, with little effect on the results. (The detonation velocities for this run, not plotted, are within 50 m/s of those for the central point.)

Mixture Theory

The one-fluid theory* gives a rigorous upper bound to the mixture free energy, and large positive deviations from ideal mixing; it is probably much too "hard". The very "soft" pseudo-pair-potential theory, which gives a rigorous lower bound to the free energy, is too complicated for use in the calculation. The softest theory we have used is the CS theory chosen for the central point, which gives relatively small negative

---

*The one-fluid theory gives a very complicated calculational recipe for any potential other than the Lennard-Jones form. Therefore, the mixture rule which gives the average parameters was written in this case for the L-J, n = 9 potential, which is comparable to the MM, $\alpha = 13$ form used in all other parts of the calculation. While this procedure must be regarded as empirical from the statistical-mechanical point of view, it is thermodynamically consistent, and, we believe, a good approximation to the more exact method.

deviations from ideal mixing. We have done calculations with the one-fluid theory (run 11), and also with ideal mixing (run 12), which gives results between those of the one-fluid theory and the CS theory (run 2).

Heat of Formation of Solid Carbon

Since any solid carbon present is probably in the form of very small particles, there may be an appreciable surface energy due to interface interactions with gas molecules, which are neglected in the calculation. To take this effect into account, we have increased the heat of formation of the solid up to about ten per cent of the sublimation energy (runs 13, 14).

4.4 Compensated Parameter Variations

Since some of the parameter variations of Section 4.3 caused rather large changes in detonation velocity and CJ pressure, we repeated several of them with all r_i^* scaled to compensate for the variation and bring the calculated detonation velocities back to approximately the original value. In nearly all cases it was found that the required scale factor could be obtained quite closely from a simple procedure based on the reduced initial density scaling described in Ref. 3. Let subscript 1 refer to the central point (run 2) and subscript 2 refer to a calculation done with one parameter changed. If $(\rho_o)_1$ and $(\rho_o)_2$ are the densities at which the calculated detonation velocities are equal, then the required scale factor is given by

$$S_{r^*} = \text{scale factor for } r_i^* = \left[\frac{(\rho_o)_1}{(\rho_o)_2}\right]^{1/3} .$$

(See figure at the top of the next page.)

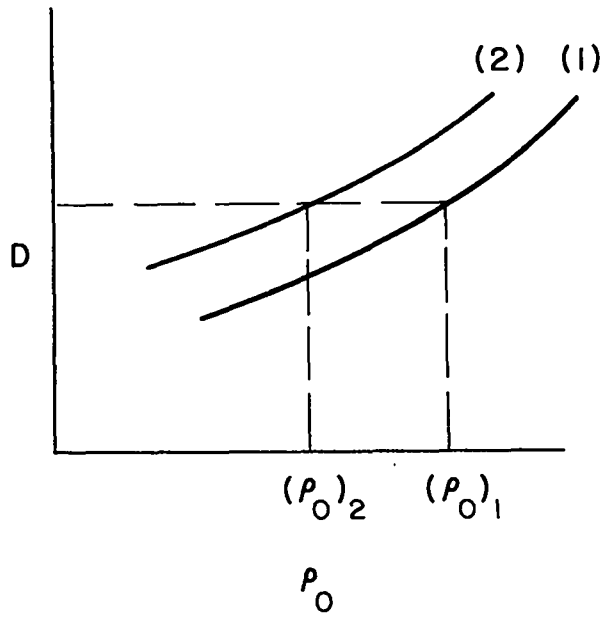

Several of the original variations were repeated, using this recipe for the compensation. These runs are listed in Table 4.3.

4.5 Discussion of the Results

The results of the calculations are given in Tables 4.2 and 4.3 and Figs. 4.1 to 4.7. The central point set of parameters, Figs. 4.3, 4.4a, gives results which compare with experiment as follows:

(1) The calculated detonation velocity for NM/HNO_3 is about 500 m/s below the experimental value; the next largest disagreement, from TNT at density 1.4, is about 300 m/s.

(2) With the exception of NM/HNO_3, the calculated Hugoniots pass close to the experimental CJ points, but the calculated CJ pressures are too low (with correspondingly high values of γ), indicating that the calculated Hugoniots are too steep near their CJ points.

(3) The calculated temperature for nitromethane is several hundred degrees too high, while that for NM/HNO_3 is about right.

(4) The hook at the end of the TNT velocity curve is due to the hook in the experimental data. None of our calculations produced anything like this for TNT, although the abrupt changes in slope associated with carbon disappearance in the other explosives, Fig. 4.6c, suggest a possible mechanism.

(5) The experimental errors, discussed in more detail in Chapter 5, are such that some of the calculated velocities are certainly wrong by several hundred meters per second; but the calculated pressures and temperatures may possibly be correct.

The parameter variations were made about this central point. We now discuss the results.

Common Potential Parameters

Figures 4.1 and 4.2 show that the potential with exponent $\alpha = 14$ is too hard: all of the claculated Hugoniots with the exception of NM/HNO_3 lie to the right of the experimental CJ points. Figure 4.3 shows that $\alpha = 13$ is about right in this respect, and it also brings the velocity deviations closer together, Fig. 4.4a. The potential with $\alpha = 12$ is

clearly too soft, Fig. 4.4b. Increasing all the molecular diameters r_i^* by about 2%, Fig. 4.4c, has about the same effect as increasing α from 13 to 14, but does not increase γ quite so much (Table 4.3). Substitution of the L-J, n = 9 potential for the MM form, Fig. 4.4d, gives results qualitatively similar to those for α = 12, except that the calculated velocity for NM/HNO_3 is even lower.

Individual Potential Parameters

Figure 4.5a-d shows that the relative sizes of the molecules have a marked effect on the calculated results, but that the variations tried do not give much better overall agreement with experiment.

Heat of Formation of Solid Carbon

This parameter has a pronounced effect on the shape of the calculated velocity curves, Fig. 4.6c and d, and also decreases the calculated values of γ appreciably. When solid carbon is present, the initial effect on velocity of increasing the heat of formation depends on the explosive and the density. The reaction

$$2H_2O + 3C(s) \rightarrow 2CO + CH_4 \qquad \Delta H_f = +44 \text{ kcal}$$

is shifted to the right; the resulting decrease in Q and in the total number of moles of products tends to decrease the calculated velocity, while the increase in the number of moles of gas tends to increase it.

Of course, when the heat of formation of the solid is increased, the solid tends to disappear. In nitromethane and in low-density Composition B

and RDX, it disappears entirely, and considerable quantities of methane are formed.

Mixture Theory

For the simple theories considered here, changing the mixture theory, Fig. 4.6a and b, gives results comparable to those obtained by changing the exponent of the potential or scaling all of the molecular sizes. The calculated values of γ remain too high.

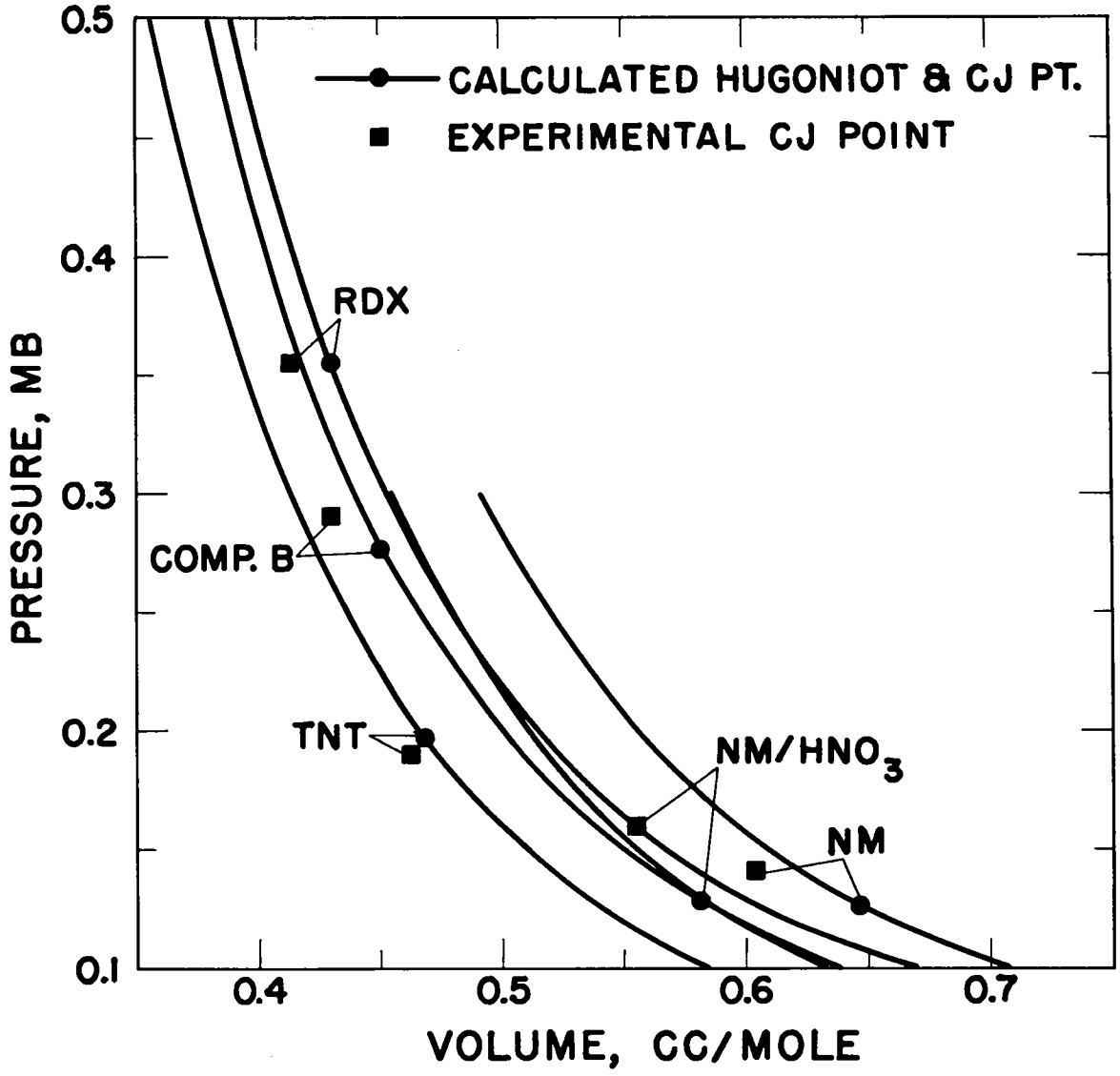

Fig. 4.1. Calculated detonation Hugoniots and experimental CJ points for the a priori set of parameters, run 1.

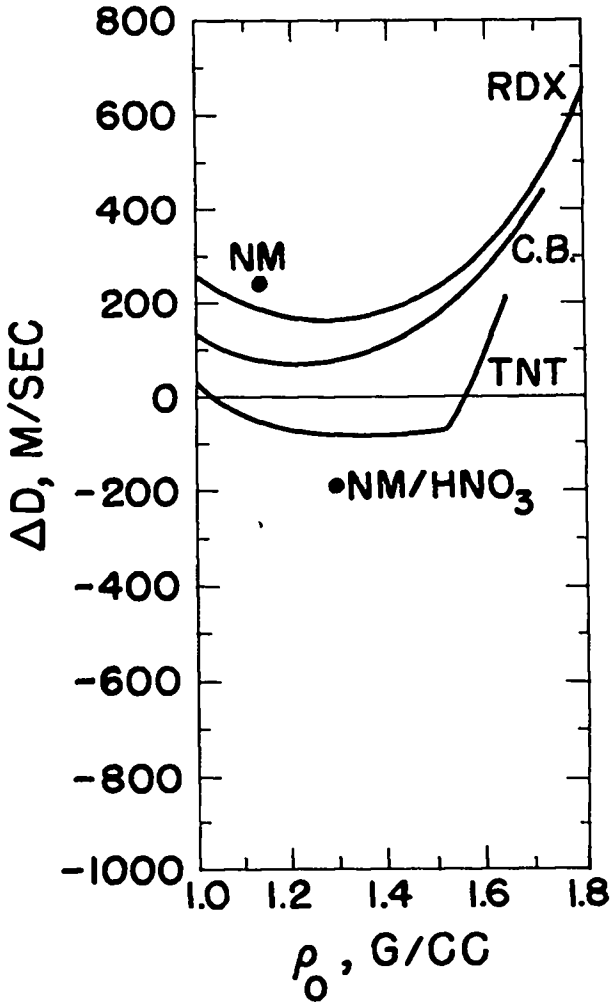

Fig. 4.2. Differences of the calculated detonation velocities from experiment for the a priori set of parameters ($\alpha = 14$), run 1. The quantity plotted is ΔD = calculated D - experimental D.

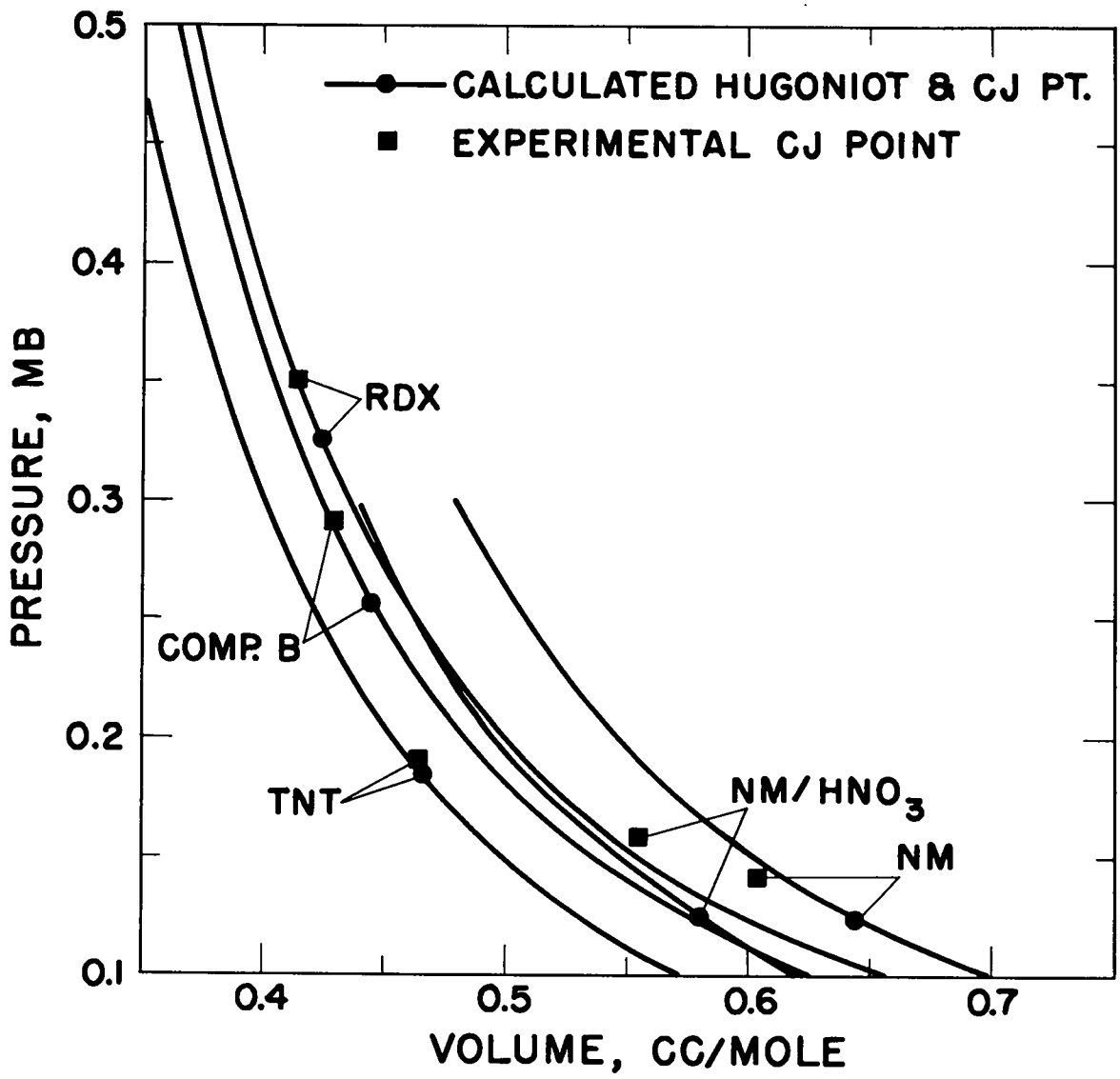

Fig. 4.3. Calculated detonation Hugoniots and experimental CJ points for the "central point" set of parameters, run 2. This set is the same as the a priori set with α changed from 14 to 13.

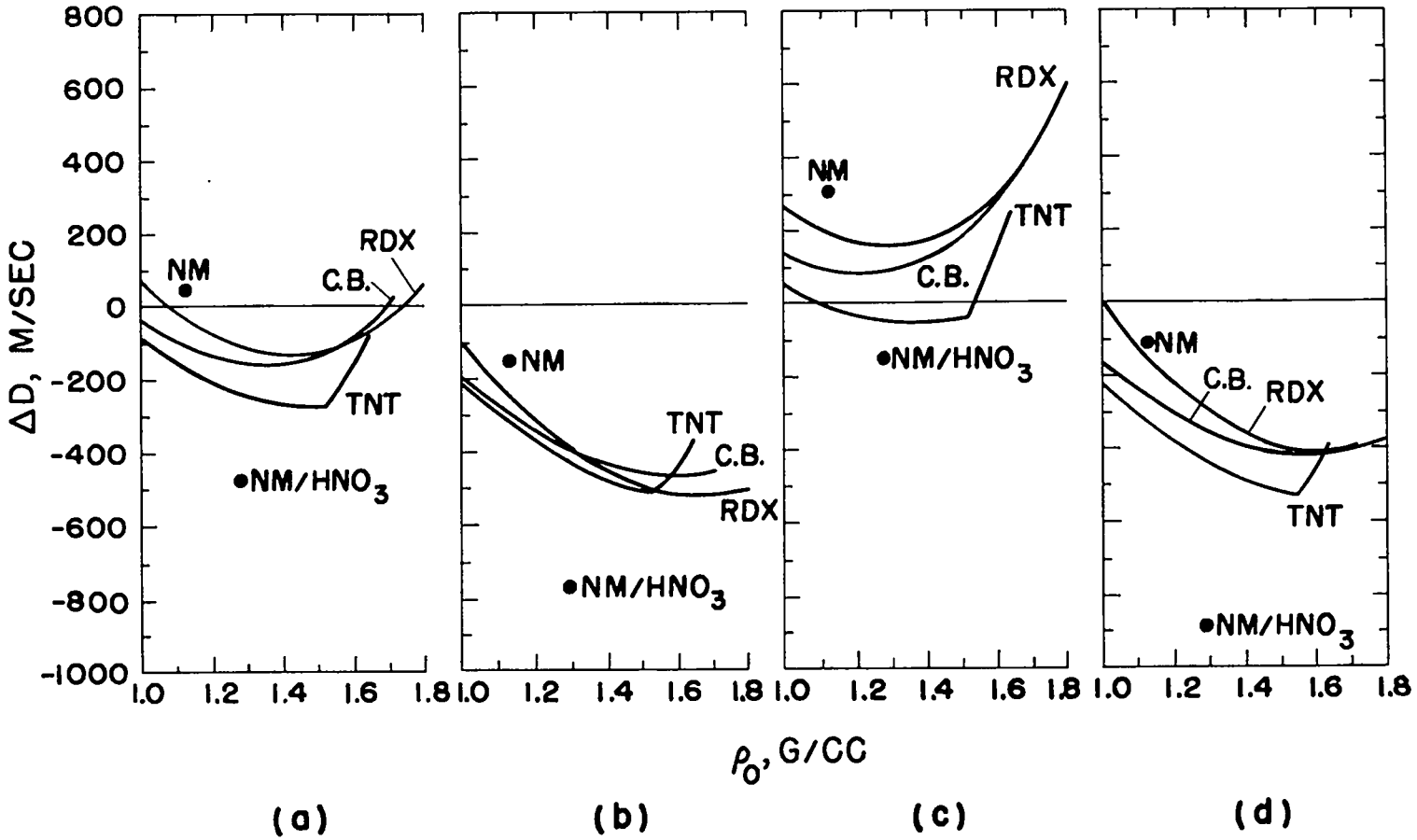

Fig. 4.4 Variations in the pair potential. (a) $\alpha = 13$ (central point), run 2; (b) $\alpha = 12$, run 3; (c) All r_i^* increased 2.03%, run 4; (d) L-J, n = 9 form, run 5.

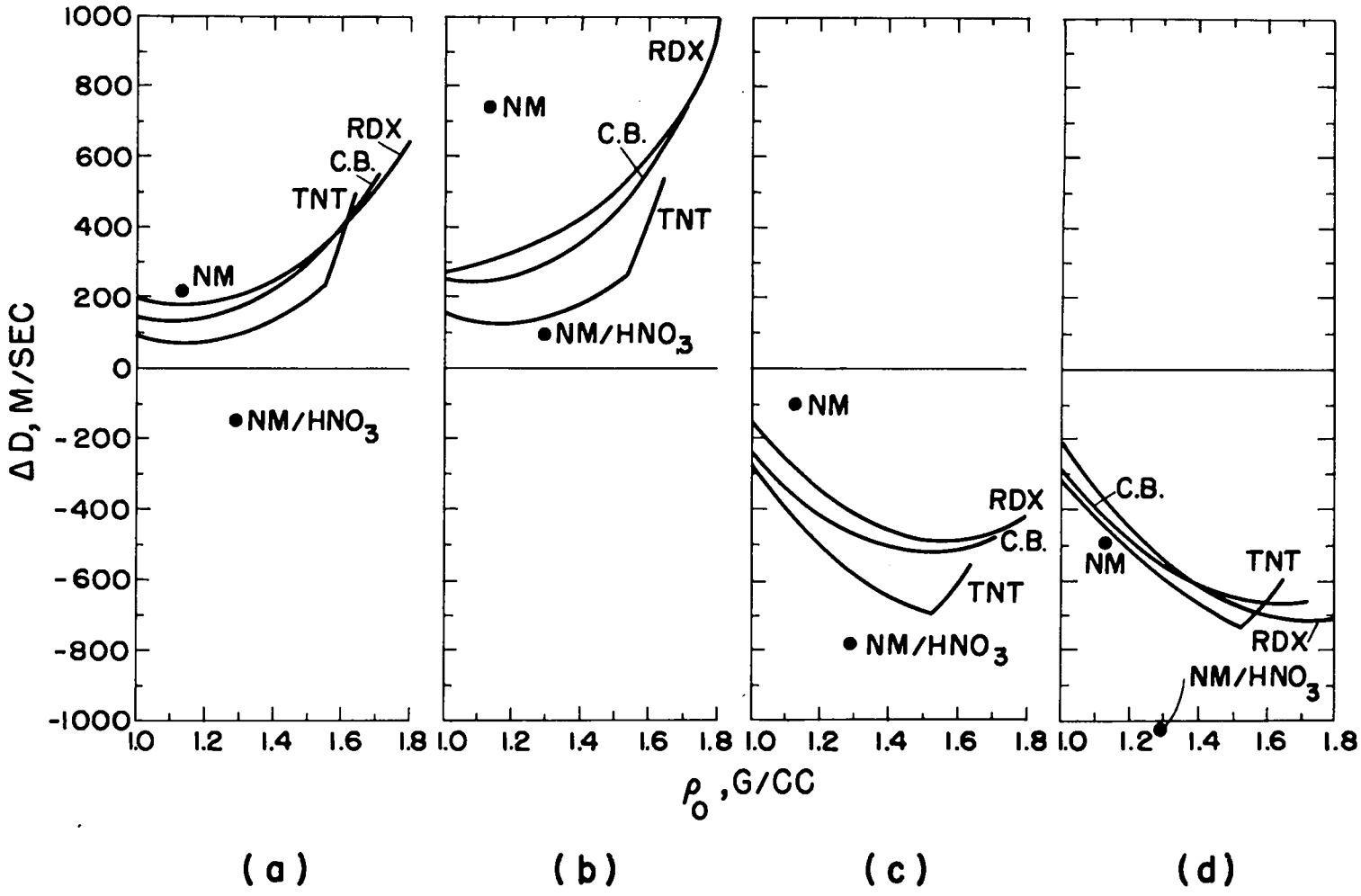

Fig. 4.5. Individual size variations. (a) CO_2 r* increased 10%, run 6; (b) H_2O r* increased 10%, run 8; (c) CO_2 r* decreased 10%, run 7; (d) H_2O r* decreased 10%, run 9.

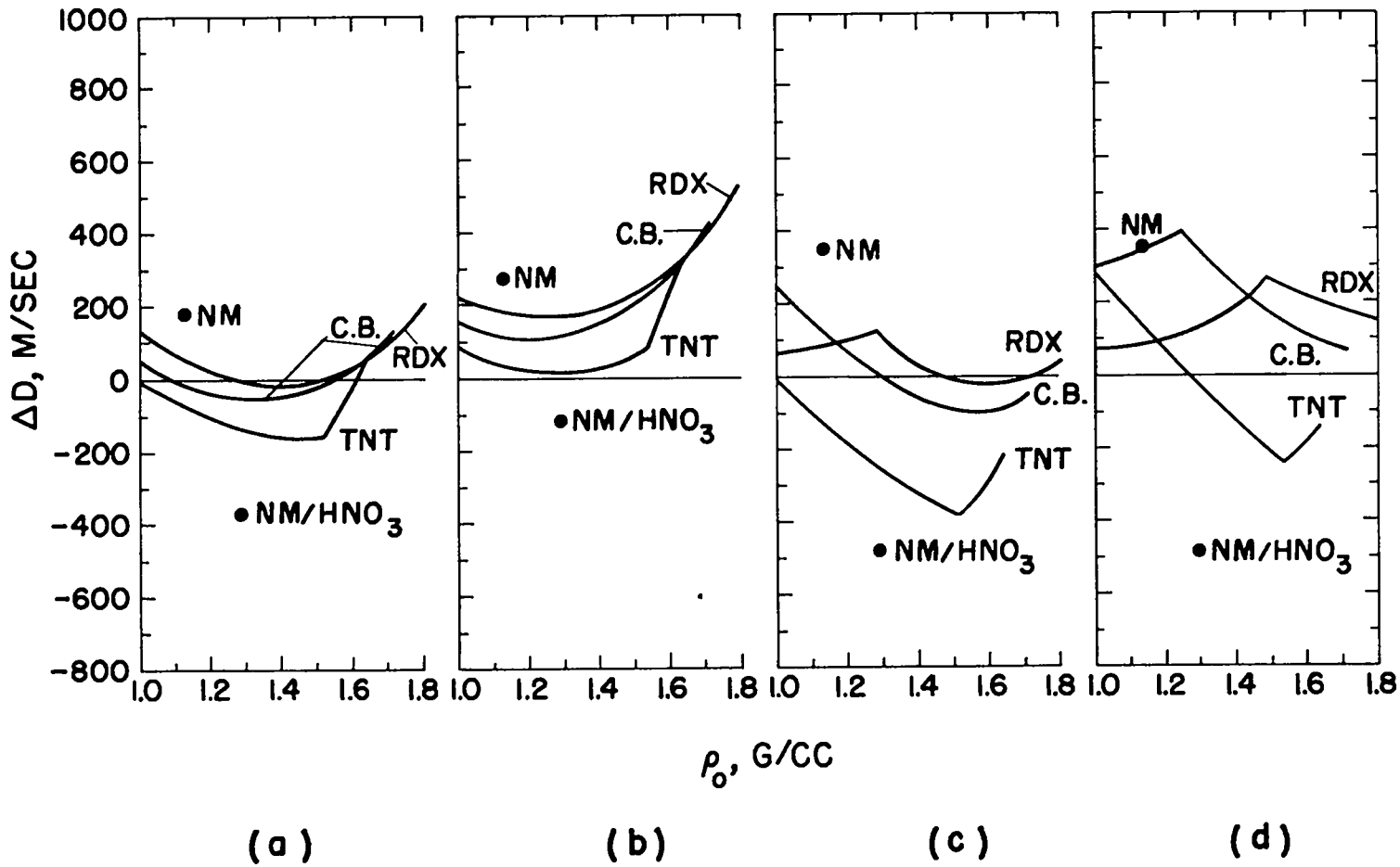

Fig. 4.6. Changes in the mixture theory and in the heat of formation of the solid. (a) Ideal mixing, run 12; (b) One-fluid mixture theory, run 11; (c) ΔH_f = 10 kcal/mole, run 13 (d) ΔH_f = + 20 kcal/mole, run 14.

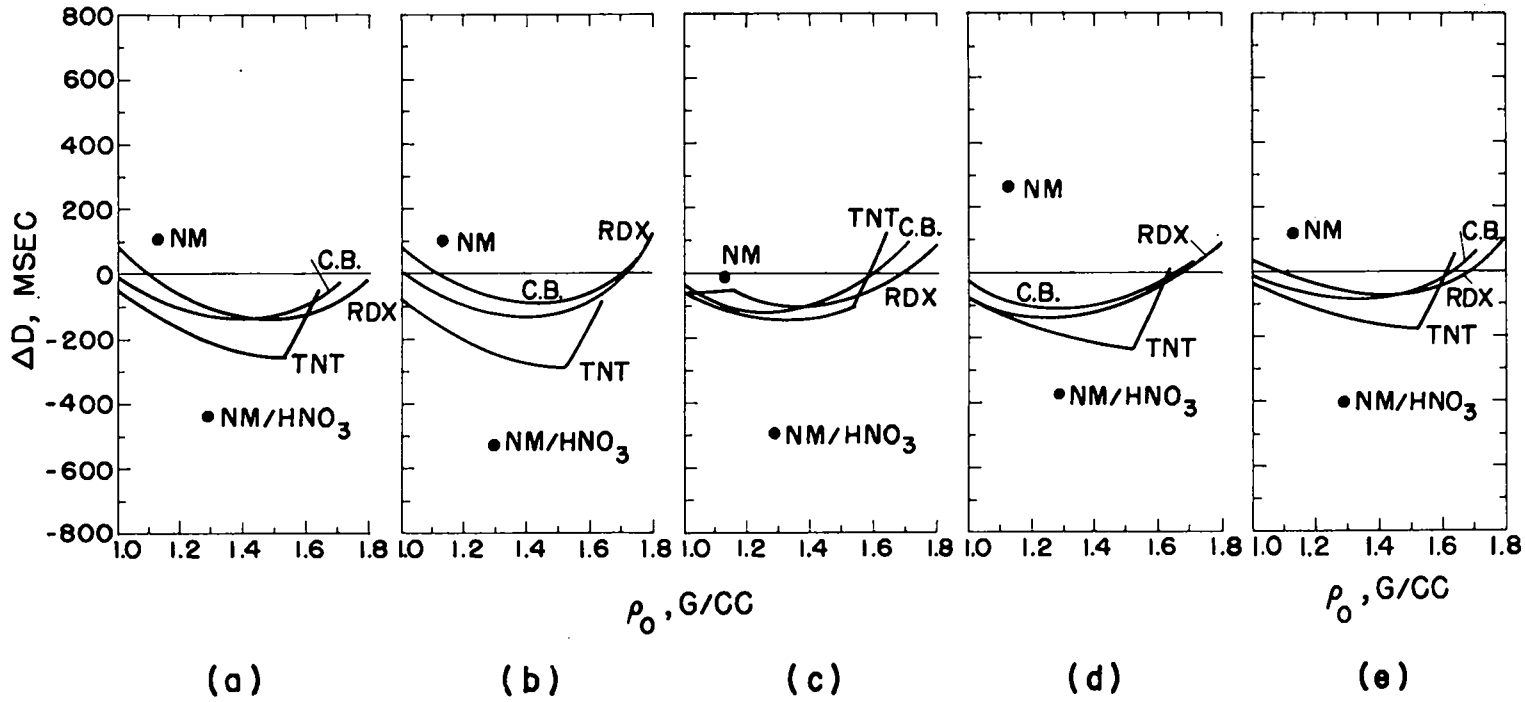

Fig. 4.7. Compensated parameter variations. (a) α = 12, run 15; (b) α = 14, run 16; (c) CO_2 r* increased 10%, run 17; (d) H_2O r* increased 10%, run 19; (e) One-fluid theory, run 19.

Table 4.2. Calculated Values of D, γ and T for Single-Parameter Variations.

Run	Description	$D_{calc} - D_{exp}$ for RDX at $\rho_o = 1.8$	RDX $\rho_o = 1.8$		Comp. B $\rho_o = 1.714$		TNT $\rho_o = 1.64$		Nitromethane $\rho_o = 1.131$		NM/HNO_3 $\rho_o = 1.293$	
			γ	T	γ	T	γ	T	γ	T	γ	T
	Experimental	0	2.90		2.77		3.17		2.13	3380	2.54	3400
1	"A priori" set, $\alpha = 14$	660	3.51	4016	3.41	3967	3.37	3684	2.74	3865	3.10	3531
2	"Central Point" set, $\alpha = 13$	55	3.29	4040	3.22	3962	3.22	3662	2.66	3803	2.95	3517
3	$\alpha = 12$	-512	3.08	4045	3.04	3943	3.08	3630	2.58	3728	2.81	3502
4	$S_{r^*} = 1.023$ (all r_i^* increased 2.3%)	590	3.40	3871	3.33	3857	3.32	3618	2.72	3815	3.07	3460
5	L-J potential with n = 9	-370	3.26	4406	3.17	4221	3.16	3799	2.64	3869	2.88	3698
6	CO_2 r* increased by 10%	626	3.37	3807	3.33	3755	3.38	3491	2.71	3751	3.07	3453
7	CO_2 r* decreased by 10%	-412	3.23	4158	3.15	4057	3.12	3734	2.61	3820	2.84	3567
8	H_2O r* increased by 10%	969	3.45	3679	3.38	3698	3.39	3508	2.94	3609	3.18	3396
9	H_2O r* decreased by 10%	-702	3.14	4254	3.07	4109	3.08	3738	2.41	3913	2.73	3603
10	All T_i^* equal	-5	3.30	4058	3.22	3987	3.19	3686	2.63	3856	2.94	3522
11	One-fluid mixture theory	550	3.35	3816	3.29	3794	3.31	3553	2.71	3779	3.07	3408
12	Ideal mixing	207	3.31	3987	3.24	3923	3.25	3636	2.67	3798	2.99	3495
13	ΔH_f for carbon = + 10 kcal/mole	50	3.23	3887	3.15	3686	3.18	3619	2.87	3626	2.95	3517
14	ΔH_f for carbon = + 20 kcal/mole	170	3.00	3804	2.91	3502	2.93	2784	2.87	3626	2.95	3517

Table 4.3. Calculated Values of D, γ and T for Compensated[a] Single-Parameter Variations.

Run	Description	S_r^* (Scale Factor for All r_i^*)	$D_{calc} - D_{exp}$ for RDX $\rho_o = 1.8$	RDX $\rho_o = 1.8$		Comp. B $\rho_o = 1.714$		TNT $\rho_o = 1.64$		Nitromethane $\rho_o = 1.131$		NM/HNO_3 $\rho_o = 1.293$	
				γ	T	γ	T	γ	T	γ	T	γ	T
15	$\alpha = 12$	1.027	8	3.19	3882	3.15	3844	3.18	3591	2.64	3749	2.93	3438
16	$\alpha = 14$	0.9776	108	3.38	4169	3.28	4060	3.25	3720	2.68	3849	2.94	3580
17	CO_2 r* increased by 10%	0.9807	85	3.30	3946	3.26	3838	3.32	3521	2.64	3728	2.95	3511
18	H_2O r* increased by 10%	0.9651	92	3.32	3924	3.25	3849	3.25	3566	2.82	3633	2.99	3496
19	One-fluid mixture theory	0.9804	99	3.27	3959	3.21	3882	3.24	3589	2.63	3775	2.97	3462

[a] In each case the r_i^* have been scaled to keep the calculated high-density RDX detonation velocity close to the experimental value.

Chapter 5

COMPARISON WITH EXPERIMENT

Having examined the effect of varying the parameters, we now make a more extensive comparison with experiment.

The "central point" set of parameters described in Chapter 4 was used for all of the calculations. To make the comparison as meaningful as possible, we considered a wide variety of explosives. The principal characteristics affecting the choice were: accuracy of the data, oxygen-balance, density, and variety of atomic composition, with particular emphasis on those explosives which lack one or more of the elements C, H, O, and N. In order to attain the desired variety, we included some explosives for which the experimental data are relatively poor.

The explosives chosen are listed in Table 5.1.

5.1 Applicability of the Hydrodynamic Theory

As often happens, the system for which a simple theory can be constructed is not the one on which experiments can be performed. The Zeldovich-von Neumann theory described in the introduction of this report

Table 5.1. Explosives for Comparison of Calculation and Experiment.

Symbol	Explosive	Empirical Formula	Composition[b] (Mole Fraction of Second Component)	Density[c] (g/cc)	Heat of Formation (kcal/mole)	Oxygen Balance to CO (%)	Oxygen Balance to CO_2 (%)	Data References for D	Data References for P	Data References for T
RDX	Cyclotrimethylene-trinitramine	$C_3H_6O_6N_6$		1.80	14.71[1]	0	-22	6, 7[h]	7, 16, 17	18, 19
Comp. B	65/35 RDX/TNT	$C_{4.4}H_{5.7}O_6N_{4.9}$		1.714	3.49[d]	-9	-40	8	8, 16, 17	—
TNT	Trinitrotoluene	$C_7H_5O_6N_3$		1.64	-17.81[2]	-25	-74	7, 9	7, 8, 16, 17	—
PETN	Pentaerythritol tetranitrate	$C_5H_8O_{12}N_4$		1.67	-123[3]	+15	-10	10, LA	LA	19, LA
HN	Hydrazine nitrate	H_5O_3N		1.63	-60[4]	—	—	4, LA	—	—
HNB	Hexanitroso-benzene	$C_6O_6N_6$		1.76	144.5(LA)[e]	0	-38	LA	—	—
TNTAB	Trinitro-triazido-benzene	$C_6O_6N_{12}$		1.74	270.6(LA)	0	-29	LA	—	—
NM/HNO_3	Nitromethane/ nitric acid/ water(T_o = 0 °C.)[a]	$C_{.4}H_2O_{2.3}N_{.9}$		1.293	-37.5(LA)	+14	-26	LA	LA	LA
NG	Nitroglycerine	$C_3H_5O_9N_3$		1.60	-82.7[3]	25	4	7, LA	—	18, LA
CT	Cyanuric triazide	C_3N_{12}		1.15	222[3]	—	—	11	—	—
NM/TNM	Nitromethane/ tetranitromethane (T_o = 0 °C.)	CH_3O_2N	0	1.131	-21.28[5]	-13	-38	7, 12, 13, LA	7, LA	18, LA
		CO_8N_4	1	1.64	8.8[5]	57	49			
CH_4/O_2	Liquid methane/ oxygen (T_o = 90 °K)	$C_{.50}H_2O$	0.5	0.765	-9.2[f]	-33	-67	14	—	—
		$C_{.22}H_{.80}O_{1.6}$	0.8	0.980	-4.3	54	42			
O_2/O_3	Liquid oxygen/ ozone (T_o = 96 °K)	$O_{2.4}$	0.4	1.258	11.4[g]	—	—	15	—	—
		O_3	1	1.554	30.9	—	—			

Notes for Table 5.1

[a]The composition of this mixture is given in Table 4.1.

[b]The extremes of composition for which measurements are available.

[c]For the solids, the maximum density is given. The detonation velocity data extend to less than 1.0 g/cc in most cases. All of the densities are given in the references below except for O_2 - O_3 for which we calculated the mixture densities from the experimental values assuming ideal mixing (molar volumes).

[d]This value was calculated from those of RDX and TNT assuming ideal mixing (molar enthalpies).

[e]LA denotes previously unpublished Los Alamos data described in Appendix C.

[f]Ideal mixing is assumed. For CH_4, the value ΔH_f = - 17.33 kcal/mole was calculated from the gaseous heat of formation given in F. D. Rossini, et al., National Bureau of Standards Circular 461 (1947), and from the heat of vaporization given in F. Din, Thermodynamics Functions of Gases (Butterworths, London, 1961), Vol. 3, p. 47, with a 10° extrapolation. For O_2, the value ΔH_f = - 1.009 kcal/mole was obtained by a small extrapolation from the data in reference 5 of this Table.

[g]Ideal mixing is assumed. For O_3, the value ΔH_f = 30.9 kcal/mole was obtained from data given in reference 5 of this Table, and the liquid heat capacity C_p = 0.45 cal/g, from Handbook of Chemistry and Physics (Chemical Rubber Publishing Co., Cleveland, Ohio, 1961), 43rd Ed., p. 2237.

[h]The data used for comparison with the calculations were selected from the references in the last three columns of the Table. Data from the underscored references were omitted in this selection.

References for Table 5.1.

Heats of Formation

1. E. J. Prosen, National Bureau of Standards, private communication. RDX

2. G. Stegeman, Report OSRD B-5306, July, 1945 (NDRC B-5306). TNT

3. A. Schmidt, Z. ges. Schiess- u Sprengstoffw. 29, 262 (1934) PETN, NG, CT

4. E. A. Christian and H. G. Snay, Report NAVORD-1508, Nov. 1956. HN

5. F. D. Rossini, et al., National Bureau of Standards Cir. 500, Feb. 1952. NM/TNM, CH_4, O_2

Detonation Velocities

6. W. Fickett, W. W. Wood, and Z. W. Salsburg, J. Chem. Phys. 27, 1324 (1957). RDX, TNT, Comp. B

7. A. N. Dremin and P. F. Pokhil, Doklady Akad. Nauk S.S.S.R. (Physical Chemistry Section) 127, 1245 (1959); 128, 989 (1959). RDX, TNT, NM/TNM, NG

8. W. E. Deal, Phys. Fluids 1, 523 (1958). Comp. B

9. M. J. Urizar, E. James, and L. C. Smith, Phys. Fluids 4, 262 (1961); A. W. Campbell, et al., Rev. Sci. Instruments 27, 567 (1956). TNT

10. D. P. MacDougall, G. H. Messerly, and M. D. Hurwitz, Report OSRD-5611, Jan. 1946. PETN

11. H. Muraour, Bull. Soc. Chim. France (4) 51, 1156 (1932); H. Kast and A. Haid, Z. Angew. Chem. 38, 43 (1925); W. Friederich, Z. ges. Schiess- u Sprengstoffw. 28, 113 (1933). The available data have been collected by A. H. Blatt, Report OSRD-2014, Feb. 1944. CT

12. A. W. Campbell, M. E. Malin, and T. E. Holland, J. Appl. Phys. 27, 963 (1956). NM

13. I. M. Voskoboinikov and G. S. Sosnova, Zhur. Prik. Mekh. Tekh. Fiz. 1961, 1933-35. NM/TNM

References for Table 5.1.
(Continued)

14. A. G. Streng and A. D. Kirshenbaum, J. Chem. and Eng. Data 4, 127 (1959). — $CH_4/O2$

15. R. O. Miller, J. Phys. Chem. 63, 1054 (1959). — O_2/O_3

Pressures

16. W. E. Deal, J. Chem. Phys. 27, 796 (1957).

17. M. A. Cook, R. T. Keyes, and W. O. Ursenbach, Third Symposium on Detonation, Princeton University, Sept. 1960, (Office of Naval Research), Vol. 2, p. 357.

RDX, Comp. B, TNT

Temperatures

18. I. M. Voskoboinikov, and A. Ya. Apin, Doklady Akad. Nauk S.S.S.R. (Physical Chemistry Section) 130, 804 (1960). — RDX, NM/TNM, NG

19. F. C. Gibson, et al., J. Appl. Phys. 29, 628 (1958). — RDX, PETN

assumes one-dimensional flow behind a plane shock front. Edge effects in the necessarily finite charges used in practice of course produce curved shock fronts followed by a two-dimensional expanding flow. The usual method of bridging the gap is to perform experiments at several charge diameters and then to extrapolate the results to infinite diameter, where the edge effects disappear. For pressed solids, of course, the particle size must be small, so that the material is as homogeneous as possible.

Recent experimental work has revealed new difficulties: apparently one-dimensional reactive flow is not always stable. White[51] has observed that the reaction zones of gas detonations are turbulent. The turbulence is probably associated with chemical reaction, for it appears close to the shock front and decays when reaction is complete. Denisov and Troshin,[52] Duff,[53] and others have shown, again for gas detonations, that transverse waves similar to those associated with spinning detonations are much more common than was once believed. These waves exhibit regular patterns which are probably associated with reflection from the tube walls. Recent experiments with liquid explosives at this laboratory[54] also show effects which suggest the presence of similar phenomena.

These poorly understood effects, if present in condensed explosives, may cause serious difficulty. They probably arise more from the unstable nature of one-dimensional flow than from edge effects, and may not be eliminated by extrapolation to infinite charge diameter.

5.2 Interpretation of the Data

Four quantities associated with the detonation will be considered: the velocity, CJ pressure, and CJ temperature of the steady unsupported detonation wave, and the strength of the shock produced in a light gas at an explosive-gas interface parallel to the front. We discuss briefly the methods of measurement and the interpretation of the data.

Detonation Velocity

The measurement of detonation velocity is relatively straightforward. The much-used smear camera method gives single velocity measurements accurate to within 50 to 100 m/s. With careful attention to detail, including the charge preparation, the more accurate pin method has given errors as small as 10 m/s, about one-sixth of one per cent, in the extrapolated infinite diameter velocity.[55] For most explosives the extrapolation to infinite diameter is facilitated by the apparently linear form of the detonation velocity as a function of reciprocal charge diameter.

Pressure

The most common method of measuring CJ pressure is an indirect one. Flat plates of metal (or other inert material) of different thicknesses are placed on the ends of explosive charges, and the free-surface velocities produced by the detonation are measured. If the metal shock Hugoniot is

known, the metal pressures can be obtained from this data. The resulting pressure-plate thickness curve,

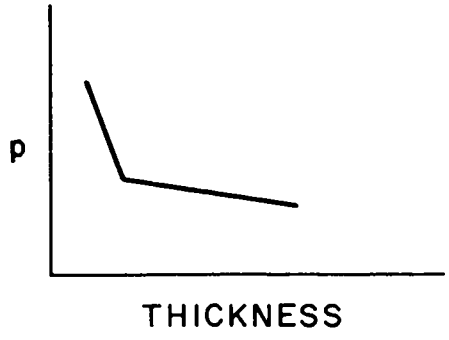

is an approximate magnified image of the pressure profile in the detonating explosive. The break in the curve is assumed to correspond to the CJ plane in the explosive, and the explosive pressure is obtained from the metal pressure at this point by the hydrodynamic conservation conditions. Again the experiment should be repeated at different charge diameters, and the results extrapolated to infinite diameter.

This is difficult to do, both because the method involves "looking behind" the CJ plane into a flow region affected by edge effects, and because the pressure depends strongly on the diameter. Careful attempts to perform the extrapolation at this laboratory suggest that perhaps the instability effects described above may be present.

The plots of pressure vs. reciprocal diameter appear to be linear with slopes on the order of 10 - 15% change in pressure per reciprocal inch of diameter.

The metal plate velocities can be measured to within 0.5%, and the pressures in any given geometry can be determined within about 2%, allowing for impurities in the material and imperfections in the charges. For the infinite-diameter figure, an error of 3 to 5% should probably be assigned, depending on the largest diameter used and the way in which the extrapolation is done. These figures do not allow for uncertainties which may be introduced by the possible presence of instability effects.

Temperature

Temperature is measured by analyzing the visible light from the detonation. A color temperature is obtained from measurements at two or more wavelengths or a brightness temperature from a single absolute measurement. In either case, it is assumed that most of the radiation seen by the detector originates near the CJ plane, and that the radiating material behaves like a blackbody. With the detector facing the oncoming wave, it is desirable that the detonation products be opaque and the cooler reaction zone thin, so that only light from the CJ plane is emitted and is transmitted unchanged through the reaction zone. There is some evidence that this is the case for many explosives and that the blackbody assumption is satisfied.

Since unreacted solid explosives are opaque, they are more difficult to measure than liquids. The technique of inserting plastic "light pipes" used by Gibson et al.[56] may be questioned on the grounds that the results are affected by the shock interactions at the explosive-plastic interface.

An alternate method (making the measurement just before the wave emerges from the end of the charge) severely limits the measurement time. Another serious difficulty is the spurious light emitted from the voids due to shocks either in the gas already present or in explosive product gases which have expanded into them.

Assuming the correctness of the assumptions, temperatures can be measured to within 100 to 150 °K for liquids and 300 °K for solids.

Gas Shock

The mass velocity of the shock produced by an explosive depends on the shape of the expansion isentrope of the detonation products, and can be computed from the Riemann integral if the expansion is assumed to be isentropic. This assumption will be more nearly satisfied as the shock moves away from the charge and the flow gradients decrease, so that measurement over some length of run is desirable as a check. Up to the point where side or end effects enter, the shock velocity should be constant if the expansion is isentropic, and this condition is met by the experimental data. For comparison with experiment, the Hugoniot of the gas must be known so that the mass velocity can be obtained from the measured shock velocity.

We use the experimental results for argon shocked by Composition B and air shocked by Composition B and TNT (Ref. 57; Ref. 58, Vol. 2, p. 386).

5.3 Results

The results of the calculation are presented and compared with experiment in Figs. 5.1 to 5.5 and Table 5.2. Some detailed numerical tabulations are given in Appendix D. We give here some comments on the data used and on the calculated results. General discussion of the comparison is given in the next chapter.

Data. We have selected for comparison those experimental data which, in our judgment, carry the smallest errors (see Table 5.1). The Russian values for the RDX velocities are within 50 m/sec of those obtained at this laboratory. The Russian velocities for TNT are also close to those obtained here, but not sufficiently accurate and detailed to confirm or deny the hook at the high-density end of the curve. The Los Alamos velocity for high-density PETN does not agree with the curve given in OSRD 5611. Both results for PETN are shown in Fig. 5.1.

For pressure, we have used the Los Alamos data exclusively, since most of the other work has been done with relatively small diameter charges and there is an appreciable diameter effect. The Russian pressure measurements on RDX and TNT indicate that γ is approximately independent of loading density down to about 1.0 g/cc.

The temperature data of Gibson et al. are omitted because all of their charges had low enough densities to give an appreciable quantity of voids. We doubt that the spurious light from this source can be entirely eliminated; the much lower value of temperature obtained for single-crystal PETN at this laboratory supports this view.

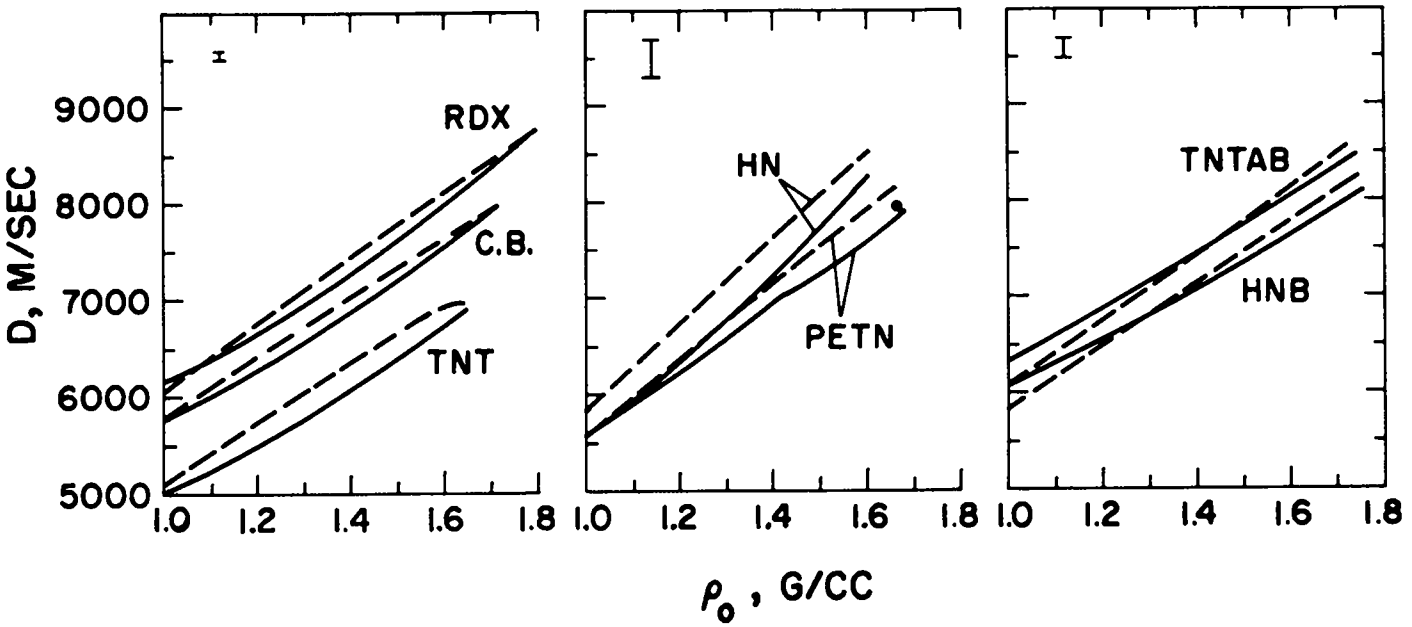

Fig. 5.1. Detonation velocities: calculated (——), experimental (- - -). The experimental error for TNT is ±10 m/s. The error on the single point shown for PETN is less than ±50 m/s.

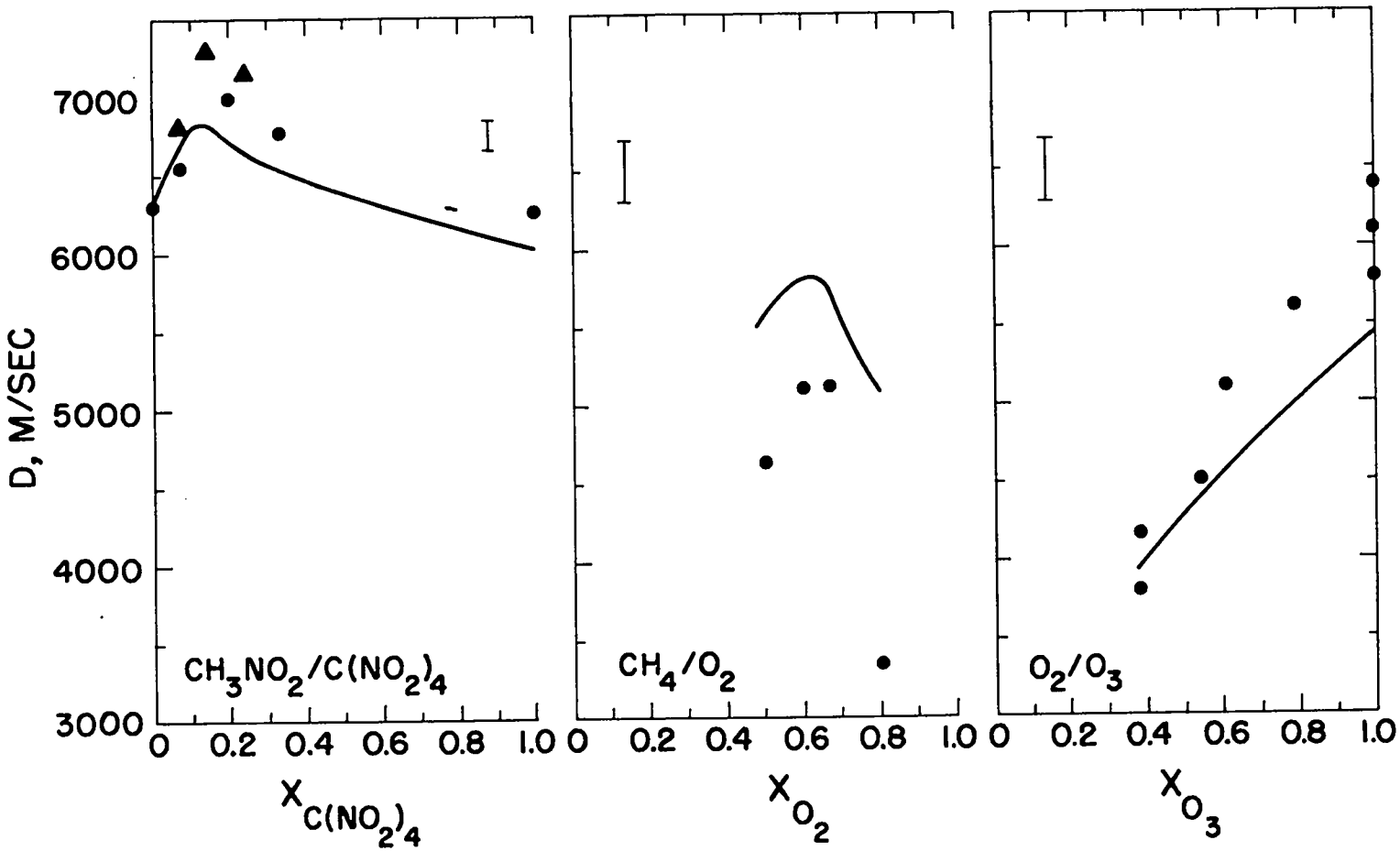

Fig. 5.2. Detonation velocities. The error for pure nitromethane is about ±40 m/s, less than that shown on the graph. For nitromethane/tetranitromethane the data shown are: ▲, Voskoboinikov and Sosnova; ●, data from this laboratory.

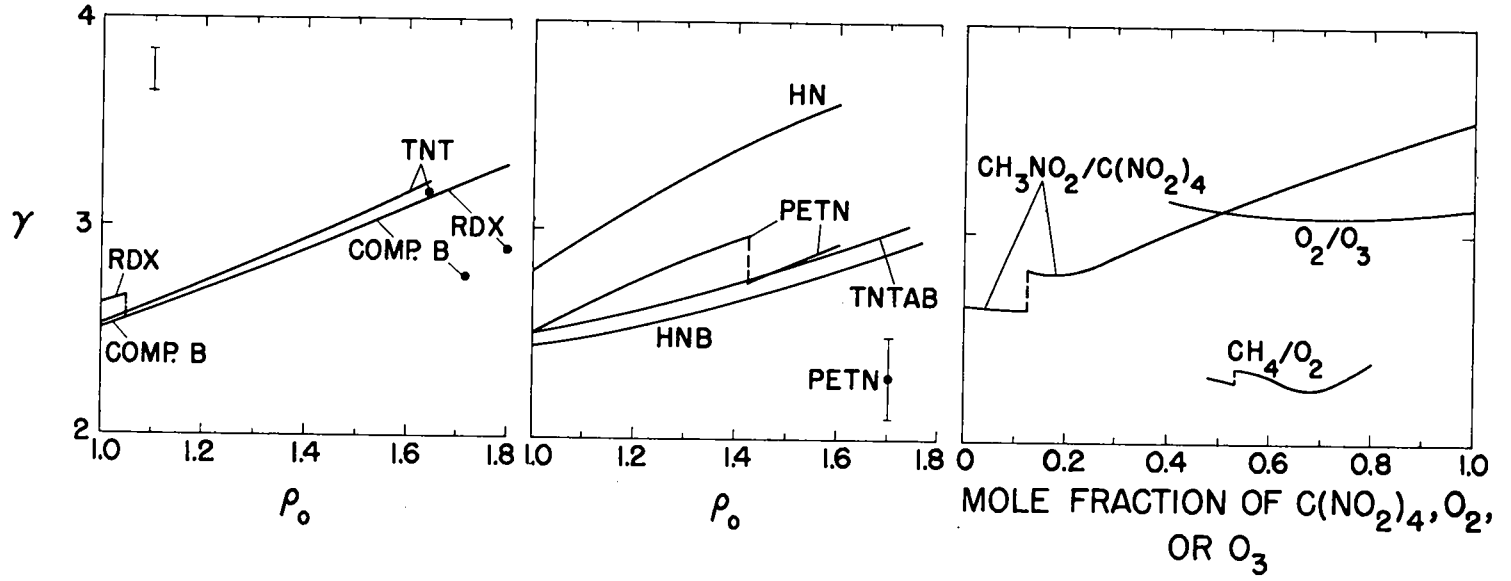

Fig. 5.3. Calculated and experimental values of $\gamma \left(= \frac{\rho_o D^2}{p} - 1 \right)$.

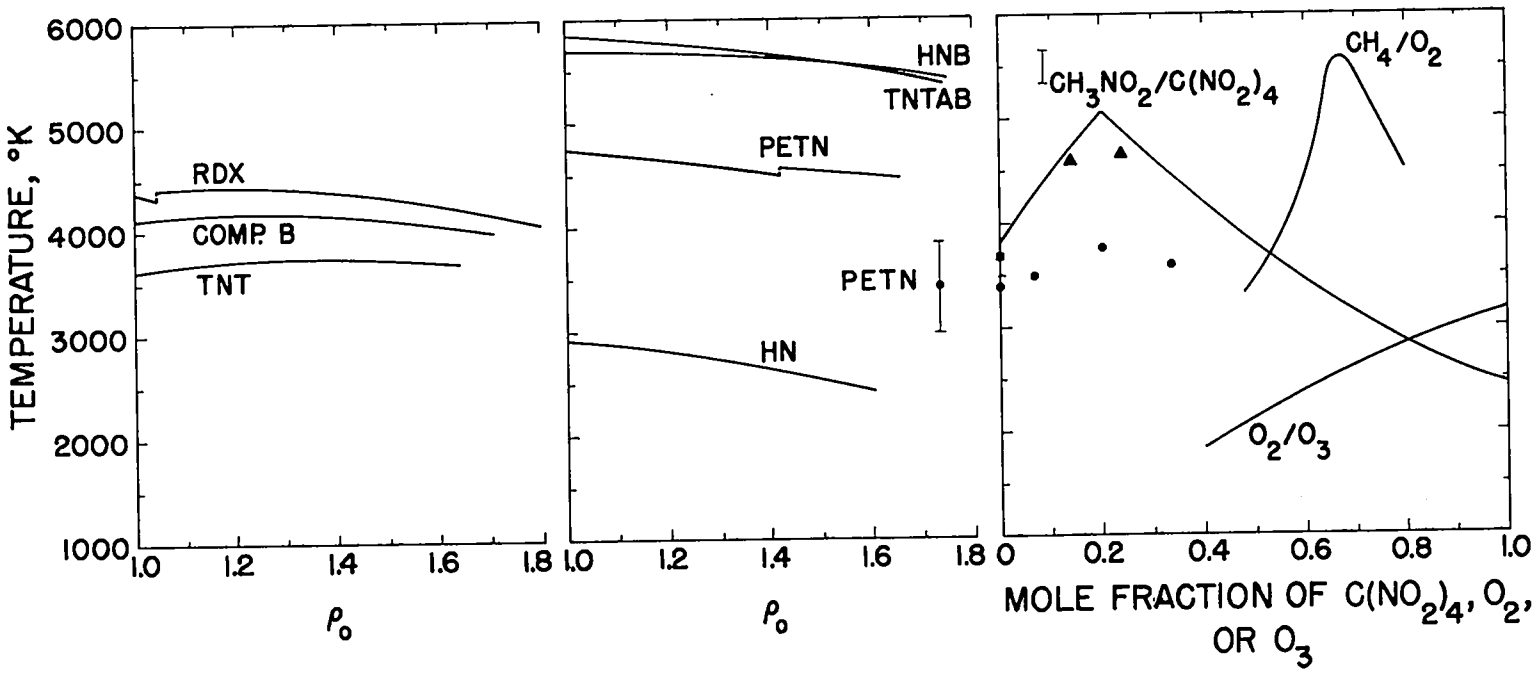

Fig. 5.4. Calculated and experimental detonation temperatures. The experimental data in the third figure are for nitromethane/tetranitromethane: ■, Voskoboinikov and Apin; ▲, Voskoboinikov and Sosnova; ●, data from this laboratory.

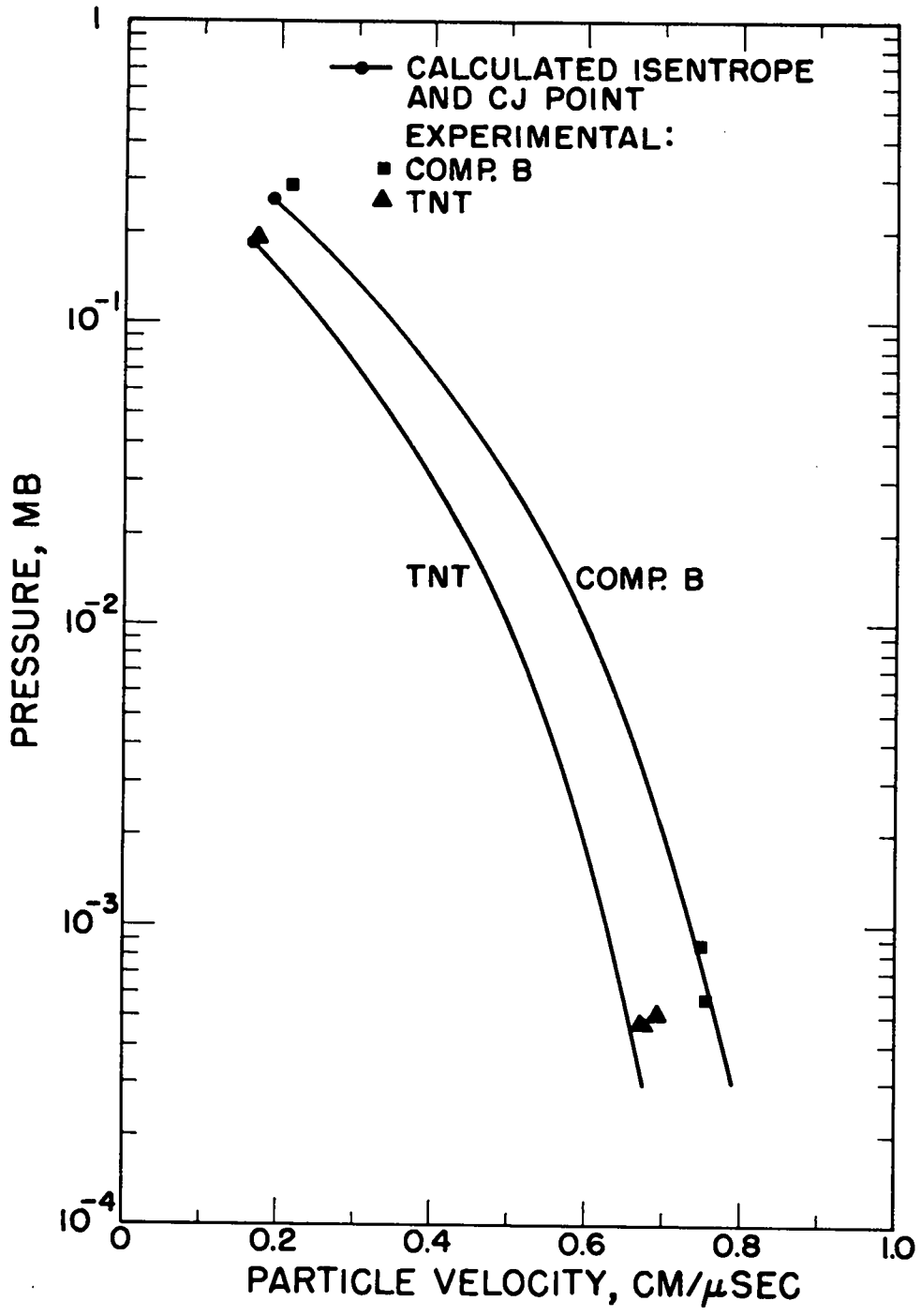

Fig. 5.5. Calculated pressures vs. particle velocities on the high-density CJ expansion isentropes compared with experimental particle velocities in gas shocks.

Table 5.2. Comparison of Calculated and Experimental Results.

Explosive	D (m/sec) calc	D (m/sec) exp	γ calc	γ exp	T (°K) calc	T (°K) exp
NM/HNO_3	6090	6580[a] ± 70	2.96	2.54 ±.25	3500	3400[a] ±100
Nitroglycerin	7286	7500[b] ± 50	3.08	2.70 ±.27	4679	3470[a] ±100
		7650[c] ±150				4000[c] ±150
						4000[d] ±100
Cyanuric triazide	6005	5545[e]	2.98	—	4261	—
		5550[f]				
		5560[g]				

[a] Davis and Mader
[b] Mautz
[c] Voskoboinikov and Apin
[d] Gibson, et al.
[e] Kast and Haid
[f] Muraour
[g] Schmidt

In Figs. 5.1 to 5.5 and Table 5.2 we have indicated rough estimates of error for the experimental data. For the most part they are the figures given by the investigators concerned, but in a few cases we have modified them in the light of more recent experience and the examination of other experimental results.

Calculations. The calculated results are shown throughout as solid lines. As mentioned earlier, the quantity

$$\gamma \equiv \left(\frac{\partial \ln p}{\partial \ln v}\right)_S$$

is used instead of the CJ pressure, since it is a much more slowly varying function of the thermodynamic state. It is related to the CJ pressure by

$$\gamma = \frac{\rho_o D^2}{p} - 1 \quad .$$

The discontinuities in the curves of the CJ γ of several explosives as a function of initial density, Fig. 5.3, and the corresponding slope discontinuities in the velocity curves, Fig. 5.1, occur at the points of disappearance of solid carbon. Separate investigation of this behavior for PETN revealed that the isentropes have the general shape shown in Fig. 5.6 (the slope change is exaggerated). The change in the logarithmic slope (γ) across the phase line is about 13%. There is actually a small range of density, on the order of 0.01 g/cc, in which there are two CJ points (tangencies of the Rayleigh line to the equilibrium detonation Hugoniot) so that the two branches of the curve overlap slightly.

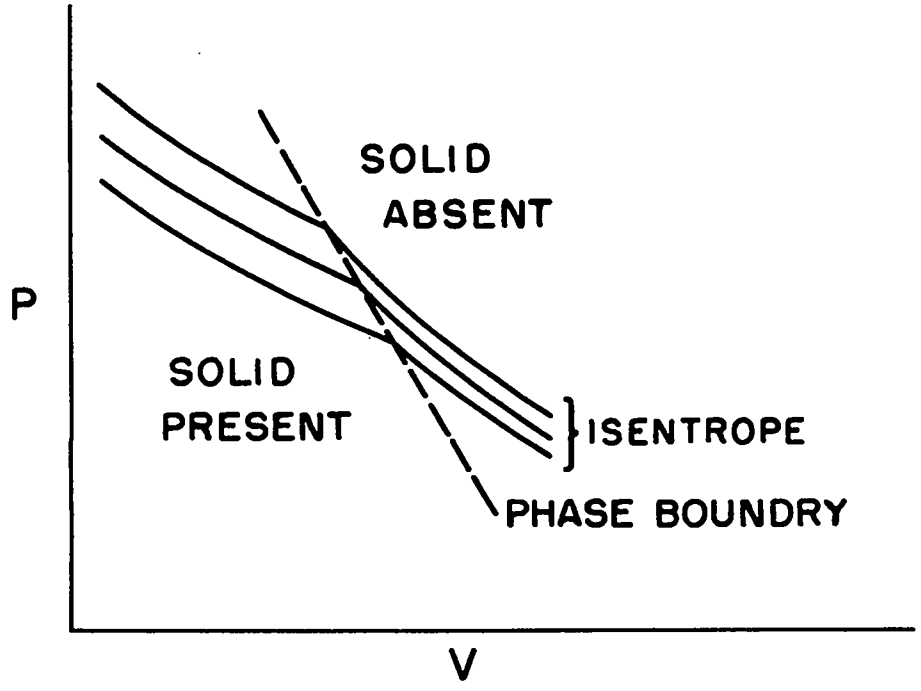

Fig. 5.6. Schematic representation of the isentropes in the neighborhood of a phase boundary.

Chapter 6

SUMMARY AND CONCLUSIONS

Under the assumption that the detonation products consist of mixtures of well-defined molecules in chemical equilibrium (plus solid carbon as a possible separate phase), we have used the best available statistical-mechanical equation of state theories consistent with a reasonable expenditure of computer time to calculate a detonation product equation of state for condensed CHON explosives. With this equation of state in the usual one-dimensional hydrodynamic model, together with the CJ hypothesis defining the thermodynamic state of the products in a plane, steady, unsupported detonation, we have tested the theory by comparing calculated and experimental results for a variety of CHON explosives. Unfortunately, there are both theoretical and experimental deficiencies in this program.

The equation of state theory is incomplete in that it assumes knowledge of the potentials of intermolecular force (pair potentials). These can be obtained experimentally from molecular-beam and low-temperature equation of state data, but many of them, particularly those for nonspherical molecules, are poorly known. Even with exact knowledge of the pair

potentials, major approximations remain in the statistical-mechanical theory. Most of the equation of state theories for mixtures are obtained by some type of perturbation from a pure fluid, and are so crude that at the pressures of interest even the sign of the deviation from ideal mixing cannot be predicted with any confidence. In our application there is another major approximation: it is assumed that the molecules are spherical, since realistic consideration of other shapes like those of CO_2 and H_2O would make the theory much more complicated.

On the experimental side, there is the difficulty that conditions corresponding to the one-dimensional hydrodynamic theory are approached only at infinite charge diameter, for the unavoidable edge effects in finite charges produce curved shock fronts and some two-dimensional flow. The usual practice is to make measurements at several charge diameters and then to extrapolate the results to infinite diameter, a procedure which increases both the amount of experimental work and the size of the error. A less transparent difficulty uncovered by recent work is the apparent instability of one-dimensional reactive flow: turbulence and other non-one-dimensional effects sometimes appear, so that comparison with a one-dimensional laminar flow theory is not entirely appropriate. Data obtained at the laboratory in careful attempts to extrapolate pressure measurements to infinite diameter have some puzzling features which may be due to such effects. In the following discussion of the comparisons between theory and experiment, these reservations should be kept in mind.

The comparison with experiment is complicated by the uncertain elements of the theory, mainly the pair potentials. Regarding these as

a set of adjustable parameters, we varied them within their ranges of uncertainty and found that the calculated detonation velocities and pressures could be placed either well above or well below the experimental values. Therefore, in making the final comparison, a single parameter, the repulsive exponent of the pair potential, was set to give approximate agreement with the experimental Hugoniots in the p-v plane for the more commonly used explosives. Calculations were then made for 13 CHON explosives and the results were compared with experiment (Chapter 5). The maximum deviations beyond experimental error were about 500 m/s in detonation velocity,* 45 kb in pressure, and 1000 °K in temperature. As a group, the oxygen-excess explosives are the worst offenders.

A possible next step is to ask whether there is some set of parameter values which lie within the ranges of uncertainty and give agreement within experimental error. A definite answer is precluded by the amount of work involved, but the parameter variations of Chapter 4 give some hints.

Although the average pair potential can be varied enough to make all of the calculated velocities and pressures too low or too high, the relative deviations from experiment and the values of CJ γ and temperature can be changed very little in this way. The same can be said for the different mixture theories. It is quite possible that the simple representations used for both of these very complex functions are inadequate. Although the forms used probably cover an adequate range of

*Excluding the extremes of composition in the liquid methane-oxygen system, where velocity deviations of about 800 and 1800 m/s are found.

"hardness", the real functions may have a much more complicated shape which could markedly affect the results.

Changing the carbon heat of formation presents interesting possibilities for changing both the CJ γ and the shape of the detonation velocity curves. Again a simple parameter is used to represent a much more complicated effect: the forces acting across the solid-fluid phase boundary.

The molecular sizes (values of r_i^* for the individual pair potentials) have the greatest effect on the calculated results. In addition to the results presented in Chapter 4, the calculations with the "geometric" sizes in Appendix E show what large changes in the results can be had from apparently reasonable changes in these values. They have been the principal source of variation in previous work of this sort with simpler equations of state, and would undoubtedly have to be varied to achieve much improvement in the agreement with experiment.

We eschew the large amount of work required to determine whether agreement with experiment might be obtained by variation of the uncertain elements of the theory and the parameters of the experimentally determined pair potentials. An affirmative result (which could signify nothing more than a cancellation of errors) might be obtained quickly, but the more interesting negative answer demonstrating the inadequacy of the theory could be established only by an exhaustive survey of all possible variations.

The conclusions are not encouraging. The possible instability of one-dimensional reactive flow casts doubt on the applicability of the

simple hydrodynamic theory. The available body of equation of state theory, supplemented by experimental knowledge of the pair potentials, is a crude approximation to the multicomponent systems of interest. With slight calibration, this crude but relatively complex theory gives only fair agreement with experiment, comparable to that obtained with simpler and more empirical forms.

However, there are some new and interesting qualitative features, particularly in comparison with results from some of the empirical equations of state (Appendix E). The dip in the isentrope, Fig. E5, resulting from the attractive portion of the potential, is not produced by any of the simple theories; it partially explains the rather surprising experimental conclusion that some isentropes have a gamma-law form. The discontinuities in the CJ γ and temperature curves and in the slopes of the detonation velocity-density curves, in Figs. 5.1 and 5.3 at the point where the solid disappears, are quite pronounced. The increased sensitivity of the results to variations in the molecular sizes should serve as a warning against a too-cavalier use of the empirical forms.

For practical purposes, probably the best course of action is to settle on some one form --- in the present state of knowledge a frankly empirical form may be as good as any and would probably have the advantage of simplicity --- and sustain a continuing program of calibration and checking as experimental data are accumulated. The present work suggests the magnitude of the errors involved, and should serve as a warning against putting too much faith in the results.

Appendix A

EQUATIONS

A.1 Gas Equation of State

The LJD cell theory is used. For a single shell of neighbors, we have

$$\frac{A'}{RT} = 1 + \frac{NZ}{2}\frac{f(t)}{\theta} - \ell n[2\pi\sqrt{2}g(1)]$$

$$\frac{E'}{RT} = \theta^{-1}\left[\frac{NZ}{2} f(t) - \frac{g(w)}{g(1)}\right]$$

$$\frac{pV}{RT} - 1 = -\theta^{-1}\left[\frac{NZ}{2}\frac{t}{3}\frac{df(t)}{dt} - \frac{g\left(\frac{t}{3}\frac{\partial w}{\partial t}\right)}{g(1)}\right]$$

$$\theta = T/T^* \quad , \tag{A.1}$$

where the cell potential w is defined by the smoothing integral

$$w(x,t) = \int_{1-x}^{1+x} x'[f(tx') - f(t)]dx' \tag{A.2}$$

and the g function by the cell integral

$$g(z) = 2\int_0^b (z)\, x^2 e^{-w(x,t)/\theta} dx \quad . \tag{A.3}$$

Here A′ is the Helmholtz free energy, N is Avogadro's number, and Z is the coordination number of the lattice. (Z = 12 for a face-centered cubic lattice.) Physically, the integration variables x and x′ may be regarded as the distance from the cell center, in units of a, the nearest-neighbor distance. The upper limit b is the distance from the cell center to its boundary in the same units. All dimensionless thermodynamic quantities are functions only of the reduced temperature θ, and the reduced volume $t^3 = \left(\frac{a}{r^*}\right)^3$ ($= \frac{V}{(N/\sqrt{2})r^{*3}}$ for a face-centered cubic lattice). The pair potential has been written in dimensionless form with a reduced argument

$$u(r) = kT^* f(r/r^*) \quad . \tag{A.4}$$

The primes denote imperfection or configurational thermodynamic functions on a volume basis, that is, the difference between the total value of the quantity at given T and V and the value for an ideal gas at the same T and V.

Explicit expressions for the cell potential w for the pair potentials used here are given in references 3 and 34.

A.2 Solid Equation of State

We sketch the derivation, as well as giving the final results. The assumptions are:

(1) E(p,v) is linear in p .

(2) E is known on the shock Hugoniot $p_H(v)$ for $v < v_o$, and on the line $p = 0$ for $v > v_o$.

(3) On $p = 0$:

$$E = C_p(T_1 - T_o) \ , \tag{A.5a}$$

$$\frac{v_1}{v_o} - 1 = \alpha(T_1 - T_o), \quad \alpha \text{ and } C_p \text{ constant}, \tag{A.5b}$$

where subscript zero denotes the initial point (normal p and T) and subscript 1 denotes values on the line $p = o$. These assumptions lead immediately to

$$E = f(v)p + g(v) \tag{A.6a}$$

$$f(v) = \frac{v}{G} \tag{A.6b}$$

$$g(v) = p_H(v)\left[\tfrac{1}{2}(v_o - v) - \frac{v}{G}\right] + E_o \text{ for } v < v_o \tag{A.6c}$$

$$= \frac{C_p}{\alpha}\left(\frac{v}{v_o} - 1\right) \text{ for } v > v_o \ . \tag{A.6d}$$

Differential equations for p and T on an isentrope are given by the thermodynamic relations

$$-\left(\frac{\partial p}{\partial v}\right)_s = \frac{p + \left(\frac{\partial E}{\partial v}\right)_p}{\left(\frac{\partial E}{\partial p}\right)_v} \ , \qquad -\left(\frac{\partial \ell n\ T}{\partial \ell n\ v}\right)_s = \frac{1}{\left(\frac{\partial E}{\partial pv}\right)_v} \ . \tag{A.7}$$

With the above expression for p, these become

$$-\left(\frac{\partial p}{\partial v}\right)_s = \frac{p + pf'(v) + g'(v)}{f(v)} \ , \qquad \left(\frac{\partial \ell n\ T}{\partial \ell n\ v}\right)_s = -G \ . \tag{A.8}$$

The solutions are

$$p = Gv^{-(G+1)}\int_{v_1}^{v} v^{(G+1)}g'(v)dv, \tag{A.9a}$$

$$\frac{T}{T_1} = \left(\frac{v}{v_1}\right)^{-G} \quad . \tag{A.9b}$$

Given p and T, we can, in effect, write a single equation determining v as follows:

(1) Guess v.

(2) Solve Eq. A.9a for v_1. (When the integral is written out, v, appears only in an additive term of the form $(v_1/v)^{(G+1)}$.)

(3) Solve Eq. A.5b for T_1, and Eq. A.9b for T.

(4) Compare the calculated T with the given T.

(5) Guess a new v, and iterate until agreement is obtained in T.

A.3 Thermodynamic Functions

Tabular values of the enthalpy are fit with a polynomial in T. This fit is then differentiated and integrated to give the heat capacity and entropy, so that a thermodynamically consistent set of functions is obtained.[59] All numerical values except those for methane[60] are from the NBS Tables.[23]

A.4 Mixture Theories

We give here the equations for the most-used mixture theories. Equations for the others can be found in reference 36 and sources quoted there. The independent variables are T, p, and the mole fractions x_i ($i = 1 \ldots\ldots c$ with c components); the dependent variables are F', H', V, and μ_i' (molar Gibbs free energy, molar enthalpy, molar volume, and

chemical potential of species i, with primes denoting imperfection quantities on a pressure basis). It is assumed that all pure, or reference, fluids obey the same equation of state, denoted by the subscript r and given as a function of T, p, and the constants of the pair potential:

$$F'_r = F'_r\left(\frac{T}{T^*_r}, \frac{pV^*_r}{kT^*_r}\right) \quad , \qquad V^*_r = (N/\sqrt{2})r^{*3} \quad . \tag{A.10}$$

Ideal Mixing

The free energy is given by

$$F'(T,p,\vec{x}) = \sum_{i=1}^{c} x_i F'_r\left(\frac{T}{T^*_i}, \frac{pV^*_i}{RT^*_i}\right) \quad , \tag{A.11}$$

with similar expressions for volume and enthalpy. The imperfection chemical potential of species i is just the free energy of the pure substance at the same T and p

$$\mu'_i(T,p,\vec{x}) = F'_r\left(\frac{T}{T^*_i}, \frac{pV^*_i}{RT^*_i}\right) \quad . \tag{A.12}$$

Corresponding States (CS) Theory

A reference fluid is chosen with potential constants

$$\overline{T^*} = T^*_r = \sum_{i,j=1}^{c} x_i x_j T^*_{ij}; \qquad \overline{r^*} = r^*_r = \sum_{i,j=1}^{c} x_i x_j r^*_{ij} \quad . \tag{A.13}$$

The LH equation (2.11) is used with this substance as reference fluid. Thus, the sums in Eq. 2.11 vanish, and F', H', and V for the mixture are

the same as those for the reference fluid. The equations for the chemical potentials can be written as

$$\mu_i' - F_r' = E_r'\left[\frac{n}{\bar{T}^*}\left(\frac{\partial \bar{T}^*}{\partial n_i}\right)_{n_j, j\neq i}\right] + 3(pV_r - RT)\left[\frac{n}{\bar{r}^*}\left(\frac{\partial \bar{r}^*}{\partial n_i}\right)_{n_j, j\neq i}\right] , \qquad (A.14)$$

with

$$\frac{n}{\bar{T}^*}\left(\frac{\partial \bar{T}^*}{\partial n_i}\right)_{n_j} = 2\left(\sum_{j=1}^{c} x_j \frac{T_{ij}^*}{T_r^*} - 1\right), \qquad \frac{n}{\bar{r}^*}\left(\frac{\partial \bar{r}^*}{\partial n_i}\right)_{n_j} = 2\left(\sum_{j=1}^{c} x_j \frac{r_{ij}^*}{r_r^*} - 1\right) . \qquad (A.15)$$

One-Fluid Theory

The mixture is replaced by a single substance with mean parameters given (for the LJ potential) by:

$$\bar{T}^* = \frac{[\Sigma(m)]^{n/(n-m)}}{[\Sigma(n)]^{m/(n-m)}}; \qquad \bar{r}^* = \left[\frac{\Sigma(n)}{\Sigma(m)}\right]^{1/(n-m)}; \qquad \Sigma(n) = \sum_{i,j=1}^{c} x_i x_j T_{ij}^* \left(r_{ij}^*\right)^n ;$$

$$\Sigma(m) = \sum_{i,j=1}^{c} x_i x_j T_{ij}^* \left(r_{ij}^*\right)^m . \qquad (A.16)$$

The chemical potentials are given by Eq. A.14, with

$$\frac{n}{\bar{T}^*}\left(\frac{\partial \bar{T}^*}{\partial n_i}\right)_{n_j} = \frac{2}{n-m}\left[\frac{\sum_{j=1}^{c} x_j T^*_{ij}\left(r^*_{ij}\right)^n}{\Sigma(n)} - \frac{\sum_{j=1}^{c} x_j T^*_{ij}\left(r^*_{ij}\right)^m}{\Sigma(m)}\right],$$

$$\frac{n}{\bar{r}^*}\left(\frac{\partial \bar{r}^*}{\partial n_i}\right)_{n_j} = -2 - \frac{2}{n-m}\left[m\frac{\sum_{j=1}^{c} x_j T^*_{ij}\left(r^*_{ij}\right)^n}{\Sigma(n)} - n\frac{\sum_{j=1}^{c} x_j T^*_{ij}\left(r^*_{ij}\right)^m}{\Sigma(m)}\right]. \quad \text{(A.17)}$$

A.5. Gas-Solid Mixture

The molar quantities for the mixture are linear combinations of those for the solid and gas (sub s and sub g).

$$V = x_s V_s(T,p) + x_g V_g(T,p)$$

$$H = X_s\left[H_s^{(id)}(T) + H_s'(T,p)\right] + x_g\left[H_g^{(id)}(T) + H_g'(T,p)\right]$$

etc.

$$x_s = \frac{n_s}{n_s + n_g}; \qquad x_g = \frac{n_g}{n_s + n_g},$$

where n_s and n_g are the number of moles of solid and gas products, and the superscript (id) denotes ideal thermodynamic functions.

As described in Appendix B, the principal independent variables are T and p; but T and V are used in the gas equation of state. The gas imperfection functions relative to ideal gas at the same T and p are related to those relative to ideal gas at the same T and V by

$$\begin{Bmatrix} E'(T,p) \\ H'(T,p) \end{Bmatrix} = \begin{Bmatrix} E'(T,V) \\ H'(T,V) \end{Bmatrix}$$

$$\begin{Bmatrix} A'(T,p) \\ F'(T,p) \end{Bmatrix} = \begin{Bmatrix} A'(T,V) \\ F'(T,V) \end{Bmatrix} - \ell n \frac{pV}{RT} \quad , \tag{A.18}$$

where

$$F'(T,p) = F - F^{(id)}(T,p)$$

$$F'(T,V) = F - F^{(id)}(T,V), \text{ etc.} \tag{A.19}$$

Specific quantities are obtained by multiplying the molar ones by $\frac{n}{M_o}$, where n is the total number of moles of products ($n = n_s + n_g$) and M_o is the number of grams of material considered (ordinarily the molecular weight of the undetonated substance). The zero of energy is taken as elements at 0 °K.

A.6 Hugoniot Equation and Heat of Explosion

The Hugoniot equation is given by

$$h - h_o - \tfrac{1}{2}(p - p_o)(v_o + v) = 0; \qquad v = \frac{n}{M_o}V; \qquad h = \frac{n}{M_o}H \quad , \tag{A.20}$$

where h_o is the specific enthalpy of formation of the explosive from elements at T^o, and h is calculated as above but with elements at T_o for the zero of energy.

The specific energy of explosion is given by

$$Q = \frac{n}{M_o}\left\{ \sum_{(gas)}^{i} x_i\left[\Delta H_f(T_o)\right]_i + x_s\left[\Delta H_f(T_o)\right]_s \right\} - h_o - \frac{n}{M_o}RT_o \quad , \tag{A.21}$$

where x_i is the mole fraction of species i in the gas phase, and the ΔH_f are the enthalpies of formation at T_o.

Appendix B

CODE AND METHOD OF CALCULATION

The machine used was the IBM 7090. Much of the coding was done in the FORTRAN II system, but for both speed and convenience, some parts were done in longhand using the FAP assembly program.

B.1 Major Subroutines

Most of the computational work is done by six major subroutines. We give here a brief description and abbreviated set of specifications for each.

FROOT - Equation Solver

At many points in the calculation, the solution of a non-linear or transcendental equation is required. This is obtained by writing the equation as a function whose root is the desired solution, and locating the root by an iterative search. Given a code to calculate the function, FROOT controls the interation by supplying successively improved guesses for the independent variable and testing for convergence at each stage.

The method of regula falsi is used, with some added logical control which ensures convergence for any monotone function and often helps when the root lies near a pole or an extremum of a more complicated function.

The detonation calculation consists of a hierarchy of iterations. At the top, a nonlinear equation such as the Hugoniot relation must be solved, but the calculation of the function for this iteration requires the iterative solution of another nonlinear equation, and so on through several stages. The routine is coded in such a way that it can simultaneously control any number of iterations interlocked in this way.

GES - Gas Equation of State

This routine calculates the pure-component equation of state for the gaseous mixture, using the LJD cell theory. The cell integrals are done numerically using the 16-point Gauss method. The inner (smoothing) integral, which gives the cell potential, can be evaluated analytically for all of the forms of the pair potential used here.

The integrands of the cell integral have the general form

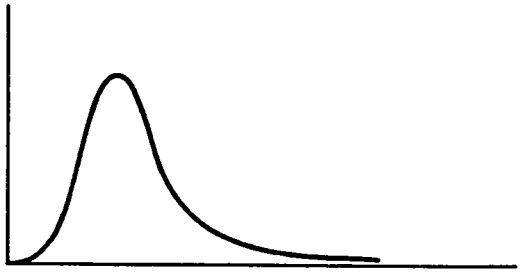

At high densities they are squeezed up into a small fraction of the nominal

range of integration. Accuracy is preserved by testing for the point at which the integrand effectively vanishes and setting the sixteen arguments for the Gauss quadrature accordingly. It is perhaps worth noting that our form of the g integral (given in Appendix A) represents an improvement over that used by Hirschfelder[34] and by Wood and Fickett[61] in that the infinite slope of the integrand at the origin and the resulting numerical complication have been removed.

Temperature and volume are the natural independent variables. Given these, the pressure and energy, and all of their derivatives with respect to temperature and volume, are also calculated. While this requires the calculation of several more integrals, it costs little in additional computing time.

Unfortunately, temperature and pressure are more convenient for the other parts of the detonation calculation, so an iterative loop controlled by FROOT is used to determine the gas volume for a given pressure and temperature.

The specifications are:

Input: (1) T and p.

(2) Intermolecular potential constants:

α (or n), r*, T*.

Output: Gas volume and all imperfection thermodynamic functions and their derivatives.

Time: About 0.15 sec. for the primary calculation at given T and V; two to four times this for the overall calculation at given T and p.

SES - Solid Equation of State

This routine calculates the solid equation of state by the method outlined in Appendix A. The required iteration is controlled by FROOT. The specifications are:

Input: (1) Constants characterizing the solid.

(2) T and p.

Output: Volume and imperfection thermodynamic functions of the solid.

Time: Less than 0.02 sec.

ITF - Ideal Gas Thermodynamic Functions

This routine calculates the ideal gas thermodynamic functions from analytic fits of calculated results, using the approach described in reference 59 in which all thermodynamic functions are derived by appropriate operations on the energy fit and are thus internally consistent. The specifications are:

Input: (1) Coefficients of the energy fit and heats of formation.

(2) T, p, and mole fractions.

Output: Ideal gas thermodynamic functions for the gas mixture including chemical potentials with appropriate energy zero for each individual species.

Time: Less than 0.02 sec.

EQ - Equilibrium Composition

The method of Brinkley (Ref. 46, p. 58) is used with some refinements. The necessary matrix equation is solved to allow specification of the system in terms of its atomic composition rather than amounts of a set of compounds from which it could be prepared. The entire list of chemical formulas is given as input, and a convenient means for specifying the subset of independent components is provided. The special method for homogeneous systems is used, modified to allow for one additional pure phase; this results in an iteration set of linear equations which is of lower degree than that given by the general theory. Automatic determination of the correct number of phases is provided. The specifications are:

Input: (1) Atomic composition of the system.

(2) Chemical formulas of the species.

(3) Specification of the independent components.

(4) Standard free energies of each species for the calculation of the equilibrium constants

$$F_i^\dagger = \mu_i - \ell n\, x_i,$$

where μ_i and x_i are the total chemical potential and mole fraction of species i. (For the solid, $F^\dagger$ is just its total free energy.)

Unfortunately, the $F_i^\dagger$ in general depend on the composition so that an outer iteration becomes necessary. The procedure used is:

(1) Given the x_i, calculate a set of $F_i^\dagger$.

(2) Using this set of $F_i^\dagger$ as input, calculate a new set of x_i.

(3) Take the mean of input and output x_i, and repeat steps (1) and (2) until the input and output x_i agree.

The time required for calculating a set of x_i from given $F_i^\dagger$ is about 0.1 sec. The complete process takes several times as long.

MIX - Mixture Theory

This code calculates the chemical potentials at each cycle of the outer iteration of the equilibrium calculation, and the thermodynamic functions of the gas phase when the final composition has been found. The amount of calculation done in the equilibrium iteration depends on which mixture theory is used. For ideal mixing, the chemical potentials are independent of the composition and the outer iteration is completely eliminated, but the time-consuming GES calculation must be executed once at the beginning for each species present in order to get all the chemical potentials. For the LH theory, one execution of GES is sufficient; the chemical potentials must be recomputed for each cycle of the outer iteration, but since the reference fluid is fixed, the GES calculation need not be redone. The equations for the chemical potentials are quite simple, so this theory gives the fastest calculation. For the CS and one-fluid theories, the GES calculation must be repeated at each cycle of the outer iteration because the reference-fluid potential constants depend on the composition. The calculation time can be appreciably shortened by applying the LH type of expansion to the pure fluid to simulate the results of a

new GES calculation with the slightly changed values of $\overline{T}^*$ and $\overline{r}^*$ resulting from the successive changes in composition. As a check, the genuine GES calculation is repeated after the composition has converged, and if it differs significantly from the simulated one the whole process is repeated.

The LH theory gives the shortest calculation time; with the above shortcut the CS and one-fluid theories are next, and ideal mixing takes longest. The actual calculation time for MIX is small compared to the time required by EQ to calculate a new composition from the chemical potentials. The overall time differences arise from the different ways in which MIX controls the outer equilibrium iteration, as described above.

B.2 Control

A small control code named MES (mixture equation of state) causes the major subroutines to be executed, then uses the resulting information to calculate the properties of the two-phase mixture comprising the detonation products. The rest of the code is based on this routine.

At the next higher level, control codes calculate various curves such as the detonation Hugoniot and isentropes. The Hugoniot equation is solved by FROOT, taking p as the independent variable and iterating on T, with use of MES to calculate the energy and volume at each step. The calculation of other curves is similar; for example, isentrope points are calculated at given p by varying T under control of FROOT until the entropy

takes on a specified value.

The calculation of the CJ state is somewhat more involved. A value of p is guessed, and a Hugoniot point is calculated at this p. The derivative $(\partial p/\partial v)_S$ is then gotten from a routine which calculates adjacent points on appropriate curves and gets thermodynamic derivatives by numerical differencing. This value for the slope of the isentrope is compared with the slope of the ray from the Hugoniot point to (p_o, v_o) to test the CJ condition. The pressure is then varied under control of FROOT until the CJ condition is satisfied.

Calculation times are about 1.5 sec. for an equation of state point at given temperature and pressure, 5 sec. for a Hugoniot or isentrope point, and 30 sec. for a CJ point.

Appendix C

EXPERIMENTAL DATA FROM THIS LABORATORY

The unpublished data obtained at this laboratory which were used in the comparisons of Chapter 5 are presented in Table C.1. Comments follow.

The velocity measurements on HNB and TNTAB were terminated before completion for safety reasons. A similar study of hydrazine nitrate, terminated before completion for the same reason, gave velocities within 50 m/s of the straight-line fit referenced in Table 5.1.

The pressure measurements are subject to the uncertainties discussed in Chapter 5. The value for nitromethane is for infinite diameter, obtained by extrapolating results at different diameters. The values for PETN and NM/HNO_3 are for the charge diameters shown. Infinite-diameter values for these explosives were estimated from pressure vs. reciprocal diameter data for other explosives and are shown in parentheses with corresponding larger errors. The error estimates shown do not allow for possible deviations from plane wave, laminar-flow values due to instability effects.

Table C.1. Explosives Data, Los Alamos Scientific Laboratory

Explosive	Composition Mole Fraction of TNM	Density (g/cc)	Charge Diameter (in.)	Velocity Measurement Method	Detonation Velocity (m/s)	Pressure (kb)	γ	Temperature[5] (°K)
PETN		1.671	1 2/3	pins	7974±25 (1)	300±6 (323±32)[d]	(2.29±0.23) (1)	3400±400
HNB		1.76	1/4[a]	pins	8262±100 (2) $D=2630+3200\rho_o \pm 100$ (2) $0.8 \leq \rho_o \leq 1.76$			
TNTAB		1.74	1/4	pins	8576±100 (2) $D=2730+3360\rho_o \pm 100$ (2) $0.8 \leq \rho_o \leq 1.76$			
NM/HNO_3		1.293	1 1/2	smear camera	6580±70 (3)	145±3 (3) (158±16)	(2.54±0.25) (3)	3400±100
NG		1.60	1 1/4	smear camera	7500±50 (4)			3470±100 (?)
NM/TNM	0	1.131	1 3/4	pins,[b]	6247±40 (5)	141[e], (1) ±7	2.13	3380±100
	0.067	1.20	3/4	arrival time[c]	6530±100 (5)			3480±100
	0.20	1.31	3/4	"	7000±100 (5)			3750±100
	0.333	1.40	3/4	"	6780±100 (5)			3580±100
	1.0	1.64	3/4	"	6250±100 (5)			3075±100 (?)
				pins[c]	6361±40 (5)			

[a] Some 1/2 in. shots were fired to check the diameter effect, found to be small. Brass confinement was used.
[b] Velocities were obtained relative to nitromethane by comparing the arrival time of the wave at the end of a tube of known length with that for a simultaneously fired tube of nitromethane. The second velocity listed for pure tetranitromethane was obtained by an independent method: pins placed outside of the confining tube.
[c] The velocity for pure nitromethane is that given in Table 5.1, included here for completeness.
[d] Estimated infinite-diameter values for PETN and NM/HNO_3 are given in parentheses. See text.
[e] The pressure for NM is an infinite-diameter value obtained by extrapolation from data at several diameters.
(1) B. G. Craig (2) M. J. Urizar (3) W. C. Davis, J. B. Ramsay (4) C. W. Mautz (5) W. C. Davis, C. Mader.

Temperatures were obtained from measurements of the absolute intensity of visible radiation from the detonation. Absolute brightness was measured to an accuracy of about 100 °K, and relative brightness to an accuracy of about 25 °K. If the radiation has blackbody character and most of it comes from the detonation products in the neighborhood of the CJ plane, then the CJ temperatures are known to about this degree of accuracy. There is some evidence that these assumptions may not be satisfied for nitroglycerin and tetranitromethane, where the detonation products appear to be quite transparent to visible radiation. The error estimates shown do not allow for the possible failure of these assumptions.

The heats of formation of HNB and TNTAB listed in Table 5.1 were obtained by A. Popolato of this laboratory.

Appendix D

NUMERICAL RESULTS

We give here machine lists of the results of some of the calculations. Table D.1 is a partial listing of the CJ points from the calculations described in Chapter 5. Table D.2 is a detailed listing of points on the detonation Hugoniot, CJ locus, and CJ isentrope of Composition B. The parameter set for all of these results is the "central point" set described in Chapter 4 and used for all of the calculations in Chapter 5:

(1) The LJD equation of state, with the CS mixture theory.

(2) The MM potential form with $\alpha = 13$.

(3) The experimental individual potential constants r_i^* and T_i^* from Table 2.1.

(4) Zero for the carbon heat of formation.

A key to the labels precedes the tables.

KEY FOR TABLES D.1 AND D.2[a]

Symbol	Definition	Units
RHO	initial density	g/cc
P	pressure	mb
V/V_o	relative volume	---
T	temperature	°K
U[b]	mass velocity	cm/μsec
D	detonation velocity	cm/μsec
V (line 2)	specific volume	cc/g
E	specific energy	mb-cc/g relative to elements at 0 °K
RBAR	mean r* for the product mixture $\overline{r^*} = \sum_{gas} x_i x_j r^*_{ij}$	Å
VBAR	close packed volume of a system of spheres of diameter $\overline{r^*}=(N/\sqrt{2})\overline{r^*}^3$	cc/mole gas
TBAR	mean T* for the product mixture $\overline{T^*} = \sum_{gas} x_i x_j T^*_{ij}$	°K
Q	heat of detonation	kcal/g
NS	moles of solid	moles/mole H.E.[c]
NG	moles of gas	moles/mole H.E.
N	total moles of products	moles/mole H.E.
VS	volume of solid	cc/mole solid
VG	volume of gas	cc/mole gas
V (line 3)	total volume of products	cc/mole products
C(S), N_2, etc.	composition (C(S) is solid carbon)	moles/mole H.E.
GAMMA	$(\partial \ln p/\partial \ln v)_S$	---
ALPHA	$(\partial E/\partial pv)_p$	---
BETA	$(\partial E/\partial pv)_v$	---
C	sound speed	cm/μsec

[a]Where two or more successively listed explosives have the same column headings, the headings are given only with the first explosive.

[b]In the "CJ Isentrope" portion of Table D.2, U appears on the last line of the list. The quantity W appearing in the space normally occupied by U is the work done, in kcal/g, on the surroundings by the explosive product gases when they have expanded to the pressure P in a hypothetical experiment which keeps the products in a uniform state (in space) at all times.[50]

[c]The molecular weights of the explosives are given with the labels.

Table D. 1. Calculated CJ Points for the Explosives of Table 5.1.

RDX M= 222

1 RHO	P	V/V0	T	U	D
2 V	E	RBAR	VBAR	TBAR	Q
3 NS	NG	N	VS	VG	V
C(S)	N2	CO	H2O	NO	H2
CO2	O2	CH4			
GAMMA	ALPHA	BETA	C		
1.8000E 00	3.2451E-01	7.6698E-01	4.0396E 03	2.0496E-01	8.7959E-01
4.2610E-01	2.7402E-02	3.8024E 00	2.3420E 01	1.4084E 02	1.4944E 00
1.4275E 00	7.5642E 00	8.9917E 00	3.7974E 00	1.1796E 01	1.0526E 01
1.4275E 00	2.9990E 00	1.0481E-01	2.9671E 00	1.9918E-03	2.3513E-02
1.4630E 00	2.2713E-05	4.6715E-03	0.	0.	0.
3.2916E 00	3.6375E 00	1.4089E CO	6.7464E-01		
1.4000E 00	1.9189E-01	7.4177E-01	4.3790E 03	1.8813E-01	7.2855E-01
5.2984E-01	2.4094E-02	3.8197E 00	2.3742E 01	1.3595E 02	1.4330E 00
9.8082E-01	7.9182E 00	8.8990E 00	4.3414E 00	1.4326E 01	1.3225E 01
9.8082E-01	2.9981E 00	6.7849E-01	2.7391E 00	3.8360E-03	1.5792E-01
1.2892E 00	4.7595E-05	5.1470E-02	0.	0.	0.
2.8727E 00	2.5621E 00	1.2400E 00	5.4043E-01		
1.0000E 00	1.0353E-01	7.2485E-01	4.3739E 03	1.6878E-01	6.1340E-01
7.2485E-01	2.0640E-02	3.8491E CO	2.4295E 01	1.2572E 02	1.2946E 00
0.	8.7449E 00	8.7449E 00	4.8109E 00	1.8412E 01	1.8412E 01
0.	2.9981E 00	1.9569E 00	2.2100E 00	3.7188E-03	5.3301E-01
9.1465E-01	4.0143E-05	1.2848E-01	0.	0.	0.
2.6344E 00	2.7485E 00	1.4229E 00	4.4462E-01		

COMP. B M= 224

1.7140E 00	2.5915E-01	7.6301E-01	3.9629E 03	1.8929E-01	7.9873E-01
4.4516E-01	2.1966E-02	3.8022E 00	2.3417E 01	1.4245E 02	1.4181E 00
2.6640E 00	7.0085E 00	9.6724E CO	4.0370E 00	1.2684E 01	1.0302E 01
2.6640E 00	2.4817E CO	1.8742E-01	2.7721E 00	1.5630E-03	3.7025E-02
1.5194E 00	1.8103E-05	9.1803E-03	0.	0.	0.
3.2195E 00	3.6281E 00	1.4375E 00	6.0944E-01		
1.4000E CO	1.6974E-01	7.4283E-01	4.1465E 03	1.7658E-01	6.8663E-01
5.3059E-01	1.9640E-02	3.8178E 00	2.3707E 01	1.3778E 02	1.3648E 00
2.2782E 00	7.3179E 00	9.5961E 00	4.4395E 00	1.4849E 01	1.2377E 01
2.2782E 00	2.4814E 00	6.9808E-01	2.5872E 00	2.2818E-03	1.4517E-01
1.3562E 00	2.6884E-05	4.7558E-02	0.	0.	0.
2.8885E 00	2.7589E 00	1.3013E 00	5.1005E-01		
1.0000E 00	9.4590E-02	7.1489E-01	4.1233E 03	1.6422E-01	5.7599E-01
7.1489E-01	1.7534E-02	3.8542E 00	2.4390E 01	1.2692E 02	1.2242E 00
1.2444E 00	8.1515E 00	9.3959E 00	4.8546E 00	1.8891E 01	1.7032E 01
1.2444E 00	2.4815E 00	2.0241E 00	2.0459E 00	1.9415E-03	4.8652E-01
9.6401E-01	1.7903E-05	1.4752E-01	0.	0.	0.
2.5075E 00	2.1784E 00	1.2676E 00	4.1177E-01		

TNT M= 227

1 RHO	P	V/V0	T	U	D
2 V	E	RBAR	VBAR	TBAR	Q
3 NS	NG	N	VS	VG	V
C(S)	N2	CO	H2O	NO	H2
CO2	O2	CH4			
GAMNA	ALPHA	BETA	C		
1.6400E 00	1.8376E-01	7.6320E-01	3.6620E 03	1.6289E-01	6.8787E-01
4.6537E-01	1.2958E-02	3.8000E 00	2.3376E 01	1.4696E 02	1.2808E 00
5.0459E 00	5.9260E 00	1.0972E 01	4.3531E 00	1.4130E 01	9.6336E 00
5.0459E 00	1.4997E 00	3.0390E-01	2.4235E 00	6.1273E-04	4.8126E-02
1.6360E 00	7.0253E-06	1.4208E-02	0.	0.	0.
3.2232E 00	3.9081E 00	1.5228E 00	5.2500E-01		
1.4000E 00	1.3062E-01	7.4696E-01	3.7203E 03	1.5365E-01	6.0722E-01
5.3354E-01	1.1496E-02	3.8138E 00	2.3632E 01	1.4224E 02	1.2373E 00
4.7367E 00	6.1803E 00	1.0917E 01	4.6273E 00	1.6062E 01	1.1100E 01
4.7367E 00	1.4996E 00	7.3628E-01	2.2924E 00	7.0429E-04	1.2423E-01
1.4853E 00	7.7187E-06	4.1682E-02	0.	0.	0.
2.9519E 00	3.1813E 00	1.4165E 00	4.5357E-01		
1.0000E 00	7.0933E-02	7.1639E-01	3.6306E 03	1.4184E-01	5.0010E-01
7.1639E-01	9.7508E-03	3.8497E 00	2.4306E 01	1.3003E 02	1.1081E 00
3.8071E 00	6.9492E 00	1.0756E 01	4.9835E 00	2.0684E 01	1.5127E 01
3.8071E 00	1.4997E 00	1.9978E 00	1.8555E 00	5.0086E-04	4.0053E-01
1.0731E 00	4.0151E-06	1.2199E-01	0.	0.	0.
2.5259E 00	2.5524E 00	1.4064E 00	3.5827E-01		

PETN M= 316

1.6000E 00	2.3129E-01	7.4564E-01	4.5005E 03	1.9175E-01	7.5385E-01
4.6602E-01	5.5371E-03	3.8378E 00	2.4080E 01	1.5126E 02	1.4887E 00
4.6502E-01	1.0501E 01	1.0966E 01	4.1699E 00	1.3846E 01	1.3436E 01
4.6502E-01	1.9968E 00	9.0239E-01	3.8627E 00	6.4084E-03	1.0024E-01
3.6141E 00	1.8858E-04	1.8527E-02	0.	0.	0.
2.9315E 00	2.6989E 00	1.2618E 00	5.6211E-01		
1.4000E 00	1.7098E-01	7.4695E-01	4.5159E 03	1.7580E-01	6.9471E-01
5.3353E-01	2.6050E-03	3.8440E 00	2.4197E 01	1.4640E 02	1.4347E 00
0.	1.0937E 01	1.0937E 01	4.4475E 00	1.5424E 01	1.5424E 01
0.	1.9965E 00	1.6733E 00	3.7326E 00	7.0932E-03	2.0056E-01
3.2933E 00	2.1110E-04	3.3421E-02	0.	0.	0.
2.9517E 00	3.5429E 00	1.5391E 00	5.1891E-01		
1.0000E 00	8.9596E-02	7.1529E-01	4.7535E 03	1.5971E-01	5.6098E-01
7.1529E-01	-9.3367E-05	3.8388E 00	2.4100E 01	1.4503E 02	1.4169E 00
0.	1.1022E 01	1.1022E 01	4.9133E 00	2.0518E 01	2.0518E 01
0.	1.9807E 00	1.8141E 00	3.7682E 00	3.8662E-02	2.3004E-01
3.1850E 00	4.4836E-03	8.7414E-04	0.	0.	0.
2.5124E 00	3.5847E 00	1.8249E 00	4.0126E-01		

HYDRAZINE NITRATE M= 95

1 RHO	P	V/V0	T	U	D
2 V	E	RBAR	VBAR	TBAR	Q
3 NS	NG	N	VS	VG	V
SOL	N2	H2O	NO	H2	O2
GAMMA	ALPHA	BETA	C		
1.6000E 00	2.3539E-01	7.8324E-01	2.4356E 03	1.7858E-01	8.2384E-01
4.8952E-01	-5.4973E-03	3.6195E 00	2.0201E 01	1.3093E 02	9.0540E-01
0.	4.2500E 00	4.2500E 00	4.0809E 00	1.0951E 01	1.0951E 01
0.	1.4785E 00	2.5000E 00	4.2958E-02	2.4792E-07	2.2852E-01
3.6134E 00	3.8579E 00	1.3444E 00	6.4527E-01		
1.4000E 00	1.6613E-01	7.7229E-01	2.6536E 03	1.6438E-01	7.2188E-01
5.5163E-01	-7.9319E-03	3.6195E 00	2.0201E 01	1.3087E 02	9.0280E-01
0.	4.2500E 00	4.2500E 00	4.4002E 00	1.2341E 01	1.2341E 01
0.	1.4728E 00	2.5000E 00	5.4389E-02	3.8745E-06	2.2281E-01
3.3915E 00	3.6947E 00	1.3843E 00	5.5750E-01		
1.0000E 00	8.0548E-02	7.3714E-01	2.9256E 03	1.4551E-01	5.5356E-01
7.3714E-01	-1.0856E-02	3.6196E 00	2.0202E 01	1.3079E 02	8.9935E-01
0.	4.2501E 00	4.2501E 00	4.8897E 00	1.6491E 01	1.6491E 01
0.	1.4653E 00	2.4999E 00	6.9313E-02	1.0655E-04	2.1540E-01
2.8042E 00	3.3145E 00	1.5386E 00	4.0804E-01		

HNB M= 252

1 RHO	P	V/V0	T	U	D
2 V	E	RBAR	VBAR	TBAR	Q
3 NS	NG	N	VS	VG	V
C(S)	N2	CO	NO	CO2	O2
GAMMA	ALPHA	BETA	C		
1.7600E 00	2.9054E-01	7.4651E-01	5.4207E 03	2.0457E-01	8.0699E-01
4.2415E-01	4.7225E-02	4.1091E 00	2.9558E 01	1.4927E 02	1.6347E 00
2.5874E 00	6.4293E 00	9.0167E 00	3.9640E 00	1.5036E 01	1.1859E 01
2.5874E 00	2.9845E 00	8.5854E-01	3.0928E-02	2.5540E 00	1.2342E-03
2.9449E 00	2.9073E 00	1.3268E 00	6.0242E-01		
1.4000E 00	1.9077E-01	7.2659E-01	5.6437E 03	1.9302E-01	7.0597E-01
5.1899E-01	4.4929E-02	4.0894E 00	2.9135E 01	1.3920E 02	1.5252E 00
1.9210E 00	7.0965E 00	9.0174E 00	4.3936E 00	1.7248E 01	1.4509E 01
1.9210E 00	2.9836E 00	2.1929E 00	3.2724E-02	1.8861E 00	1.0786E-03
2.6575E 00	2.2870E 00	1.2369E 00	5.1295E-01		
1.0000E 00	1.0873E-01	7.0840E-01	5.7046E 03	1.7806E-01	6.1062E-01
7.0840E-01	4.2154E-02	4.0656E 00	2.8627E 01	1.2743E 02	1.3588E 00
8.8075E-01	8.1313E 00	9.0120E 00	4.8364E 00	2.1439E 01	1.9817E 01
8.8075E-01	2.9884E 00	4.2626E 00	2.3104E-02	8.5669E-01	4.7713E-04
2.4294E 00	2.1218E 00	1.2850E 00	4.3257E-01		

TNTAB M= 336

1 RHO	P	V/VG	T	U	D
2 V	E	RBAR	VBAR	TBAR	Q
3 NS	NG	N	VS	VG	V
C(S)	N2	CO	NO	CO2	O2
GAMMA	ALPHA	BETA	C		
1.7400E 00	3.1129E-01	7.5177E-01	5.3650E 03	2.1073E-01	8.4894E-01
4.3205E-01	5.8388E-02	4.0903E 00	2.9153E 01	1.3960E 02	1.6046E 00
2.5981E 00	9.4238E 00	1.2022E 01	3.8859E 00	1.4342E 01	1.2083E 01
2.5981E 00	5.9793E 00	8.4753E-01	4.1449E-02	2.5544E 00	1.1228E-03
3.0285E 00	2.8738E 00	1.2791E 00	6.3820E-01		
1.4000E 00	2.0525E-01	7.3332E-01	5.6759E 03	1.9773E-01	7.4145E-01
5.2380E-01	5.5733E-02	4.0766E 00	2.8862E 01	1.3284E 02	1.5148E 00
1.8787E 00	1.0146E 01	1.2025E 01	4.3269E 00	1.6555E 01	1.4645E 01
1.8787E 00	5.9762E 00	2.2924E 00	4.7584E-02	1.8289E 00	1.1004E-03
2.7498E 00	2.3235E 00	1.2086E 00	5.4372E-01		
1.0000E 00	1.1460E-01	7.1368E-01	5.8588E 03	1.8115E-01	6.3266E-01
7.1368E-01	5.2591E-02	4.0593E 00	2.8495E 01	1.2443E 02	1.3801E 00
7.5185E-01	1.1266E 01	1.2018E 01	4.8078E 00	2.0976E 01	1.9965E 01
7.5185E-01	5.9824E 00	4.5326E 00	3.5281E-02	7.1557E-01	5.0137E-04
2.4925E 00	2.2159E 00	1.2902E 00	4.5151E-01		

NM/HNO3 M= 56

1 RHO	P	V/VO	T	U	D
2 V	E	RBAR	VBAR	TBAR	Q
3 NS	NG	N	VS	VG	V
C(S)	N2	CO	H2O	NO	H2
CO2	O2	CH4			
GAMMA	ALPHA	BETA	C		
1.2930E 00	1.2118E-01	7.4732E-01	3.5002E 03	1.5389E-01	6.0902E-01
5.7797E-01	-1.2656E-02	3.7109E 00	2.1770E 01	1.4467E 02	1.0886E 00
0.	2.0660E 00	2.0660E 00	4.6709E 00	1.5537E 01	1.5537E 01
0.	4.0262E-01	4.2718E-04	9.9989E-01	4.7251E-02	1.0915E-04
4.2587E-01	1.8984E-01	7.5162E-13	0.	0.	0.
2.9575E 00	3.7792E 00	1.6159E 00	4.5513E-01		

NITROGLYCERIN M= 227

1.6000E 00	2.0797E-01	7.5514E-01	4.6789E 03	1.7840E-01	7.2860E-01
4.7196E-01	4.0319E-03	3.8605E 00	2.4511E 01	1.5672E 02	1.5047E 00
0.	7.2705E 00	7.2705E 00	4.2784E 00	1.4736E 01	1.4736E 01
0.	1.4083E 00	3.7726E-02	2.4967E 00	1.8334E-01	3.2588E-03
2.9623E 00	1.7883E-01	2.4740E-08	0.	0.	0.
3.0841E 00	4.1253E 00	1.6619E 00	5.5020E-01		

CYURANIC TRIAZIDE M= 204

1 RHO	P	V/VO	T	U	D
2 V	E	RBAR	VBAR	TBAR	Q
3 NS	NG	N	VS	VG	V
C(S) N2					
GAMMA	ALPHA	BETA	C		
1.1500E 00	1.0424E-01	7.4863E-01	4.2612E 03	1.5095E-01	6.0050E-01
6.5098E-01	5.9630E-02	4.0500E 00	2.8300E 01	1.2000E 02	1.1144E 00
3.0000E 00	6.0000E 00	9.0000E 00	4.8017E 00	1.9732E 01	1.4756E 01
3.0000E 00	6.0000E 00	0.	0.	0.	0.
2.9781E 00	3.5414E 00	1.5249E 00	4.4955E-01		

NM/TNM MOLE FRACTION OF TNM = 0.0 M= 61.0

1 RHO	P	V/V0	T	U	D
2 V	E	RBAR	VBAR	TBAR	Q
3 NS	NG	N	VS	VG	V
C(S)	N2	CO	H2O	NO	H2
CO2	O2	CH4			
GAMMA	ALPHA	BETA	C		
1.1310E 00	1.2480E-01	7.2662E-01	3.8030E 03	1.7368E-01	6.3531E-01
6.4246E-01	4.8783E-03	3.7041E 00	2.1650E 01	1.3338E 02	1.3746E 00
3.6688E-01	2.4297E 00	2.7965E 00	4.6631E 00	1.5436E 01	1.4023E 01
3.6688E-01	4.9989E-01	2.4641E-01	1.1835E 00	2.1028E-04	1.1291E-01
2.8493E-01	1.7576E-06	1.0178E-01	0.	0.	0.
2.6580E 00	2.5028E 00	1.3178E 00	4.6164E-01		

NM/TNM MOLE FRACTION OF TNM = 0.067 M= 70.1

1.2000E 00	1.4704E-01	7.2475E-01	4.2502E 03	1.8365E-01	6.6721E-01
6.0396E-01	9.4326E-03	3.7513E 00	2.2489E 01	1.3545E 02	1.4477E 00
1.4454E-01	2.7353E 00	2.8799E 00	4.5599E 00	1.5235E 01	1.4699E 01
1.4454E-01	5.9962E-01	3.6364E-01	1.1725E 00	7.6095E-04	1.0703E-01
4.3156E-01	1.0540E-05	6.0258E-02	0.	0.	0.
2.6331E 00	2.3029E 00	1.2544E 00	4.8357E-01		

NM/TNM MOLE FRACTION OF TNM = 0.200 M= 88.0

1.3100E 00	1.5569E-01	7.3650E-01	5.0389E 03	1.7697E-01	6.7159E-01
5.6221E-01	1.2042E-02	3.8161E 00	2.3674E 01	1.4882E 02	1.6208E 00
0.	3.0458E 00	3.0458E 00	4.5456E 00	1.6251E 01	1.6251E 01
0.	7.7291E-01	8.0687E-02	1.1890E 00	5.4175E-02	1.0969E-02
9.1931E-01	1.8744E-02	2.0873E-06	0.	0.	0.
2.7950E 00	3.7825E 00	1.7110E 00	4.9463E-01		

NM/TNM MOLE FRACTION OF TNM = 0.333 M= 106.0

1.4000E 00	1.5295E-01	7.4556E-01	4.4570E 03	1.6673E-01	6.5528E-01
5.3254E-01	1.2804E-02	3.8513E 00	2.4336E 01	1.4648E 02	1.2994E 00
0.	3.5041E 00	3.5041E 00	4.5370E 00	1.6110E 01	1.6110E 01
0.	8.9854E-01	7.3463E-03	9.9922E-01	2.0291E-01	7.8346E-04
9.9265E-01	4.0261E-01	1.8449E-10	0.	0.	0.
2.9302E 00	3.8195E 00	1.6448E 00	4.8855E-01		

NM/TNM MOLE FRACTION OF TNM = 1.0 M= 196.0

1 RHO	P	V/V0	T	U	D
2 V	E	RBAR	VBAR	TBAR	Q
3 NS	NG	N	VS	VG	V
C(S)	N2	CO	NO	CO2	O2
GAMMA	ALPHA	BETA	C		
1.6400E 00	1.3236E-01	7.7987E-01	2.4418E 03	1.3329E-01	6.0550E-01
4.7553E-01	1.3467E-02	3.9163E 00	2.5589E 01	1.3776E 02	5.3188E-01
0.	6.0000E 00	6.0000E 00	4.5658E 00	1.5537E 01	1.5537E 01
0.	1.9505E 00	2.8174E-06	9.8917E-02	10.0000E-01	2.9505E 00
9.9265E-01	4.0261E-01	1.8449E-10	0.	0.	0.
3.5427E 00	3.3906E 00	1.2393E 00	4.7221E-01		

CH4/O2 MOLE FRACTION OF O2 = 0.5 M= 24.0

1 RHO	P	V/V0	T	U	D
2 V	E	RBAR	VBAR	TBAR	Q
3 NS	NG	N	VS	VG	V
C(S)	CO	H2O	H2	CO2	O2
CH4					
GAMMA	ALPHA	BETA	C		
7.6500E-01	7.1952E-02	6.9743E-01	3.4426E 03	1.6870E-01	5.5754E-01
9.1167E-01	-1.1161E-02	3.6645E 00	2.0964E 01	1.2743E 02	1.5349E 00
4.9004E-02	1.1645E 00	1.2135E 00	4.9683E 00	1.8596E 01	1.8046E 01
4.9004E-02	2.0076E-01	5.8527E-01	1.2822E-01	1.0698E-01	1.7391E-07
1.4325E-01	0.	0.	0.	0.	0.
2.3051E 00	2.3977E 00	1.4740E 00	3.8885E-01		

CH4/O2 MOLE FRACTION OF O2 = 0.6 M= 25.6

8.3000E-01	8.4660E-02	6.9920E-01	4.4126E 03	1.7516E-01	5.8232E-01
8.4241E-01	-7.2302E-03	3.6106E 00	2.0052E 01	1.2942E 02	1.7594E 00
0.	1.1717E 00	1.1717E 00	4.9296E 00	1.8419E 01	1.8419E 01
0.	2.3323E-01	6.6146E-01	1.1027E-01	1.5263E-01	2.0130E-05
1.4135E-02	0.	0.	0.	0.	0.
2.3245E 00	3.0784E 00	1.7545E 00	4.0716E-01		

CH4/O2 MOLE FRACTION OF O2 = 0.6667 M= 26.68

8.7900E-01	8.7594E-02	6.9316E-01	5.5680E 03	1.7486E-01	5.6988E-01
7.8857E-01	2.8336E-03	3.6284E 00	2.0350E 01	1.5041E 02	2.1416E 00
0.	1.0344E 00	1.0344E 00	4.9619E 00	2.0340E 01	2.0340E 01
0.	5.5414E-02	6.5270E-01	1.3793E-02	2.7789E-01	3.4556E-02
1.2310E-06	0.	0.	0.	0.	0.
2.2589E 00	3.9155E 00	2.1760E 00	3.9501E-01		

CH4/O2 MOLE FRACTION OF O2 = 0.8 M= 28.81

9.8000E-01	7.4619E-02	7.0476E-01	4.4981E 03	1.4993E-01	5.0784E-01
7.1914E-01	4.9121E-03	3.6820E 00	2.1266E 01	1.4803E 02	1.3639E 00
0.	1.0019E 00	1.0019E 00	4.9985E 00	2.0679E 01	2.0679E 01
0.	3.2384E-03	3.9937E-01	6.2698E-04	2.1896E-01	3.7973E-01
3.5033E-11	0.	0.	0.	0.	0.
2.3871E 00	3.5897E 00	1.9227E 00	3.5791E-01		

02/03 MOLE FRACTION OF 03 = 0.4 M= 38.4

1 RHO	P	V/VO	T	U	D
2 V	E	RBAR	VBAR	TBAR	Q
3 NS	NG	N	VS	VG	V
02					
GAMMA	ALPHA	BETA	C		
1.2580E 00	4.4553E-02	7.6020E-01	1.8118E 03	9.2155E-02	3.8430E-01
6.0430E-01	1.7519E-02	3.7300E 00	2.2108E 01	1.3200E 02	3.0232E-01
0.	1.2000E 00	1.2000E 00	5.0783E 00	1.9337E 01	1.9337E 01
0.	1.2000E 00	0.	0.	0.	0.
3.1701E 00	2.4159E 00	1.0775E 00	2.9214E-01		

02/03 MOLE FRACTION OF 03 = 0.6 M= 41.6

1.3440E 00	6.4394E-02	7.5532E-01	2.3695E 03	1.0827E-01	4.4251E-01
5.6200E-01	2.4728E-02	3.7300E 00	2.2108E 01	1.3200E 02	4.3601E-01
0.	1.3000E 00	1.3000E 00	4.9653E 00	1.7984E 01	1.7984E 01
0.	1.3000E 00	0.	0.	0.	0.
3.0870E 00	2.5441E 00	1.1481E 00	3.3424E-01		

02/03 MOLE FRACTION OF 03 = 0.8 M= 44.8

1.4410E 00	8.5935E-02	7.5487E-01	2.8049E 03	1.2091E-01	4.9323E-01
5.2385E-01	3.0961E-02	3.7300E 00	2.2108E 01	1.3200E 02	5.5038E-01
0.	1.4000E 00	1.4000E 00	4.8505E 00	1.6763E 01	1.6763E 01
0.	1.4000E 00	0.	0.	0.	0.
3.0795E 00	2.6506E 00	1.1855E 00	3.7233E-01		

02/03 MOLE FRACTION OF 03 = 1.0 M= 48.0

1.5540E 00	1.1125E-01	7.5700E-01	3.1423E 03	1.3189E-01	5.4277E-01
4.8713E-01	3.6505E-02	3.7300E 00	2.2108E 01	1.3200E 02	6.4971E-01
0.	1.5000E 00	1.5000E 00	4.7129E 00	1.5588E 01	1.5588E 01
0.	1.5000E 00	0.	0.	0.	0.

Table D. 2. Detonation Hugoniot, CJ Locus, and CJ Isentrope for Composition B.

DETONATION HUGONIOT

1 RHO	P	V/V0	T	U	D
2 V	E	RBAR	VBAR	TBAR	Q
3 NS	NG	N	VS	VG	V
C(S)	N2	CO	H2O	NO	H2
CO2	O2	CH4			
GAMMA	ALPHA	BETA	C		
1.7140E 00	5.0000E-01	6.2931E-01	4.9420E 03	3.2884E-01	8.8710E-01
3.6716E-01	5.8118E-02	3.7989E 00	2.3356E 01	1.4348E 02	1.4274E 00
2.7493E 00	6.9403E 00	9.6897E 00	3.2962E 00	1.0536E 01	8.4821E 00
2.7493E 00	2.4780E 00	7.2940E-02	2.8072E 00	9.0380E-03	1.5253E-02
1.5552E 00	2.1922E-04	2.5383E-03	0.	0.	0.
3.1670E 00	4.0083E 00	1.5814E 00	7.6250E-01		
1.7140E 00	4.0000E-01	6.7099E-01	4.5112E 03	2.7709E-01	8.4221E-01
3.9148E-01	4.2441E-02	3.7997E 00	2.3371E 01	1.4329E 02	1.4264E 00
2.7298E 00	6.9544E 00	9.6842E 00	3.5667E 00	1.1201E 01	9.0490E 00
2.7298E 00	2.4802E 00	9.6770E-02	2.7998E 00	4.5120E-03	1.9552E-02
1.5494E 00	8.2256E-05	4.0789E-03	0.	0.	0.
3.2198E 00	3.8605E 00	1.5095E 00	7.1007E-01		
1.7140E 00	3.5000E-01	6.9768E-01	4.3128E 03	2.4846E-01	8.2186E-01
4.0705E-01	3.4917E-02	3.8004E 00	2.3383E 01	1.4310E 02	1.4247E 00
2.7132E 00	6.9672E 00	9.6804E 00	3.7195E 00	1.1630E 01	9.4126E 00
2.7132E 00	2.4809E 00	1.1830E-01	2.7926E 00	3.1410E-03	2.3618E-02
1.5429E 00	4.9182E-05	5.6300E-03	0.	0.	0.
3.2350E 00	3.7496E 00	1.4682E 00	6.7888E-01		
1.7140E 00	3.0000E-01	7.3047E-01	4.1263E 03	2.1720E-01	8.0584E-01
4.2618E-01	2.7638E-02	3.8015E 00	2.3405E 01	1.4279E 02	1.4214E 00
2.6869E 00	6.9876E 00	9.6745E 00	3.8872E 00	1.2158E 01	9.8610E 00
2.6869E 00	2.4814E 00	1.5241E-01	2.7805E 00	2.1720E-03	3.0211E-02
1.5324E 00	2.9025E-05	8.3302E-03	0.	0.	0.
3.2362E 00	3.6030E 00	1.4224E 00	6.4324E-01		
1.7140E 00	2.5000E-01	7.7254E-01	3.9511E 03	1.8214E-01	8.0078E-01
4.5072E-01	2.0638E-02	3.8035E 00	2.3442E 01	1.4227E 02	1.4157E 00
2.6424E 00	7.0217E 00	9.6641E 00	4.0733E 00	1.2836E 01	1.0440E 01
2.6424E 00	2.4818E 00	2.0946E-01	2.7593E 00	1.4930E-03	4.1491E-02
1.5148E 00	1.6891E-05	1.3341E-02	0.	0.	0.
3.2142E 00	3.4104E 00	1.3721E 00	6.0182E-01		
1.7140E 00	2.0000E-01	8.3013E-01	3.7842E 03	1.4079E-01	8.2881E-01
4.8432E-01	1.3961E-02	3.8073E 00	2.3512E 01	1.4134E 02	1.4053E 00
2.5607E 00	7.0832E 00	9.6439E 00	4.2821E 00	1.3758E 01	1.1242E 01
2.5607E 00	2.4820E 00	3.1163E-01	2.7186E 00	1.0139E-03	6.2248E-02
1.4843E 00	9.5864E-06	2.3304E-02	0.	0.	0.
3.1562E 00	3.1638E 00	1.3192E 00	5.5293E-01		
1.7140E 00	1.5000E-01	9.1745E-01	3.6166E 03	8.4996E-02	1.0296E 00
5.3527E-01	7.6624E-03	3.8150E 00	2.3654E 01	1.3957E 02	1.3845E 00
2.3973E 00	7.2041E 00	9.6013E 00	4.5193E 00	1.5128E 01	1.2479E 01
2.3973E 00	2.4822E 00	5.1124E-01	2.6341E 00	6.6216E-04	1.0439E-01
1.4270E 00	5.0846E-06	4.4495E-02	0.	0.	0.
3.0385E 00	2.8652E 00	1.2721E 00	4.9393E-01		
1.7140E 00	10.0000E-02	1.0759E 00	3.4226E 03	6.6525E-02	8.7701E-01
6.2769E-01	1.8375E-03	3.8314E 00	2.3960E 01	1.3586E 02	1.3386E 00
2.0344E 00	7.4717E 00	9.5062E 00	4.7912E 00	1.7501E 01	1.4781E 01
2.0344E 00	2.4823E 00	9.4809E-01	2.4406E 00	3.7791E-04	2.0287E-01
1.3055E 00	2.1795E-06	9.2007E-02	0.	0.	0.
2.8305E 00	2.5439E 00	1.2520E 00	4.2151E-01		

CJ LOCUS (D VS. RHO)

1 RHO	P	V/V0	T	U	D
2 V	E	RBAR	VBAR	TBAR	Q
3 NS	NG	N	VS	VG	V
C(S)	N2	CO	H2O	NO	H2
CO2	O2	CH4			
GAMMA	ALPHA	BETA	C		
1.7140E 00	2.6004E-01	7.6311E-01	3.9854E 03	1.8958E-01	8.0029E-01
4.4522E-01	2.2020E-02	3.8030E 00	2.3432E 01	1.4240E 02	1.4172E 00
2.6534E 00	7.0133E 00	9.6667E 00	4.0343E 00	1.2684E 01	1.0310E 01
2.6534E 00	2.4817E 00	1.9535E-01	2.7647E 00	1.6107E-03	3.8678E-02
1.5191E 00	1.8858E-05	1.2055E-02	0.	0.	0.
3.2214E 00	3.4532E 00	1.3824E 00	6.1071E-01		
1.7000E 00	2.5521E-01	7.6236E-01	3.9981E 03	1.8888E-01	7.9486E-01
4.4844E-01	2.1888E-02	3.8035E 00	2.3441E 01	1.4226E 02	1.4156E 00
2.6422E 00	7.0221E 00	9.6643E 00	4.0539E 00	1.2770E 01	1.0587E 01
2.6422E 00	2.4817E 00	2.1008E-01	2.7593E 00	1.6562E-03	4.1635E-02
1.5144E 00	1.9476E-05	1.3269E-02	0.	0.	0.
3.2081E 00	3.4072E 00	1.3738E 00	6.0593E-01		
1.6000E 00	2.2315E-01	7.5666E-01	4.0756E 03	1.8422E-01	7.5707E-01
4.7291E-01	2.1020E-02	3.8079E 00	2.3522E 01	1.4108E 02	1.4023E 00
2.5431E 00	7.0990E 00	9.6421E 00	4.1898E 00	1.3411E 01	1.0979E 01
2.5431E 00	2.4815E 00	3.3781E-01	2.7110E 00	1.9551E-03	6.7599E-02
1.4746E 00	2.3478E-05	2.4453E-02	0.	0.	0.
3.1098E 00	3.0998E 00	1.3183E 00	5.7288E-01		
1.5000E 00	1.9520E-01	7.5034E-01	4.1322E 03	1.8025E-01	7.2196E-01
5.0023E-01	2.0294E-02	3.8139E 00	2.3633E 01	1.3956E 02	1.3845E 00
2.4089E 00	7.2016E 00	9.6106E 00	4.3169E 00	1.4105E 01	1.1651E 01
2.4089E 00	2.4814E 00	5.0768E-01	2.6439E 00	2.1916E-03	1.0307E-01
1.4231E 00	2.6423E-05	4.0276E-02	0.	0.	0.
3.0054E 00	2.8374E 00	1.2768E 00	5.4172E-01		
1.4000E 00	1.7056E-01	7.4364E-01	4.1689E 03	1.7673E-01	6.8937E-01
5.3117E-01	1.9667E-02	3.8213E 00	2.3772E 01	1.3769E 02	1.3619E 00
2.2370E 00	7.3327E 00	9.5697E 00	4.4363E 00	1.4862E 01	1.2425E 01
2.2370E 00	2.4813E 00	7.2330E-01	2.5564E 00	2.3425E-03	1.4962E-01
1.3590E 00	2.7868E-05	6.0760E-02	0.	0.	0.
2.9007E 00	2.6190E 00	1.2476E 00	5.1264E-01		
1.3000E 00	1.4863E-01	7.3679E-01	4.1865E 03	1.7347E-01	6.5908E-01
5.6676E-01	1.9097E-02	3.8301E 00	2.3936E 01	1.3546E 02	1.3342E 00
2.0257E 00	7.4944E 00	9.5201E 00	4.5490E 00	1.5699E 01	1.3327E 01
2.0257E 00	2.4813E 00	9.8737E-01	2.4474E 00	2.3927E-03	2.0902E-01
1.2814E 00	2.7577E-05	8.5563E-02	0.	0.	0.
2.7993E 00	2.4407E 00	1.2291E 00	4.8560E-01		
1.2000E 00	1.2893E-01	7.2999E-01	4.1858E 03	1.7032E-01	6.3080E-01
6.0832E-01	1.8555E-02	3.8399E 00	2.4120E 01	1.3291E 02	1.3011E 00
1.7744E 00	7.6887E 00	9.4631E 00	4.6557E 00	1.6636E 01	1.4390E 01
1.7744E 00	2.4813E 00	1.3015E 00	2.3160E 00	2.3371E-03	2.8333E-01
1.1900E 00	2.5587E-05	1.1407E-01	0.	0.	0.
2.7034E 00	2.2980E 00	1.2199E 00	4.6047E-01		
1.1000E 00	1.1109E-01	7.2335E-01	4.1675E 03	1.6715E-01	6.0420E-01
6.5759E-01	1.8020E-02	3.8504E 00	2.4318E 01	1.3004E 02	1.2625E 00
1.4834E 00	7.9168E 00	9.4003E 00	4.7571E 00	1.7702E 01	1.5659E 01
1.4834E 00	2.4814E 00	1.6662E 00	2.1616E 00	2.1816E-03	3.7501E-01
1.0850E 00	2.2204E-05	1.4543E-01	0.	0.	0.
2.6147E 00	2.1868E 00	1.2188E 00	4.3705E-01		
1.0000E 00	9.4844E-02	7.1701E-01	4.1320E 03	1.6383E-01	5.7892E-01
7.1701E-01	1.7470E-02	3.8612E 00	2.4523E 01	1.2690E 02	1.2184E 00
1.1541E 00	8.1798E 00	9.3339E 00	4.8534E 00	1.8937E 01	1.7196E 01
1.1541E 00	2.4815E 00	2.0801E 00	1.9834E 00	1.9415E-03	4.8701E-01
9.6727E-01	1.7928E-05	1.7856E-01	0.	0.	0.
2.5337E 00	2.1043E 00	1.2252E 00	4.1509E-01		

CJ ISENTROPE

1 RHO	P	V/V0	T	W	D
2 V	E	RBAR	VBAR	TBAR	Q
3 NS	NG	N	VS	VG	V
C(S)	N2	CO	H2O	NO	H2
CO2	O2	CH4			
GAMMA	ALPHA	BETA	C	U	
1.7140E 00	2.5916E-01	7.6300E-01	3.9629E 03	-4.2822E-01	7.9873E-01
4.4516E-01	2.1968E-02	3.8022E 00	2.3417E 01	1.4245E 02	1.4181E 00
2.6640E 00	7.0085E 00	9.6724E 00	4.0370E 00	1.2684E 01	1.0302E 01
2.6640E 00	2.4817E 00	1.8741E-01	2.7721E 00	1.5632E-03	3.7021E-02
1.5194E 00	1.8105E-05	9.1792E-03	0.	0.	0.
3.2195E 00	3.6282E 00	1.4375E 00	6.0945E-01		
1.7140E 00	7.0000E-01	5.6086E-01	4.7855E 03	-1.6498E 00	7.9873E-01
3.2722E-01	7.3076E-02	3.7975E 00	2.3330E 01	1.4410E 02	1.4339E 00
2.7896E 00	6.9044E 00	9.6940E 00	2.8247E 00	9.4678E 00	7.5561E 00
2.7896E 00	2.4785E 00	1.3361E-02	2.8243E 00	8.0240E-03	2.9046E-03
1.5769E 00	2.1803E-04	1.2426E-04	0.	0.	0.
3.1532E 00	4.9111E 00	1.8746E 00	8.4986E-01		
1.7140E 00	5.0000E-01	6.2307E-01	4.5125E 03	-1.1353E 00	7.9873E-01
3.6352E-01	5.1552E-02	3.7981E 00	2.3342E 01	1.4385E 02	1.4321E 00
2.7701E 00	6.9207E 00	9.6908E 00	3.2844E 00	1.0443E 01	8.3969E 00
2.7701E 00	2.4801E 00	4.0652E-02	2.8176E 00	4.7412E-03	8.2754E-03
1.5684E 00	9.4913E-05	8.3305E-04	0.	0.	0.
3.2338E 00	4.5260E 00	1.7088E 00	7.6666E-01		
1.7140E 00	3.0000E-01	7.2920E-01	4.0876E 03	-5.5968E-01	7.9873E-01
4.2544E-01	2.7467E-02	3.8008E 00	2.3391E 01	1.4288E 02	1.4226E 00
2.6980E 00	6.9810E 00	9.6790E 00	3.8860E 00	1.2140E 01	9.8393E 00
2.6980E 00	2.4815E 00	1.4166E-01	2.7876E 00	2.0477E-03	2.7914E-02
1.5343E 00	2.6883E-05	6.0129E-03	0.	0.	0.
3.2395E 00	3.8193E 00	1.4877E 00	6.4301E-01		
1.7140E 00	2.0000E-01	8.2746E-01	3.7398E 03	-2.2345E-01	7.9873E-01
4.8277E-01	1.3399E-02	3.8055E 00	2.3478E 01	1.4152E 02	1.4079E 00
2.5874E 00	7.0685E 00	9.6559E 00	4.2805E 00	1.3722E 01	1.1192E 01
2.5874E 00	2.4820E 00	2.8694E-01	2.7354E 00	9.2546E-04	5.7513E-02
1.4884E 00	8.4717E-06	1.7294E-02	0.	0.	0.
3.1669E 00	3.3293E 00	1.3670E 00	5.5297E-01	**2.3679E-01**	
1.7140E 00	1.5000E-01	9.0713E-01	3.4917E 03	-3.0912E-02	7.9873E-01
5.2925E-01	5.3436E-03	3.8105E 00	2.3570E 01	1.4030E 02	1.3941E 00
2.4796E 00	7.1499E 00	9.6295E 00	4.5143E 00	1.5004E 01	1.2303E 01
2.4796E 00	2.4823E 00	4.2066E-01	2.6801E 00	4.7803E-04	8.6706E-02
1.4494E 00	3.2855E-06	3.0363E-02	0.	0.	0.
3.0902E 00	3.0684E 00	1.3165E 00	4.9530E-01	**2.8485E-01**	
1.7140E 00	10.0000E-02	1.0371E 00	3.1499E 03	1.9128E-01	7.9873E-01
6.0508E-01	-3.9531E-03	3.8193E 00	2.3734E 01	1.3842E 02	1.3718E 00
2.2984E 00	7.2806E 00	9.5790E 00	4.7795E 00	1.7095E 01	1.4140E 01
2.2984E 00	2.4824E 00	6.3140E-01	2.5791E 00	1.6187E-04	1.3734E-01
1.3947E 00	7.0564E-07	5.5542E-02	0.	0.	0.
2.9657E 00	2.8298E 00	1.2922E 00	4.2347E-01	**3.4632E-01**	
1.7140E 00	7.0000E-02	1.1741E 00	2.8633E 03	3.4999E-01	7.9873E-01
6.8499E-01	-1.0593E-02	3.8318E 00	2.3968E 01	1.3688E 02	1.3502E 00
2.0901E 00	7.4044E 00	9.4945E 00	4.9549E 00	1.9310E 01	1.6150E 01
2.0901E 00	2.4825E 00	8.3091E-01	2.4466E 00	5.2788E-05	1.8534E-01
1.3612E 00	1.4701E-07	9.7773E-02	0.	0.	0.
2.8452E 00	2.7029E 00	1.3014E 00	3.6936E-01	**3.9503E-01**	
1.7140E 00	5.0000E-02	1.3247E 00	2.6141E 03	4.7427E-01	7.9873E-01
7.7287E-01	-1.5793E-02	3.8409E 00	2.4139E 01	1.3565E 02	1.3337E 00
1.9320E 00	7.5010E 00	9.4330E 00	5.0781E 00	2.1757E 01	1.8341E 01
1.9320E 00	2.4825E 00	9.7977E-01	2.3408E 00	1.6545E-05	2.2967E-01
1.3397E 00	2.8960E-08	1.2851E-01	0.	0.	0.
2.7300E 00	2.7011E 00	1.3557E 00	3.2480E-01	**4.3692E-01**	

1.7140E 00	3.0000E-02	1.6075E 00	2.2817E 03	6.2696E-01	7.9873E-01
9.3785E-01	-2.2182E-02	3.8537E 00	2.4381E 01	1.3436E 02	1.3156E 00
1.7327E 00	7.6083E 00	9.3409E 00	5.2046E 00	2.6408E 01	2.2475E 01
1.7327E 00	2.4825E 00	1.1350E 00	2.1895E 00	2.3819E-06	2.8898E-01
1.3377E 00	1.9441E-09	1.7453E-01	0.	0.	0.
2.5528E 00	2.8413E 00	1.5047E 00	2.6800E-01	**4.9399E-01**	
1.7140E 00	2.0000E-02	1.8924E 00	2.0589E 03	7.2422E-01	7.9873E-01
1.1041E 00	-2.6251E-02	3.8628E 00	2.4555E 01	1.3386E 02	1.3079E 00
1.6166E 00	7.6551E 00	9.2716E 00	5.2676E 00	3.1173E 01	2.6656E 01
1.6166E 00	2.4825E 00	1.1917E 00	2.0831E 00	4.5931E-07	3.2599E-01
1.3626E 00	1.9778E-10	2.0919E-01	0.	0.	0.
2.4203E 00	3.0698E 00	1.6815E 00	2.3118E-01	**5.3461E-01**	
1.7140E 00	1.5000E-02	2.1359E 00	1.9219E 03	7.8302E-01	7.9873E-01
1.2461E 00	-2.8711E-02	3.8688E 00	2.4670E 01	1.3377E 02	1.3056E 00
1.5548E 00	7.6692E 00	9.2240E 00	5.2985E 00	3.5299E 01	3.0242E 01
1.5548E 00	2.4825E 00	1.1994E 00	2.0150E 00	1.3831E-07	3.4649E-01
1.3928E 00	3.7468E-11	2.3298E-01	0.	0.	0.
2.3335E 00	3.2918E 00	1.8392E 00	2.0885E-01	**5.6118E-01**	
1.7140E 00	10.0000E-03	2.5525E 00	1.7555E 03	8.5416E-01	7.9873E-01
1.4892E 00	-3.1685E-02	3.8769E 00	2.4825E 01	1.3394E 02	1.3063E 00
1.4913E 00	7.6669E 00	9.1582E 00	5.3284E 00	4.2443E 01	3.6399E 01
1.4913E 00	2.4825E 00	1.1735E 00	1.9278E 00	2.5094E-08	3.6790E-01
1.4493E 00	3.5265E-12	2.6588E-01	0.	0.	0.
2.2212E 00	3.6867E 00	2.1100E 00	1.8187E-01	**5.9591E-01**	
1.7140E 00	7.0000E-03	3.0043E 00	1.6367E 03	9.0799E-01	7.9873E-01
1.7528E 00	-3.3940E-02	3.8800E 00	2.4884E 01	1.3422E 02	1.3111E 00
1.4909E 00	7.6431E 00	9.1339E 00	5.3437E 00	5.0294E 01	4.2957E 01
1.4909E 00	2.4825E 00	1.1112E 00	1.8890E 00	6.1510E-09	3.8245E-01
1.4999E 00	5.1070E-13	2.7803E-01	0.	0.	0.
2.2061E 00	4.1818E 00	2.3488E 00	1.6453E-01	**6.2395E-01**	
1.7140E 00	5.0000E-03	3.5057E 00	1.5444E 03	9.5042E-01	7.9873E-01
2.0453E 00	-3.5715E-02	3.8838E 00	2.4957E 01	1.3456E 02	1.3156E 00
1.4836E 00	7.6190E 00	9.1026E 00	5.3530E 00	5.9051E 01	5.0299E 01
1.4836E 00	2.4825E 00	1.0528E 00	1.8474E 00	1.7712E-09	3.9278E-01
1.5499E 00	9.2066E-14	2.9368E-01	0.	0.	0.
2.2474E 00	5.0484E 00	2.6913E 00	1.5160E-01	**6.4807E-01**	
1.7140E 00	3.0000E-03	4.3665E 00	1.4392E 03	9.9811E-01	7.9873E-01
2.5475E 00	-3.7711E-02	3.8957E 00	2.5188E 01	1.3520E 02	1.3187E 00
1.4045E 00	7.5987E 00	9.0032E 00	5.3618E 00	7.4057E 01	6.3340E 01
1.4045E 00	2.4825E 00	1.0030E 00	1.7388E 00	3.4448E-10	4.0191E-01
1.6291E 00	9.5101E-15	3.4338E-01	0.	0.	0.
2.4599E 00	7.1926E 00	3.3305E 00	1.3711E-01	**6.7965E-01**	
1.7140E 00	2.0000E-03	5.1347E 00	1.3781E 03	1.0248E 00	7.9873E-01
2.9957E 00	-3.8829E-02	3.9080E 00	2.5427E 01	1.3576E 02	1.3191E 00
1.3091E 00	7.5905E 00	8.8996E 00	5.3659E 00	8.7421E 01	7.5351E 01
1.3091E 00	2.4825E 00	9.8454E-01	1.6332E 00	1.1742E-10	4.0394E-01
1.6911E 00	2.1166E-15	3.9520E-01	0.	0.	0.
2.5466E 00	9.1546E 00	3.9875E 00	1.2352E-01	**7.0078E-01**	
1.7140E 00	1.5000E-03	5.7545E 00	1.3424E 03	1.0400E 00	7.9873E-01
3.3573E 00	-3.9462E-02	3.9165E 00	2.5593E 01	1.3618E 02	1.3196E 00
1.2445E 00	7.5839E 00	8.8283E 00	5.3677E 00	9.8217E 01	8.5128E 01
1.2445E 00	2.4825E 00	9.7171E-01	1.5623E 00	5.9753E-11	4.0349E-01
1.7330E 00	8.2278E-16	4.3083E-01	0.	0.	0.
2.4987E 00	1.0409E 01	4.5660E 00	1.1218E-01	**7.1416E-01**	
1.7140E 00	10.0000E-04	6.8259E 00	1.2983E 03	1.0583E 00	7.9873E-01
3.9824E 00	-4.0231E-02	3.9262E 00	2.5784E 01	1.3676E 02	1.3214E 00
1.1779E 00	7.5686E 00	8.7465E 00	5.3691E 00	1.1695E 02	1.0192E 02
1.1779E 00	2.4825E 00	9.4277E-01	1.4820E 00	2.4733E-11	4.0198E-01
1.7876E 00	2.3999E-16	4.7174E-01	0.	0.	0.
2.2179E 00	1.1399E 01	5.5903E 00	9.3982E-02	**7.3178E-01**	

```
1.7140E 00  7.0000E-04  8.1702E 00  1.2611E 03  1.0739E 00  7.9873E-01
4.7668E 00 -4.0884E-02  3.9312E 00  2.5882E 01  1.3725E 02  1.3254E 00
1.1611E 00  7.5445E 00  8.7057E 00  5.3696E 00  1.4061E 02  1.2257E 02
1.1611E 00  2.4825E 00  8.9515E-01  1.4417E 00  1.1327E-11  4.0142E-01
1.8315E 00  8.1158E-17  4.9217E-01  0.          0.          0.
1.7411E 00  1.0709E 01  6.7253E 00  7.6221E-02  7.4701E-01

1.7140E 00  5.0000E-04  1.0292E 01  1.2222E 03  1.0912E 00  7.9873E-01
6.0046E 00 -4.1606E-02  3.9307E 00  2.5873E 01  1.3771E 02  1.3328E 00
1.2062E 00  7.5047E 00  8.7109E 00  5.3692E 00  1.7824E 02  1.5431E 02
1.2062E 00  2.4825E 00  8.1454E-01  1.4461E 00  4.8123E-12  4.0233E-01
1.8697E 00  2.5021E-17  4.8955E-01  0.          0.          0.
1.2241E 00  8.5841E 00  7.8295E 00  6.0623E-02  7.6260E-01

1.7140E 00  3.0000E-04  1.6814E 01  1.1519E 03  1.1257E 00  7.9873E-01
9.8101E 00 -4.3047E-02  3.9206E 00  2.5674E 01  1.3849E 02  1.3509E 00
1.3856E 00  7.4113E 00  8.7969E 00  5.3676E 00  2.9530E 02  2.4963E 02
1.3856E 00  2.4825E 00  6.3035E-01  1.5347E 00  8.9337E-13  3.9971E-01
1.9175E 00  2.5287E-18  4.4656E-01  0.          0.          0.
9.9740E-01  7.2676E 00  8.2892E 00  5.4179E-02

1.7140E 00  2.0000E-04  2.4918E 01  1.0982E 03  1.1530E 00  7.9873E-01
1.4538E 01 -4.4193E-02  3.9136E 00  2.5535E 01  1.3920E 02  1.3640E 00
1.5137E 00  7.3407E 00  8.8544E 00  5.3659E 00  4.4222E 02  3.6754E 02
1.5137E 00  2.4825E 00  5.0005E-01  1.6030E 00  2.1009E-13  3.8888E-01
1.9485E 00  3.5228E-19  4.1781E-01  0.          0.          0.
1.0691E 00  7.5884E 00  8.0331E 00  5.5754E-02

1.7140E 00  1.5000E-04  3.2458E 01  1.0625E 03  1.1711E 00  7.9873E-01
1.8937E 01 -4.4948E-02  3.9101E 00  2.5468E 01  1.3974E 02  1.3720E 00
1.5850E 00  7.2964E 00  8.8814E 00  5.3647E 00  5.7981E 02  4.7729E 02
1.5850E 00  2.4825E 00  4.2234E-01  1.6410E 00  7.3566E-14  3.7791E-01
1.9683E 00  8.4117E-20  4.0431E-01  0.          0.          0.
1.1073E 00  7.7003E 00  7.8575E 00  5.6082E-02

1.7140E 00 10.0000E-05  4.6575E 01  1.0144E 03  1.1949E 00  7.9873E-01
2.7173E 01 -4.5944E-02  3.9065E 00  2.5397E 01  1.4051E 02  1.3819E 00
1.6688E 00  7.2394E 00  8.9083E 00  5.3630E 00  8.3899E 02  6.8282E 02
1.6688E 00  2.4825E 00  3.2754E-01  1.6869E 00  1.5814E-14  3.5881E-01
1.9928E 00  1.0284E-20  3.9087E-01  0.          0.          0.
1.1369E 00  7.6690E 00  7.6251E 00  5.5582E-02

1.7140E 00  7.0000E-05  6.3636E 01  9.7339E 02  1.2145E 00  7.9873E-01
3.7127E 01 -4.6765E-02  3.9039E 00  2.5347E 01  1.4121E 02  1.3897E 00
1.7324E 00  7.1934E 00  8.9258E 00  5.3614E 00  1.1541E 03  9.3111E 02
1.7324E 00  2.4825E 00  2.5572E-01  1.7247E 00  3.7746E-15  3.3861E-01
2.0098E 00  1.4473E-21  3.8208E-01  0.          0.          0.
1.1497E 00  7.5138E 00  7.4049E 00  5.4663E-02

1.7140E 00  5.0000E-05  8.5218E 01  9.3545E 02  1.2321E 00  7.9873E-01
4.9719E 01 -4.7500E-02  3.9018E 00  2.5305E 01  1.4187E 02  1.3963E 00
1.7865E 00  7.1531E 00  8.9396E 00  5.3600E 00  1.5546E 03  1.2456E 03
1.7865E 00  2.4825E 00  1.9704E-01  1.7605E 00  8.9392E-16  3.1661E-01
2.0212E 00  2.0123E-22  3.7520E-01  0.          0.          0.
1.1569E 00  7.2943E 00  7.1697E 00  5.3627E-02

1.7140E 00  3.0000E-05  1.3239E 02  8.7860E 02  1.2570E 00  7.9873E-01
7.7241E 01 -4.8545E-02  3.8987E 00  2.5246E 01  1.4288E 02  1.4050E 00
1.8604E 00  7.0974E 00  8.9578E 00  5.3577E 00  2.4348E 03  1.9302E 03
1.8604E 00  2.4825E 00  1.2445E-01  1.8175E 00  8.1590E-17  2.7777E-01
2.0290E 00  7.5611E-24  3.6610E-01  0.          0.          0.
1.1652E 00  6.8720E 00  6.7559E 00  5.1962E-02

1.7140E 00  2.0000E-05  1.8741E 02  8.3384E 02  1.2755E 00  7.9873E-01
1.0934E 02 -4.9317E-02  3.8963E 00  2.5198E 01  1.4366E 02  1.4109E 00
1.9135E 00  7.0581E 00  8.9715E 00  5.3558E 00  3.4664E 03  2.7282E 03
1.9135E 00  2.4825E 00  8.0837E-02  1.8662E 00  9.8205E-18  2.4281E-01
2.0265E 00  4.1445E-25  3.5923E-01  0.          0.          0.
1.1722E 00  6.4939E 00  6.3931E 00  5.0630E-02
```

1.7140E 00	1.5000E-05	2.3952E 02	8.0218E 02	1.2879E 00	7.9873E-01
1.3974E 02	-4.9834E-02	3.8944E 00	2.5162E 01	1.4419E 02	1.4145E 00
1.9489E 00	7.0329E 00	8.9818E 00	5.3545E 00	4.4464E 03	3.4828E 03
1.9489E 00	2.4825E 00	5.7028E-02	1.9030E 00	1.9021E-18	2.1633E-01
2.0200E 00	4.3590E-26	3.5410E-01	0.	0.	0.
1.1777E 00	6.2189E 00	6.1299E 00	4.9685E-02		
1.7140E 00	10.0000E-06	3.3782E 02	7.5771E 02	1.3043E 00	7.9873E-01
1.9709E 02	-5.0522E-02	3.8915E 00	2.5106E 01	1.4489E 02	1.4187E 00
1.9968E 00	7.0015E 00	8.9983E 00	5.3526E 00	6.2999E 03	4.9031E 03
1.9968E 00	2.4825E 00	3.2559E-02	1.9579E 00	1.5028E-19	1.7790E-01
2.0048E 00	1.3387E-27	3.4587E-01	0.	0.	0.
1.1861E 00	5.8388E 00	5.7658E 00	4.8350E-02		
1.7140E 00	7.0000E-06	4.5624E 02	7.1881E 02	1.3178E 00	7.9873E-01
2.6618E 02	-5.1088E-02	3.8885E 00	2.5048E 01	1.4543E 02	1.4218E 00
2.0382E 00	6.9777E 00	9.0159E 00	5.3510E 00	8.5378E 03	6.6089E 03
2.0382E 00	2.4825E 00	1.8454E-02	2.0090E 00	1.2612E-20	1.4444E-01
1.9863E 00	4.4631E-29	3.3703E-01	0.	0.	0.
1.1939E 00	5.5264E 00	5.4664E 00	4.7166E-02		
1.7140E 00	5.0000E-06	6.0475E 02	6.8247E 02	1.3298E 00	7.9873E-01
3.5283E 02	-5.1589E-02	3.8852E 00	2.4985E 01	1.4587E 02	1.4243E 00
2.0780E 00	6.9586E 00	9.0366E 00	5.3494E 00	1.1349E 04	8.7402E 03
2.0780E 00	2.4825E 00	1.0062E-02	2.0595E 00	9.6453E-22	1.1458E-01
1.9652E 00	1.3094E-30	3.2672E-01	0.	0.	0.
1.2013E 00	5.2586E 00	5.2098E 00	4.6036E-02		
1.7140E 00	3.0000E-06	9.2479E 02	6.2829E 02	1.3466E 00	7.9873E-01
5.3955E 02	-5.2292E-02	3.8791E 00	2.4867E 01	1.4634E 02	1.4272E 00
2.1415E 00	6.9354E 00	9.0770E 00	5.3471E 00	1.7413E 04	1.3306E 04
2.1415E 00	2.4825E 00	3.4640E-03	2.1395E 00	1.2033E-23	7.4934E-02
1.9285E 00	3.1874E-33	3.0651E-01	0.	0.	0.
1.2124E 00	4.9039E 00	4.8697E 00	4.4299E-02		
1.7140E 00	2.0000E-06	1.2923E 03	5.8647E 02	1.3588E 00	7.9873E-01
7.5394E 02	-5.2803E-02	3.8733E 00	2.4755E 01	1.4654E 02	1.4291E 00
2.1961E 00	6.9218E 00	9.1179E 00	5.3453E 00	2.4381E 04	1.8510E 04
2.1961E 00	2.4825E 00	1.2943E-03	2.2055E 00	2.3455E-25	4.9885E-02
1.8966E 00	1.2493E-34	2.8604E-01	0.	0.	0.
1.2210E 00	4.6612E 00	4.6367E 00	4.2908E-02		
1.7140E 00	1.5000E-06	1.6364E 03	5.5758E 02	1.3669E 00	7.9873E-01
9.5471E 02	-5.3142E-02	3.8686E 00	2.4664E 01	1.4660E 02	1.4302E 00
2.2372E 00	6.9145E 00	9.1517E 00	5.3441E 00	3.0906E 04	2.3352E 04
2.2372E 00	2.4825E 00	5.9353E-04	2.2533E 00	1.0953E-26	3.5865E-02
1.8730E 00	1.2480E-34	2.6914E-01	0.	0.	0.
1.2269E 00	4.5091E 00	4.4903E 00	4.1916E-02		
1.7140E 00	10.0000E-07	2.2783E 03	5.1812E 02	1.3776E 00	7.9873E-01
1.3292E 03	-5.3587E-02	3.8612E 00	2.4524E 01	1.4655E 02	1.4315E 00
2.2987E 00	6.9069E 00	9.2056E 00	5.3424E 00	4.3078E 04	3.2323E 04
2.2987E 00	2.4825E 00	1.7453E-04	2.3220E 00	9.6065E-29	2.1135E-02
1.8389E 00	1.2466E-34	2.4219E-01	0.	0.	0.
1.2352E 00	4.3160E 00	4.3038E 00	4.0520E-02		

Appendix E

COMPARISON WITH OTHER EQUATIONS OF STATE

There are two equations of state of a semi-empirical nature (the Kistiakowsky-Wilson and the constant-β) which have been extensively used at this laboratory and others for practical work. With this type of application in mind, we give here some comparisons between the present equation of state (LJD) and these two. A portion of the comparison does double duty: the detailed comparison on Composition B serves also as a graphical presentation of the illustrative numerical results for the LJD equation of state given in Table D.2 (Appendix D).

The so-called Kistiakowsky-Wilson equation of state is a fairly simple one which allows a priori calculations if a set of molecular parameters called co-volumes is assumed known. It is similar in principle to that used in the present work, but substitutes simple empirical expressions for the LJD cell theory and the mixture theory. It has been extensively compared with experimental data and used for prediction of the properties of proposed new explosives.[27,62]

The constant-β equation of state[63] is essentially an empirical recipe (based on some thermodynamic assumptions) for constructing a partial product

equation of state from experimental data on an explosive. It makes no explicit reference to the chemical composition of the detonation products, and gives the equation of state in the form

$$E = E(p,v) \quad ,$$

which is sufficient for many applications such as numerical hydrodynamic calculations.

In the first section, we compare the LJD and KW equations of state on the set of five explosives used in Chapter 4. In the second, we make fairly detailed comparisons of all three equations of state on the single explosive Composition B.

E.1 Comparison of the KW and LJD Equations of State on the Five Explosives of Chapter 4

In order to compare these two equations of state, a relationship between the KW co-volumes and the LJD potential constants must be established. There is no unique way of doing this, for the KW equation of state is not based directly on intermolecular potentials, and the co-volumes k_i have mixed dimensions:

$$\left[k_i\right] = \left[VT^{\frac{1}{2}}\right] \quad .$$

We have used the two recipes

(1) $k_i \propto (r_i^*)^3$

(2) $k_i \propto (r_i^*)^3 \, (T_i^*)^{\frac{1}{2}}$.

Much of the work with the KW equation of state has used so-called "geometric" co-volumes obtained by taking the k_i proportional to the volume swept out by the rotating molecule as calculated from bond lengths and Van der Waals atomic radii.[27,62] We have done some calculations with this set of co-volumes and a corresponding set of geometric r_i^* for the LJD equation of state calculated from them according to the first recipe above. We have also used co-volumes computed from the potential constants given in Chapter 2 according to both of the above recipes. The constant of proportionality was chosen to give the geometric value of 380 for the N_2 co-volume in each case. Some of the values used are listed in Table E.1. The other constants in the KW equation of state were taken to be $\alpha = 0.5$, $\beta = 0.09$, and $\kappa = 11.85$, as in reference 27.

Results are given in Table E.2 and Figs. E.1 through E.3. As in Chapter 4, some of the variations were repeated with compensation, i.e., rescaling of the molecular sizes to give the experimental RDX detonation velocity. The KW equation of state gives detonation velocity curves of a qualitatively different shape, lower temperature, and values of γ which are lower and closer to the experimental values. In evaluating these results, it should be remembered that the KW geometric co-volumes have already been scaled to give agreement with experiment for several CHON explosives.[27]

Table E.1. Values of the KW Co-Volumes and the Corresponding LJD r_i^*.

	From Chapter 2		Geometric	
Species	r_i^* (A)	k_i[a] (cc/mole-°$K^{\frac{1}{2}}$)	r_i^* (A)	k_i[b] (cc/mole-°$K^{\frac{1}{3}}$)
N_2	4.05	380	4.05	380
CO	4.05	380	4.08	390
H_2O	3.35	215	3.98	360
NO	3.97	358	4.06	386
H_2	3.34	214	3.16	180
CO_2	4.20	423	4.89	670
O_2	3.73	297	3.94	350
CH_4	4.30	455	4.53	528

[a] From recipe (1): $k_i \propto (r_i^*)^3$

[b] See reference 62.

Table E.2. Calculated Values of p, γ, and T for the LJD and KW Equations of State

Run	DESCRIPTION: Equation of State	DESCRIPTION: Constants	S_{r^*} (Scale Factor for all r^*_i)	$D_{calc} - D_{exp}$ for RDX at $\rho_o = 1.8$	RDX $\rho_o = 1.8$ γ	RDX $\rho_o = 1.8$ T	Comp. B $\rho_o = 1.714$ γ	Comp. B $\rho_o = 1.714$ T	TNT $\rho_o = 1.64$ γ	TNT $\rho_o = 1.64$ T	Nitromethane $\rho_o = 1.131$ γ	Nitromethane $\rho_o = 1.131$ T	$NM/HNO_3/H_2O$ $\rho_o = 1.293$ γ	$NM/HNO_3/H_2O$ $\rho_o = 1.293$ T
		Experimental		0	2.90		2.77		3.17		2.13	3380	2.54	3400
20	LJD	geometric r^*_i		2741	3.51	2735	3.50	2923	3.54	2922	3.27	3195	3.52	3021
21	KW	k_i from experimental r^*_i[a]		-1493	2.62	3354	2.63	3346	2.72	3202	2.34	3317	2.35	2825
22	KW	k_i from experimental r^*_i and T^*_i[a]		-1104	2.68	3153	2.68	3159	2.78	3039	2.42	3169	3.96	2707
23	KW	geometric k_i		176	2.84	2661	2.82	2741	2.89	2726	2.61	2870	2.68	2408
	COMPENSATED RUNS													
24	LJD	geometric r^*_i	0.9117	51	3.36	3592	3.34	3378	3.40	3138	2.89	3353	3.07	3432
25	KW	k_i from experimental r^*_i	1.108	-75	2.84	2646	2.82	2804	2.88	2877	2.57	3148	2.49	2405

[a] Values of r^*_i and T^*_i from Chapter 2

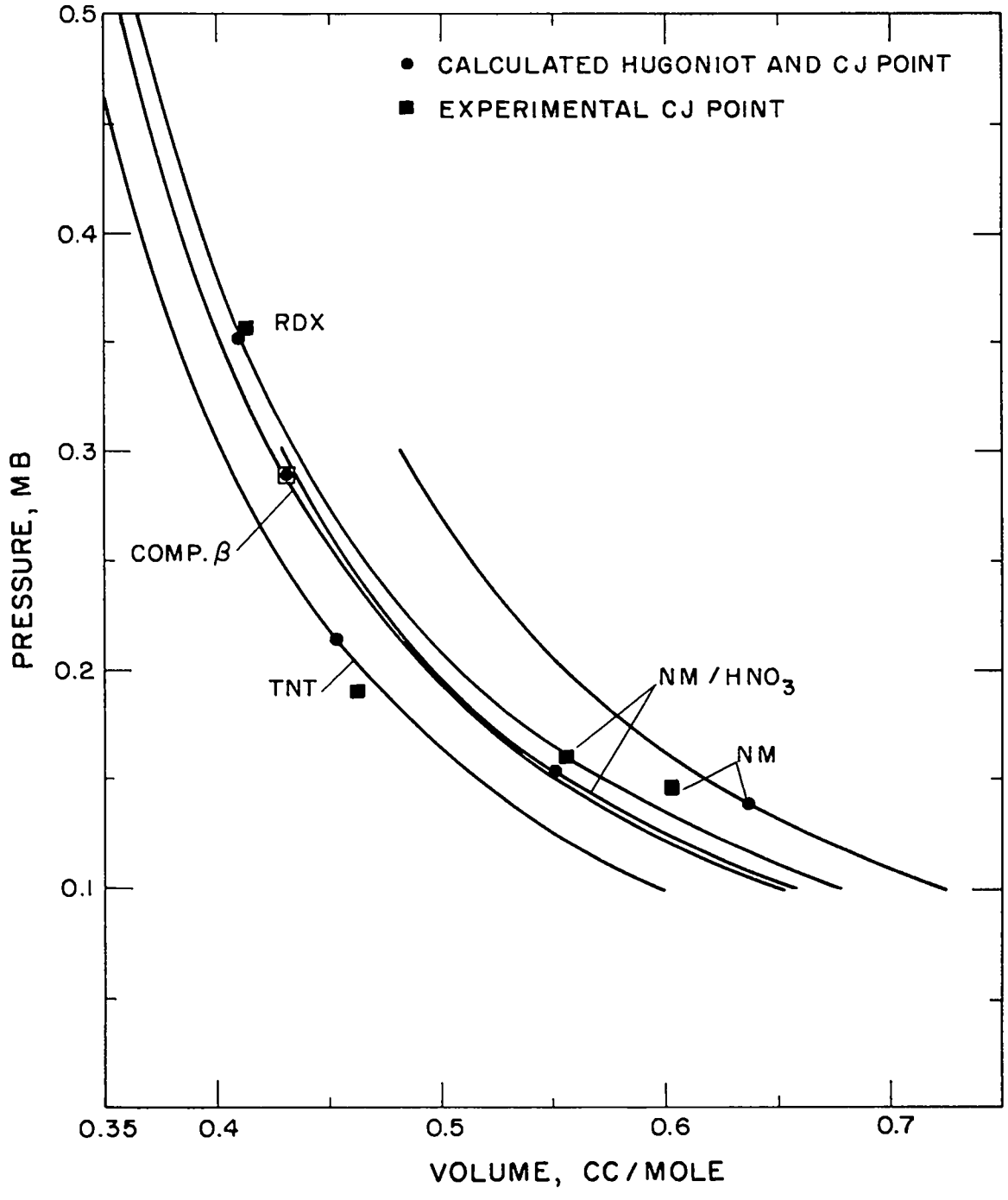

Fig. E.1. Calculated detonation Hugoniots and experimental CJ points for the KW equation of state with co-volumes k_i from the experimental r_i^* of Chapter 2 (run 25 of Table E.2). Compare with Fig. 4.1.

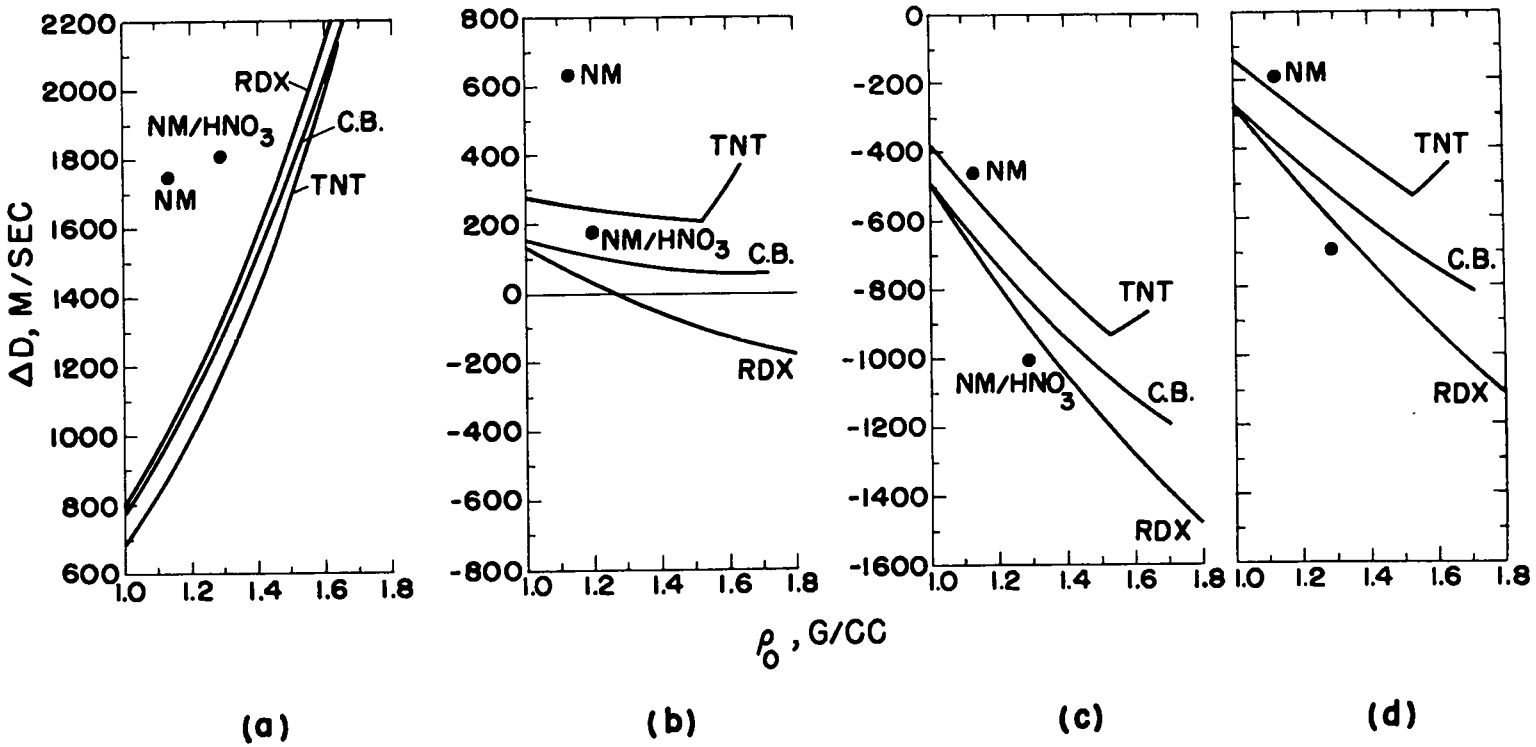

Fig. E.2. Differences of calculated and experimental detonation velocities. (a) LJD, geometric k_i^*, run 20; (b) KW, geometric k_i, run 23; (c) KW, k_i from r_i^*, run 21; (d) KW, k_i from r_i^* and T_i^*, run 22.

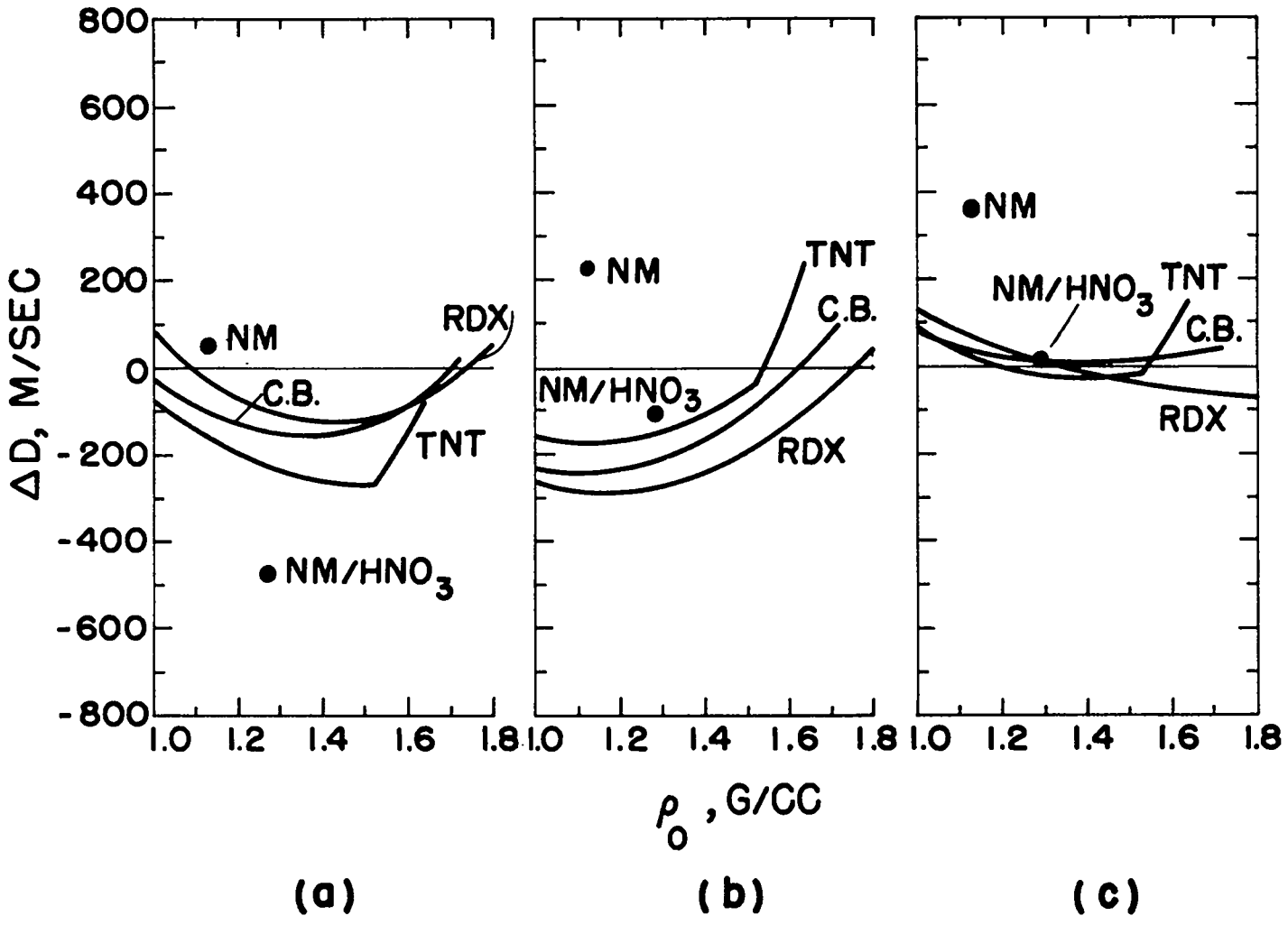

Fig. E.3. Compensated calculations (b and c): (b) LJD; geometric r_i^*, run 24; (c) KW; k_i from experimental r_i^*, run 25. For convenience, we have reproduced here for comparison: (a) Fig. 4.4(a): LJD; "central point," run 2 of Table 4.2.

E.2 Detailed Comparison of the KW, LJD, and Constant-β Equations of State on Composition B

In this section we present a detailed comparison of all three equations of state on the single explosive Composition B. The results are given in Figs. E.4 through E.8. The parameters used are the central point set for the LJD equation of state, co-volumes proportional to the cubes of these r_i^* (scaled for agreement with the experimental RDX detonation velocity) for the KW equation of state (run 25 of Table E2), and constants determined from the experimental CJ point for Composition B for the constant-β form.

The complicated form of the LJD results at intermediate pressures is probably due largely to the presence of the attractive wells in the intermolecular potential functions, a feature lacking in the other forms. The very good agreement between the calculated KW CJ point and the experimental one (indistinguishable from the calculated one in the figures) is partly fortuitous but not entirely unexpected since it has been given the advantage of the scaling of the co-volumes to give agreement with the RDX detonation velocity. The constant-β equation of state is a good approximation to the KW results in the neighborhood of the CJ point.

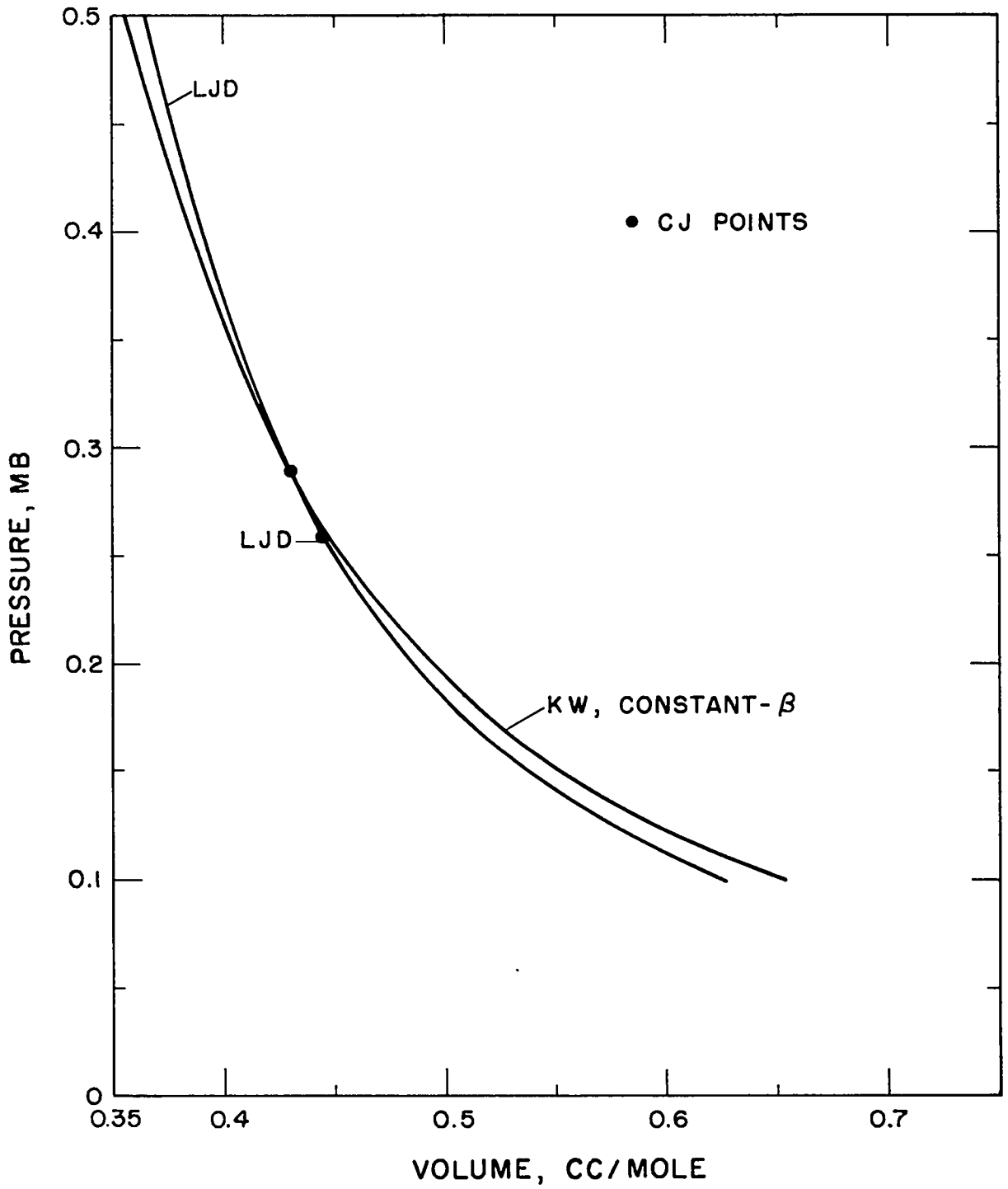

Fig. E.4. Calculated detonation Hugoniots (at $\rho_o = 1.714$) for the KW, LJD, and constant-β equations of state.

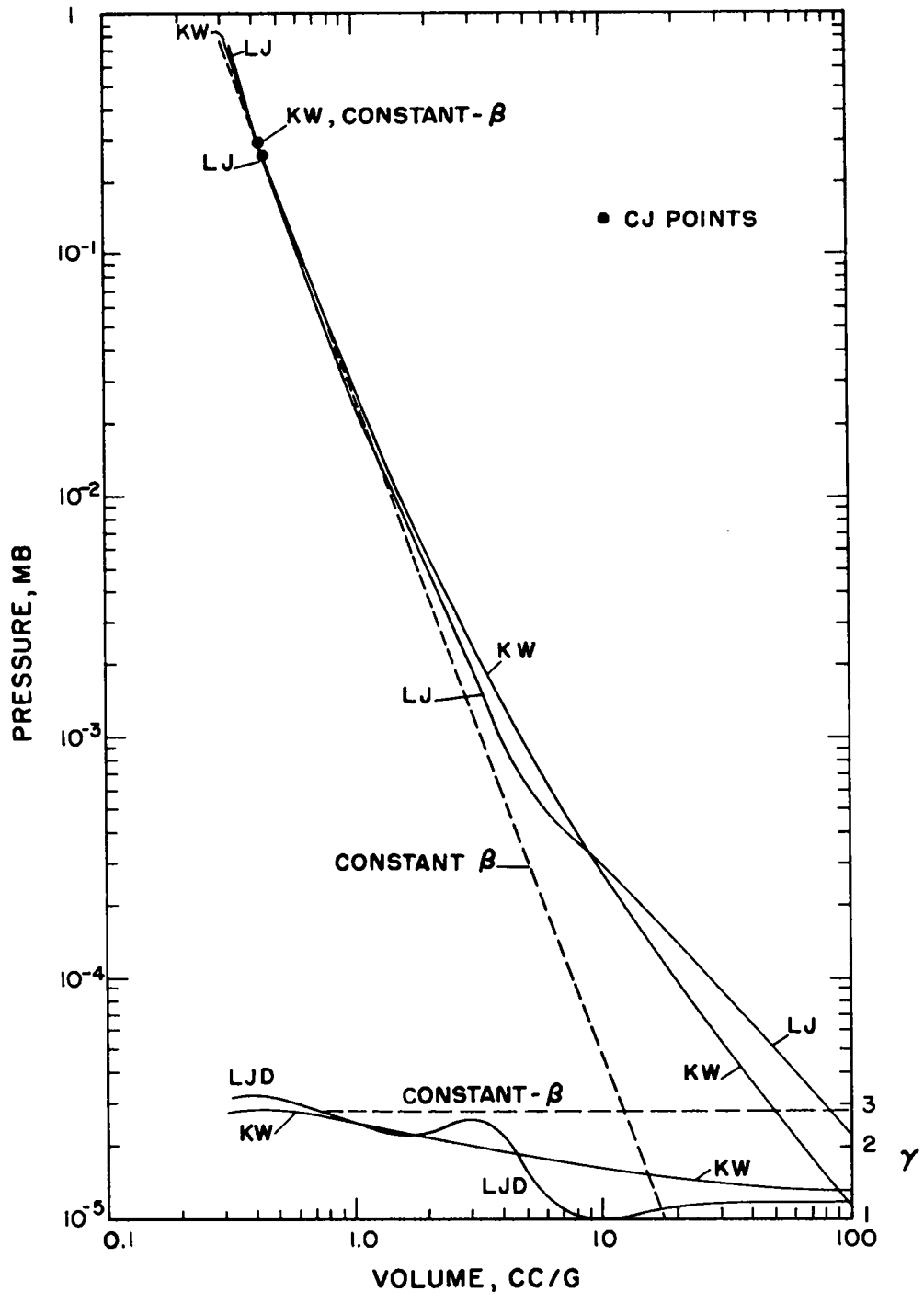

Fig. E.5. Calculated CJ isentropes (at $\rho_o = 1.714$) for the KW, LJD, and constant-β equations of state. At bottom is the logarithmic slope $\gamma = (\partial \ln p / \partial \ln v)_S$ (right hand scale).

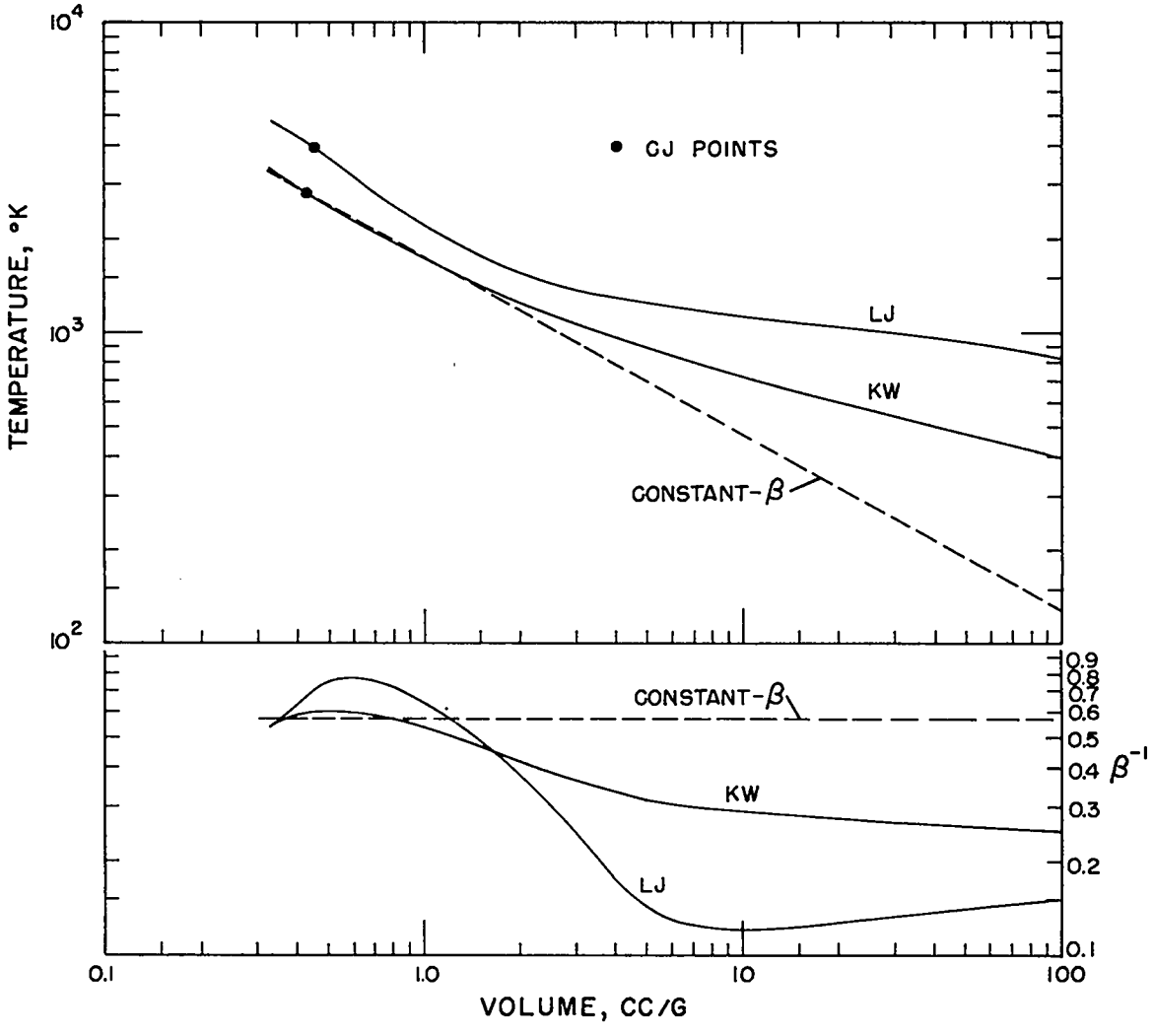

Fig. E.6. Temperatures on the isentropes of Fig. E.5. At bottom is the logarithmic slope $\beta^{-1} = (\partial \ln T/\partial \ln v)_S$. The constant-$\beta$ equation of state gives only relative temperatures; the calculated KW CJ value was arbitrarily chosen as the starting point.

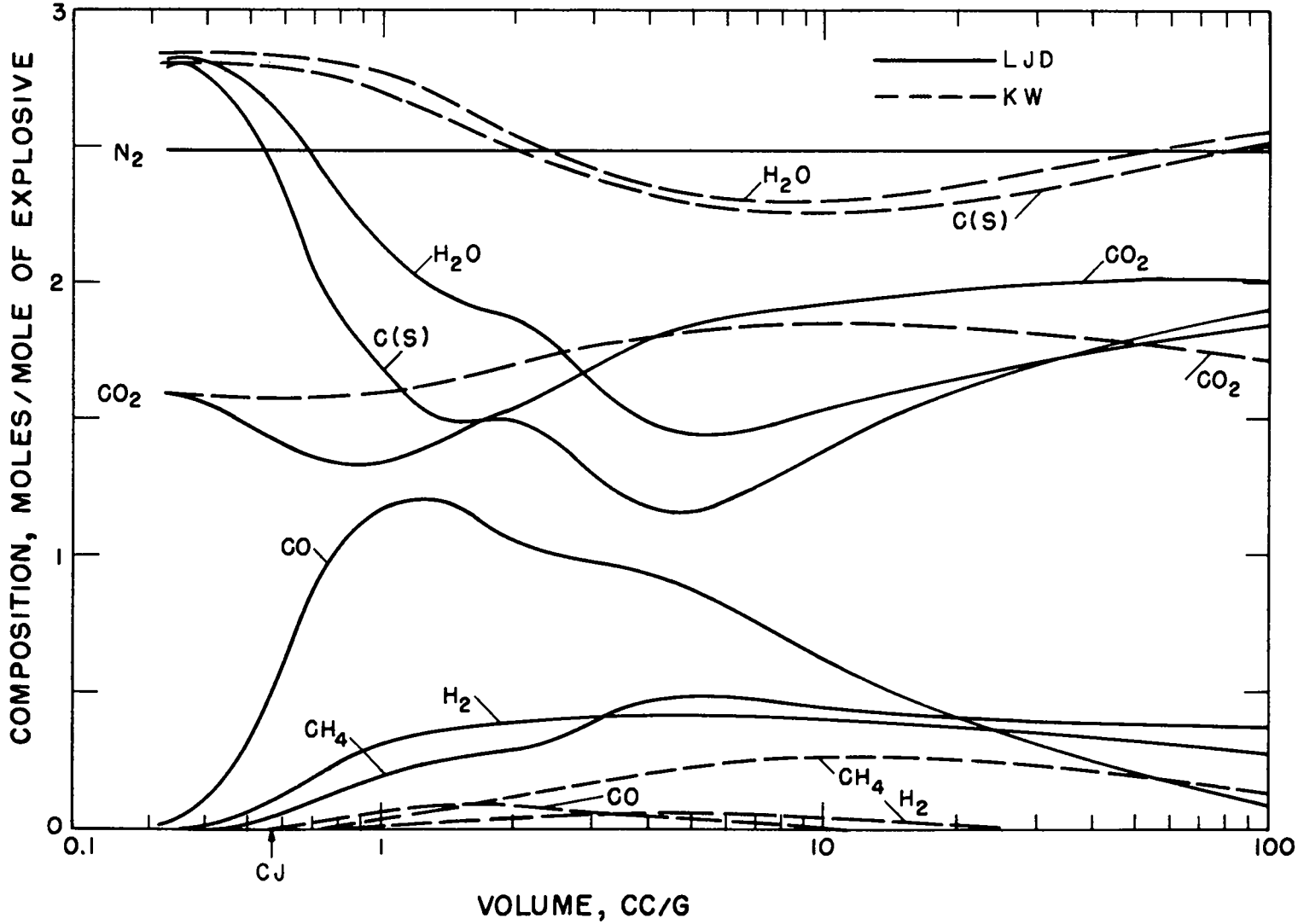

Fig. E.7. Composition on the isentropes of Fig. E.5.

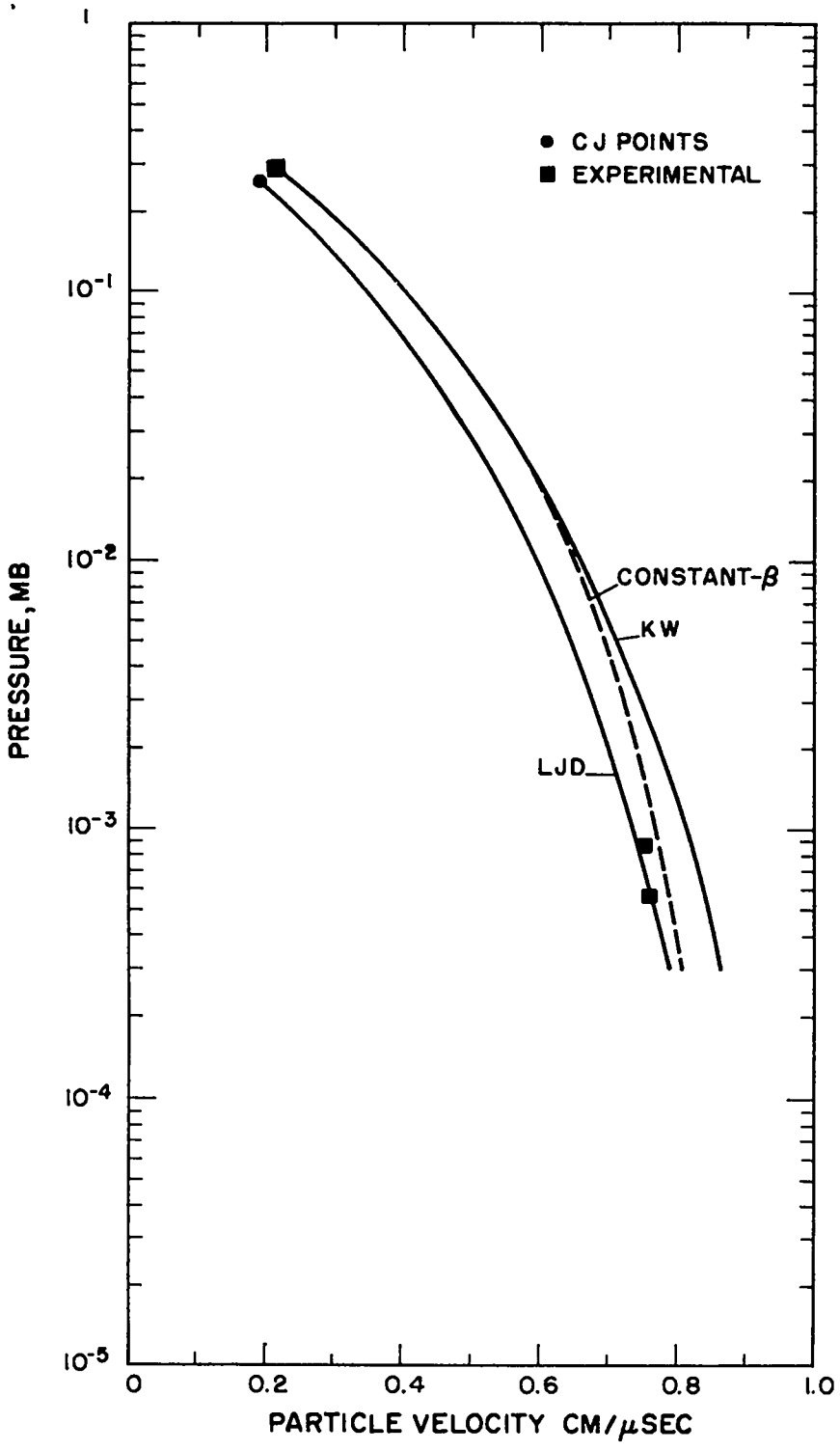

Fig. E.8. Pressure vs. particle velocity on the isentropes of Fig. E.5.

Appendix F

SHOCK HUGONIOTS OF LIQUID N_2 AND SOLID CO_2

Since the publication of ref. (31), experimental data on the shock Hugoniots of liquid N_2 and solid CO_2 have appeared.[64] We present here a comparison of some calculated shock Hugoniots with these experimental results, as a check on the pair potentials of these two species.

The results are given in Figs. F.1 and F.2. For nitrogen, the numbered curves correspond to calculations made with the following potentials:

1. The exp-six potential determined from low-energy (second virial coefficient, crystal, and viscosity) data:

   $\alpha = 17, \quad r^* = 4.01$ A, $\quad T^* = 101$ °K.

2. The exp-six potential determined from high-energy (molecular scattering) data:

   $\alpha = 15, \quad r^* = 4.05$ A, $\quad T^* = 120$ °K.

3. The MM potential used in the detonation calculations of Chapter 5 (i.e., the common value of α (= 13) and the individual values of r^* and T^* for N_2):

   $\alpha = 13, \quad r^* = 4.05$ A, $\quad T^* = 120$ °K.

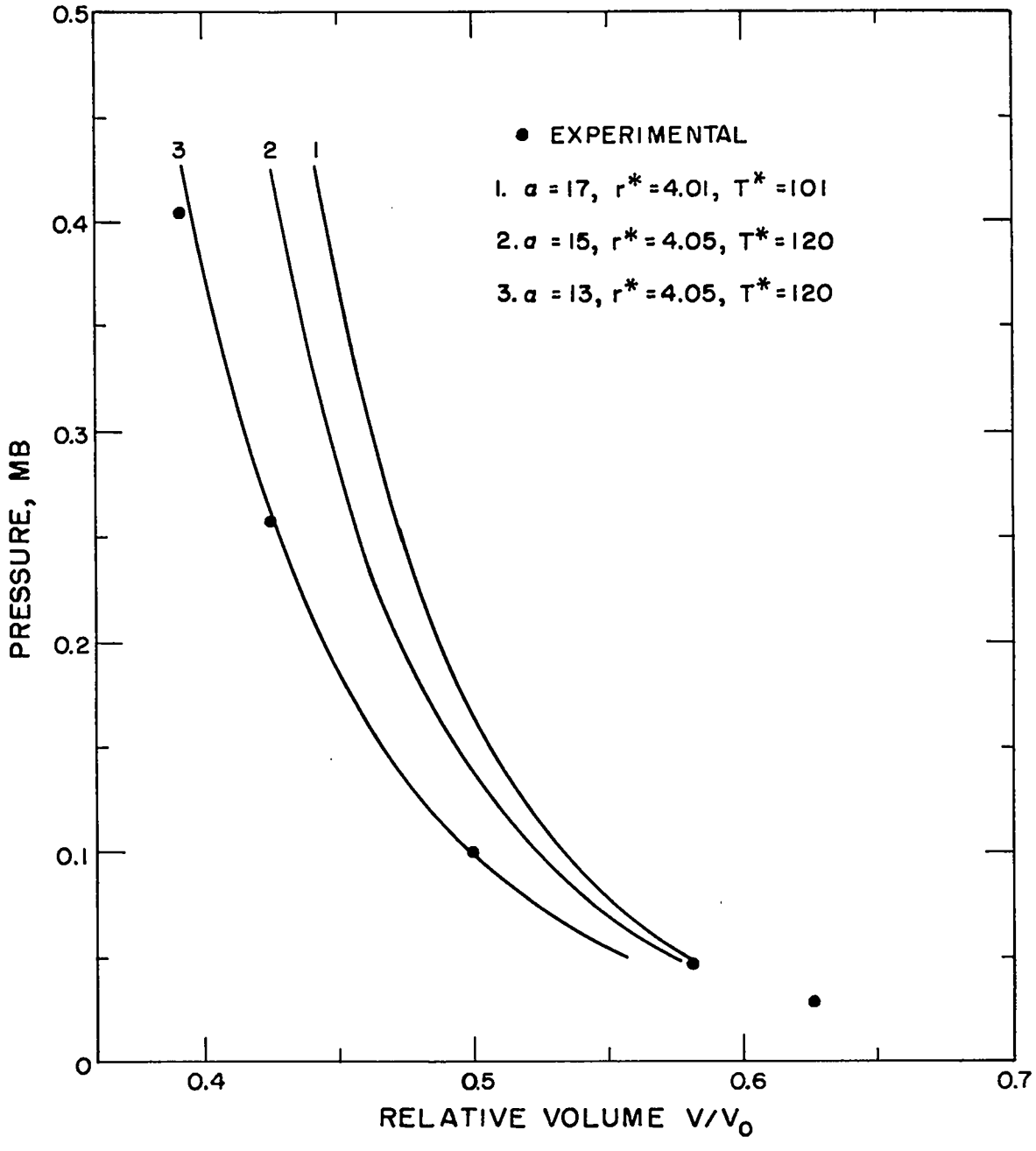

Fig. F.1. Calculated (——) and experimental (●) shock Hugoniots for liquid N_2 (see text).

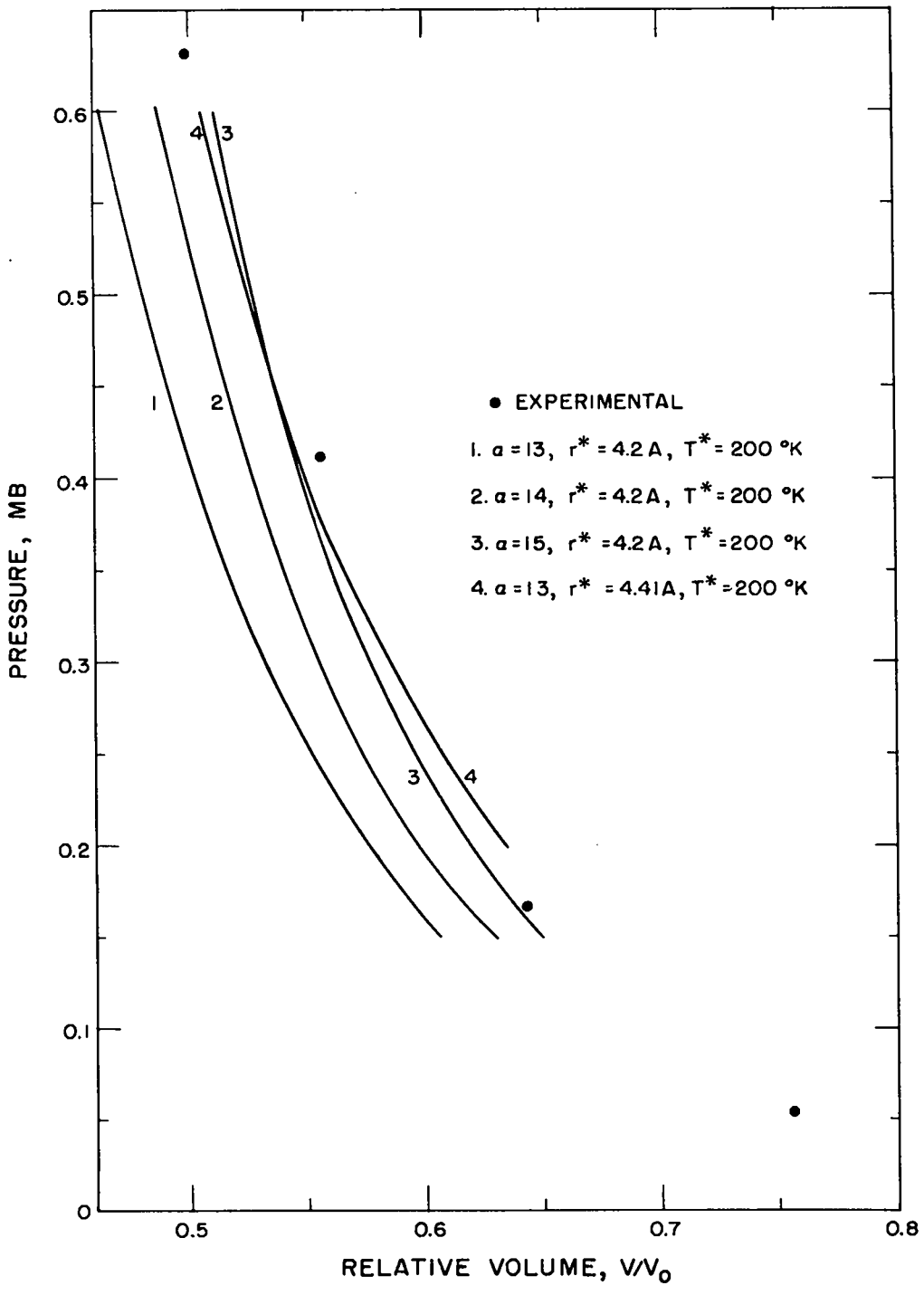

Fig. F.2. Calculated (——) and experimental (●) shock Hugoniots for solid CO_2 (see text).

It is gratifying, though perhaps fortuitous, that the Hugoniot from the potential used in the detonation calculations agrees so well with the experimental data. Potential number 2 actually fits only the low end of the molecular scattering data. As shown in Fig. 4 of ref. (31), it lies above the molecular scattering results over most of the range, so that a softer potential such as that used in the detonation calculations (number 3) is not an unreasonable choice.

For CO_2, there is no high-energy data on the pair potential, and the low-energy data yield a variety of values for r* and T*, as might be expected from an attempt to represent the potential of such an elongated molecule by a spherically-symmetric potential function. In ref. (31) the following values of r* and T*:

$$r^* = 4.2 \text{ A}, \qquad T^* = 200 \text{ }^\circ\text{K},$$

were chosen from this set for use in the detonation calculation. Since there is no high-energy data on the pair potential, we used these values of r* and T* and three values of α:

$$\alpha = 13, 14, \text{ and } 15.$$

The results are shown as curves 1, 2, and 3 of Fig. F.2. The first of these, which corresponds to the potential used in the detonation calculations, is clearly too soft, so a fourth calculation was done, again with $\alpha = 13$ but with r* increased by 5% to 4.41 A. The calculated Hugoniot for this pair potential is close to that for $\alpha = 15$, above, and is in reasonably good agreement with experiment. Had this shock Hugoniot data been available earlier, we would probably have used this value of r* in the detonation calculations.

As before,[31] the experimental initial states were used in the Hugoniot calculation since the LJD equation of state is poor at low pressures. These initial states are given in Table F.1. For CO_2, an equilibrium calculation showed that decomposition to solid carbon, CO, and O_2 occurred to only a very small extent; the calculations shown assumed no decomposition.

The use of the experimental initial states makes it impossible to calculate the Hugoniot curves down to zero pressure. This difficulty is aggravated if we use r^* as an adjustable parameter, as in Curve 4 of Fig. F.2, since this will distort the potential in the neighborhood of the well, thus making the low-pressure results even worse. The adjustment of α, as in curves 1 through 3 of Fig. F.2, is probably a better choice for the individual species, but if the resulting potential is to be used in our mixture calculation, this procedure cannot be used, since the conformal assumption (Eq. 2.9), requires the same repulsive exponent for all species.

Table F.1. Experimental Initial States[a]

	T_o °K	ρ_o g/cc	H_o kcal/mole[b]
N_2 (liquid)	77.4	0.808	-1.333
CO_2 (solid)	194.7	1.54	-97.24

[a]From ref. (64) and National Bureau of Standards Circulars 500 and 564.

[b]Enthalpy relative to elements at T.

REFERENCES

1. R. Courant and K. O. Friedrichs, Supersonic Flow and Shock Waves (Interscience, New York, 1948).

2. S. J. Jacobs, J. Am. Rocket Soc. 30, 151 (1960).

3. W. Fickett, W. W. Wood, and Z. W. Salsburg, J. Chem. Phys. 27, 1324 (1957).

4. R. B. Parlin and J. C. Giddings, Second Symposium on Detonation, Washington, D. C., February, 1955 (Office of Naval Research), p 286.

5. W. E. Deal, J. Chem. Phys. 27, 796 (1957).

6. J. O. Hirschfelder, C. F. Curtiss, and R. B. Bird, Molecular Theory of Liquids and Gases (Wiley, New York, 1954).

7. I. Amdur and E. A. Mason, J. Chem. Phys. 22, 670 (1954).

8. T. L. Cottrell, Trans. Faraday Soc. 47, 337 (1951).

9. R. Fowler and E. A. Guggenheim, Statistical Thermodynamics (Cambridge, London, 1949).

10. P. Rosen, J. Chem. Phys. 21, 1007 (1953).

11. L. Salem, Proc. Roy. Soc. 264, 379 (1961).

12. A. Shostak, J. Chem. Phys. 23, 1808 (1955).

13. R. D.Cowan, Los Alamos Scientific Laboratory Report, LA-2053 March, 1956.

14. W. Fickett and W. W. Wood, Phys. Fluids 3, 204 (1960).

15. Leighton, Principles of Modern Physics (McGraw-Hill, New York, 1959).

16. E. P. Wigner and H. B. Huntington, J. Chem. Phys. 3, 764 (1935).

17. C. A. Ten Seldam, Proc. Phys. Soc. A70, 97, 529 (1957).

18. H. P. Bovenkerk et al., Nature 184, 1094 (1959).

19. C. Zener, J. Appl. Phys. 20, 950 (1949).

20. K. D. Timmerhaus and H. G. Drickamer, J. Chem. Phys. 20, 981 (1952).

21. M. H. Rice, R. G. McQueen, and J. M. Walsh, Solid State Physics, Advances in Research and Applications (Academic Press, New York, 1958), Vol. 6.

22. R. G. McQueen and S. P. Marsh, private communication.

23. Selected Values of Chemical Thermodynamic Properties, Series III (National Bureau of Standards, Washington, D. C.).

24. J. B. Nelson and D. P. Riley, Proc. Phys. Soc. 57, 477 (1945).

25. American Institute of Physics Handbook (McGraw-Hill, New York, 1957).

26. P. W. Bridgeman, Proc. Am. Acad. Arts Sci. 76, 55 (1948).

27. R. D. Cowan and W. Fickett, J. Chem. Phys. 24, 932 (1956).

28. B. J. Ransil, J. Chem. Phys. 34, 2109 (1961).

29. I. Prigogine, The Molecular Theory of Solutions (Interscience, New York, 1957).

30. H. K. Sahoo et al., Physica 27, 994 (1961).

31. W. Fickett, Los Alamos Scientific Laboratory Report, LA-2665, April, 1962.

32. J. G. Kirkwood, J. Chem. Phys. 18, 380 (1950).

33. W. W. Wood, J. Chem. Phys. 20, 1334 (1952).

34. R. J. Buehler, R. H. Wentorf, Jr., J. O. Hirschfelder, and C. F. Curtiss, J. Chem. Phys. 19, 61 (1951).

35. J. S. Dahler and J. O. Hirschfelder, J. Chem. Phys. 32, 330 (1960).

36. Z. W. Salsburg and W. Fickett, Los Alamos Scientific Laboratory Report, LA-2667, April, 1962.

37. F. E. J. Kruseman Aretz and E. G. D. Cohen, Physica 26, 967 (1960).

38. J. D. Bernal, Nature 185, 68 (1960).

39. L. H. Nosanow, J. Chem. Phys. 30, 1596 (1959).

40. H. C. Longuet-Higgins, Proc. Roy. Soc. London A205, 247 (1951).

41. W. B. Brown, Phil. Trans. Roy. Soc. London A250, 175 (1957).

42. Z. W. Salsburg, P. J. Wojtowicz, and J. G. Kirkwood, J. Chem. Phys. 26, 1533 (1957).

43. Z. W. Salsburg and J. G. Kirkwood, J. Chem. Phys. 21, 2169 (1953); 20, 1538 (1952).

44. Z. W. Salsburg, J. Chem. Phys. 36, 1974 (1962).

45. W. B. Brown, Phil. Trans. Roy. Soc. London A250, 218 (1957).

46. S. R. Brinkley and R. W. Smith, Scientific Computation Forum (International Business Machines Co., November, 1948), p.77.

47. S. R. Brinkley, J. Chem. Phys. 15, 107 (1947).

48. W. W. Wood and Z. W. Salsburg, Phys. Fluids 3, 549 (1960).

49. L. T. Ho et al., Phys. Fluids 4, 785 (1961).

50. S. J. Jacobs, NAVORD Report 4366, September, 1956.

51. D. R. White, Phys. Fluids 4, 465 (1961).

52. Yu H. Denisov and Ya K. Troshin, Doklady Akad. Nauk S.S.S.R. (Physical Chemistry Section) 125, 110 (1959).

53. R. E. Duff, Phys. Fluids 4, 1427 (1961).

54. B. G. Craig, private communication.

55. M. J. Urizar, E. James, and L. C. Smith, Phys. Fluids 4, 262 (1961); A. W. Campbell et al., Rev. Sci. Instruments 27, 567 (1956).

56. F. C. Gibson et al., J. Appl. Phys. 29, 628 (1958).

57. W. E. Deal, Phys. Fluids 1, 523 (1958).

58. W. E. Deal, Third Symposium on Detonation, Princeton University, Princeton, N. J., September, 1960 (Office of Naval Research), p. 386.

59. W. Fickett and R. D. Cowan, Los Alamos Scientific Laboratory Report, LA-1727, September, 1954.

60. JANAF Thermochemical Panel and Thermal Laboratory, Dow Chemical Co., JANAF Interim Thermo Chemical Tables, ARPA Program, December, 1960.

61. W. Fickett and W. W. Wood, J. Chem. Phys. 20, 1624 (1952).

62. C. L. Mader, Los Alamos Scientific Laboratory Report, LA-2613. January, 1961.

63. W. Fickett and W. W. Wood, Phys. Fluids 1, 528 (1958).

64. V. N. Zubarev and G. S. Telegin, Doklady Akad. Nauk S.S.S.R. 142, 309-12 (1962). Translation: Soviet Physics - Doklady 7, 34 (1962).